Siver Andreas Moestue

Molecular and functional characterization of breast cancer through a combination of MR imaging, transcriptomics and metabolomics

Thesis for the degree of Philosophiae Doctor

Trondheim, January 2012

Norwegian University of Science and Technology
Faculty of Medicine
Department of Circulation and Medical Imaging

NTNU – Trondheim
Norwegian University of
Science and Technology

NTNU
Norwegian University of Science and Technology

Thesis for the degree of Philosophiae Doctor

Faculty of Medicine
Department of Circulation and Medical Imaging

ISBN 978-82-471-3290-6 (printed ver.)
ISBN 978-82-471-3291-3 (electronic ver.)
ISSN 1503-8181

Doctoral theses at NTNU, 2012:14

Printed by NTNU-trykk

SAMMENDRAG

Molekylær og funksjonell karakterisering av brystkreft gjennom kombinasjon av MR-avbildning, genuttrykksanalyse og metabolsk profilering

Brystkreft er den hyppigst forekommende kreftformen hos kvinner i Norge. Sykdomsutfallet er svært varierende. Noen pasienter har langsomt voksende tumorer som holder seg i brystkjertelen, mens andre har aggressive tumorer som vokser raskt og gir metastaser. Basert på genuttrykksprofiler har brystkreft blitt delt inn i minst fem undergrupper med ulike kliniske egenskaper og prognose. En bedre forståelse av egenskapene til de ulike undergruppene og hvordan de best kan behandles er nødvendig for å dra nytte av denne molekylære klassifiseringen i diagnostikk og behandling av brystkreft.

Motivasjonen for arbeidet i denne avhandlingen har vært å kartlegge forskjeller i brystkreftsvulstenes metabolisme og vaskularisering ved hjelp av magnetisk resonans (MR) avbildning og spektroskopi. Arbeidet viser hvordan ulike MR-metoder kan brukes til å studere biologien i to dyremodeller av brystkreft som representerer de molekylære undergruppene luminal-like og basal-like brystkreft. Resultatene viser ulike MR-karakteristika i de to brystkreftmodellene med henholdsvis god og dårlig prognose.

MR-spektroskopi kan brukes til å studere metabolisme i celler og vev. Siden kreftceller har et stort behov for energi og byggeklosser for å kunne vokse raskt, har de metabolske egenskaper som avviker kraftig fra friske celler. I dette arbeidet er det påvist forskjeller i kolinmetabolisme mellom luminal-like og basal-like brystkreftxenografter, og metabolittmønstrene fra dyremodellene er representative for funn i kliniske prøver. Siden kolinforbindelser ofte brukes som tumormarkør både i diagnostikk og vurdering av behandlingsrespons, kan forskjell i kolinmetabolisme mellom ulike molekylære undergrupper ha klinisk betydning. I avhandlingen er det også beskrevet hvordan glukosemetabolismen kan studeres ved hjelp av ^{13}C-anriket glukose. Bruken av en stabil, MR-detekterbar isotop gjør det mulig å måle hvor raskt glukosen omdannes til andre metabolitter som laktat og alanin, og hvorvidt glukosen er et substrat i sitronsyresyklus. Unormal glukosemetabolisme er et vanlig kjennetegn

i kreft, og utnyttes klinisk blant annet i PET-avbildning. Det er også stor interesse for hyperpolarisert MR-spektroskopi i måling av laktatproduksjon i kreft. Metoden som er etablert i dette arbeidet gjør det mulig å studere metabolisme *ex vivo* og å studere sammenhengen mellom genuttrykk og metabolismehastighet. I dyremodeller av luminal-like og basal-like brystkreft ble det vist at den minst aggressive modellen hadde raskest glukoseomsetning, noe som tyder på at veksthastighet og aggressivitet ikke er direkte knyttet til glukosemetabolisme i dyremodeller av brystkreft.

MR-avbildning kan brukes til anatomisk avbildning av kroppen, men også til studier av funksjonelle egenskaper som blodgjennomstrømning og celletetthet. I kreftsvulster er blodårene ofte uferdige og dårlig organisert. Uten tilstrekkelig blodtilførsel begrenses tumorveksten, og tumorcellenes evne til å stimulere til innvekst av nye blodkar (angiogenese) har betydning for sykdomsutfallet. Ved hjelp av kontrastforsterket MR-avbildning ble vaskularisering og nydannelse av blodårer studert i dyremodellene av luminal-like og basal-like brystkreft. Ved hjelp av dynamisk kontrastoppladet MR-avbildning og immunhistokjemi ble det vist at modellen av basal-like brystkreft har et større kontrastopptak, at den er bedre vaskularisert og at den har mer aktiv angiogenese enn modellen av luminal-like brystkreft. I en oppfølgingsstudie ble effekten av antiangiogenese-legemidlet bevacizumab studert. Dette stoffet hemmer nydannelsen av blodkar og kan derfor begrense tumorveksten. Kort tid etter behandling viste MR-avbildning en økt kontrastoppladning. Immunhistokjemi viste en reduksjon i blodåretetthet og nydannelse av blodkar. Dette ble tolket som en normalisering av blodårene i tumor og bedret vaskulær funksjon, noe som kan ha betydning for bruken av bevacizumab sammen med andre cytostatika eller stråleterapi.

Avhandlingen består av fire arbeider som alle dreier seg om bruk av MR i dyremodeller av luminal-like og basal-like brystkreft. I de to første arbeidene har høyoppløst *ex vivo* MR-spektroskopi blitt brukt i kombinasjon med genuttrykksanalyse for å beskrive tumorspesifikke metabolske egenskaper. I de to siste arbeidene har dynamisk kontrastoppladet MR-avbildning og farmakokinetisk analyse av kontrastmiddeldistribusjon blitt brukt til å beskrive tumorenes vaskularisering og hvordan denne endres ved antiangiogenesebehandling. Felles for de fire arbeidene er at de beskriver hvordan ulike MR-teknikker kan skille mellom

brystkreftmodeller av ulik aggressivitet. De viser også hvordan MR-parameterne kan beskrive molekylære og strukturelle forhold i tumorene. Avhandlingen kan derfor bidra til økt forståelse av MR-funn i diagnostikk og behandling av brystkreftpasienter. I tillegg danner den et solid fundament for videre studier i de studerte dyremodellene av luminal-like og basal-like brystkreft, særlig med tanke på identifisering av nye behandlingsregimer og bruk av MR-avbildning i vurdering av behandlingsrespons.

Kandidat: Siver Andreas Moestue
Institutt: Institutt for Sirkulasjon og bildediagnostikk
Veileder: Ingrid S. Gribbestad
Finansiering: FUGE-programmet, Forskningsrådet (prosjekt nr. 183379)

Ovennevnte avhandling er funnet verdig til å forsvares offentlig for graden Philosophiae Doctor i medisinsk teknologi.
Disputas finner sted i Auditoriet, Medisinsk teknisk forskningssenter, fredag 20.januar 2012 kl. 12.15.

ACKNOWLEDGEMENTS

The work presented in this thesis has been performed in the MR Cancer Group, Department of Circulation and Medical Imaging, NTNU, with financial support from the Research Council of Norway.

I would like to express my gratitude to my supervisor, Professor Ingrid S. Gribbestad, for giving me the opportunity to perform this work and for the support and guidance throughout my PhD period. Your long experience in MR imaging and spectroscopy and your ability to see the big picture has been of great value.

Medical technology is an interdisciplinary research field and I have had the pleasure to work with scientists from several institutions. Firstly, I would like to thank all my co-authors and all my colleagues at the MR Centre. The positivity and scientific curiosity in the MR Cancer group has been of great importance for this work. Special thanks to Dr. Else Marie Huuse for introducing me to the 7T scanner and the analysis of MRI data, to Maria T. Grinde for her efforts in analyses of ^{13}C-labeled metabolites, to Dr. Øystein Risa for all the troubleshooting and Dr. Beathe Sitter for sharing her knowledge in HR MAS MRS spectroscopy of breast cancer. Secondly, my thanks goes to Dr. Med Anna Bofin and Prof. Lars A. Akslen for histopathological goodwill. Thirdly, I would like to thank Eldrid Borgan, Dr. Med Olav Engebråten and Prof. Gunhild M. Mælandsmo at the Institute for Cancer Research, Oslo, for establishing and supplying the animal models that were used in this work, for transcriptomic analyses of the animal models and for their invariably positive attitude to my endless enquiries.

A large number of people have contributed through hands-on and technical assistance and through resolving small or large problems. This thesis could not have been completed without your help. Especially, I wish to thank Alexandr Kristian for implantation of every single xenograft tumor studied in this work, Unn S. Granli and Borgny Ytterhus who prepared sections for histopathology, Tina B. Pedersen for assistance with animal experiments, and Pål Erik Goa for thoughtfully refining our image analysis tools.

A major contribution to the work was made already before I joined the MR Cancer group. I would like to thank former GE Healthcare colleagues Dr. Svein Olaf Hustvedt, Dr. Tore Skotland and Grete Friisk for introducing me to preclinical medical imaging research, for training in scientific rigor and for encouraging creativity when approaching biological problems.

Finally, I am thankful for the continuous support from friends and family; especially my mother and father for supporting me and encouraging me to embark on the PhD studies. Most importantly, I am deeply grateful to my dear Fride, for the love and patience and your understanding for my work. Last but not least, thanks to my boys Vetle and Martin Kristoffer, for making life at home even more important and entertaining than life in the MR lab.

SUMMARY

Molecular and functional characterization of breast cancer through a combination of MR imaging, transcriptomics and metabolomics

Breast cancer is the most frequent cancer among women in Norway. The outcome of this disease is heterogeneous. Some patients have slowly growing tumors which stay confined within the mammary gland, whereas others have aggressive tumors that grow rapidly and metastasize to distant tissues. Based on gene expression profiles, breast cancer has been divided into at least five different subtypes with differences in clinical characteristics and prognosis. Improved understanding of the biology of these subtypes and how they should be treated is needed to benefit from this molecular subtyping in breast cancer diagnosis and treatment.

The motivation for this work has been to map differences in breast cancer metabolism and vascularization using different MR imaging and spectroscopy methods. The work shows how different MR methods can be used to study the biology of animal breast cancer models representing the molecular subgroups luminal-like and basal-like breast cancer. The findings represent MR characteristics in breast cancer with good and poor prognosis, respectively.

MR spectroscopy can be used to study metabolism in cells and tissues. Since cancer cells have a large need for energy and molecular building blocks in order to grow fast, they have metabolic properties that differ markedly from healthy cells. The thesis describes how MR-spectroscopy can detect differences in choline metabolism between luminal-like and basal-like breast cancer, and demonstrates how metabolic patterns found in the animal models are representative for findings in clinical samples. Since CCCs are proposed as biomarkers in diagnosis and evaluation of response to therapy in breast cancer, differences in choline metabolism between different molecular subtypes may be of clinical relevance.

The thesis also describes how glucose metabolism can be studied using ^{13}C-labeled glucose. Using a stable, MR-detectable isotope allows assessment of the metabolic fate of glucose. Abnormal glucose metabolism is a typical feature in cancer, and is the basis for PET imaging using FDG. There is also great interest for use of

hyperpolarized MR spectroscopy for measurement of lactate production in cancer. The method that is established in this work allows *ex vivo* studies of metabolism and the relationship between gene expression and metabolic rates. In the luminal-like and basal-like animal models, it was found that the least aggressive model had the highest glycolytic rate, suggesting that tumor growth rate and aggressiveness not necessarily is directly linked to glycolytic rate.

MR imaging can be used for anatomical imaging of the body, but also for studies of functional properties such as perfusion and cellular density. In tumors, the blood vessels are typically leaky, poorly organized and have suboptimal function. Without sufficient blood supply, tumor growth is limited. The tumor cells' ability to stimulate growth of new vessels has impact on disease outcome. Vascularization and neoangiogenesis was studied in the luminal-like and basal-like models. Using dynamic contrast-enhanced MR imaging and immunohistochemistry, it was found that the basal-like xenograft model had higher contrast uptake, that it is better vascularised and has more active angiogenesis than the luminal-like xenograft. In a follow-up study, the effect of the antiangiogenic agent bevacizumab was studied. This drug inhibits the formation of new blood vessels and can therefore slow down tumor growth. Shortly after treatment, MR imaging demonstrated increased contrast agent uptake in the tumors. Immunohistochemistry showed a reduction in the number of microvessels and angiogenic activity. These findings were interpreted as normalization of blood vessels and improved vascular function. MR imaging of vascular normalization may have impact on the use of bevacizumab together with other cytotoxic drugs or radiotherapy.

The thesis consists of four papers which all describe use of MR in animal xenograft models of luminal-like and basal-like breast cancer. In the two first papers, high resolution *ex vivo* MR spectroscopy has been combined with gene expression analysis for description of tumor-specific metabolic properties. In the last two papers, dynamic contrast-enhanced MR imaging and pharmacokinetic analysis of contrast agent distribution has been used to describe tumor vascularization and how this respond to antiangiogenic treatment. All four papers describe how different MR techniques can distinguish between animal models of varying aggressiveness. They also show how the MR parameters are associated with molecular or structural properties of the

tumors. The thesis may therefore contribute to improved understanding of MR findings in breast cancer diagnosis and treatment. In addition, it forms a basis for further studies of these animal xenograft models of luminal-like and basal-like breast cancer, especially with regard to identification of new treatment regimens and MR imaging for therapy response monitoring.

SYMBOLS AND ABBREVIATIONS

ADC	apparent diffusion coefficient
AIF	arterial input function
ATP	adenosine triphosphate
AUC	area under the curve
b	diffusion weighting factor
B_0	the static magnetic field
C	concentration of the contrast agent
CCC	choline-containing compound
CHKA	choline kinase alpha (gene)
Cho	choline
Cp	contrast agent concentration in plasma
DCE	dynamic contrast-enhanced
DCIS	ductal carcinoma *in situ*
DNA	deoxyribonucleic acid
DNP	dynamic nuclear polarization
DW	diffusion weighted
EES	extravascular extracellular space
EPI	echo planar imaging
ER	estrogen receptor
ERETIC	electronic reference to access in vivo concentrations
FDG	fluorodeoxyglucose
FOV	field of view
γ	gyromagnetic ratio
GEMM	genetically engineered mouse models
GPC	glycerophosphocholine
HER-2	herceptin receptor
HES	hematoxylin, eosin and saffron
HIF-1	hypoxia-inducible factor 1
HR MAS	high resolution magic angle spinning
IFP	interstitial fluid pressure
ip	intraperitoneal
iv	intravenous
K^{trans}	transfer constant
KEGG	Kyoto encyclopedia of genes and genomes
LCIS	lobular carcinoma *in situ*
MR	magnetic resonance
MRI	magnetic resonance imaging
MRS	magnetic resonance spectroscopy
MRSI	magnetic resonance spectroscopic imaging
mRNA	messenger ribonucleic acid
MVD	microvessel density
NAC	neoadjuvant chemotherapy
NBCG	Norwegian breast cancer group
ω_0	resonance frequency
PCA	principal component analysis
PCho	phosphocholine
PET	positron emission tomography

PgR	progesterone receptor
PLA	phospholipase A
PLC	phospholipase C
PLD	phospholipase D
pMVD	proliferative microvessel density
PPH3	phosphohistone H3 (mitotic marker)
ppm	parts per million
PPTT	primary patient tumor tissue
PRESS	point resolved spectroscopy
PtdCho	phosphatidylcholine
ρ	proton density
RARE	rapid acquisition with refocused echoes
RF	radiofrequency
ROI	region of interest
RSI	relative signal intensity
SCID	severe combined immunodeficient
SI	signal intensity
T_1	longitudinal relaxation time
T_2	transverse relaxation time
TE	echo time
tCho	total choline signal
TNM-system	clinical tumor staging system
TSP	trimethylsilyl-3-proprionic acid
TR	repetition time
TTP	time to peak
US	ultrasound
v_e	volume fraction of extravascular extracellular space
VEGF	vascular endothelial growth factor
v_p	volume fraction of blood plasma
XRM	X-ray mammography

PAPERS INCLUDED IN THE THESIS

Paper I:

Moestue SA, Borgan E, Huuse EM, Lindholm EM, Sitter B, Børresen-Dale AL, Engebraaten O, Mælandsmo GM, Gribbestad IS: Distinct choline metabolic profiles are associated with differences in gene expression for basal-like and luminal-like breast cancer xenograft models.

Published in BMC Cancer 2010; 10; 433

Paper II:

Grinde MT, Moestue SA, Borgan E, Risa Ø, Engebraaten O, Gribbestad IS: ^{13}C High-resolution Magic Angle Spinning MRS reveals differences in glucose metabolism between two breast cancer xenograft models with different gene expression patterns.

Published in NMR in Biomedicine 2011; 24 (10); 1243-1252.

Paper III:

Huuse EM, Moestue SA, Lindholm EM, Bathen TF, Nalwoga H, Krüger K, Bofin A, Mælandsmo GM, Akslen LA, Engebraaten O, Gribbestad IS : In vivo magnetic resonance imaging and histopathological assessment of tumor microenvironment in luminal-like and basal-like breast cancer xenografts.

Published in Journal of Magnetic Resonance Imaging 2011; Epub ahead of print December 14th 2011

Paper IV:

Moestue SA, Huuse EM, Lindholm EM, Akslen LA, Bofin A, Engebraaten O, Mælandsmo GM, Gribbestad IS: Low-molecular contrast agent DCE-MRI and DW-MRI in early assessment of bevacizumab therapy in breast cancer xenografts.

Manuscript

CONTENTS

Figures

Tables

1 Introduction

1.1 Cancer

Cancer is a group of diseases typically characterized by rapid and uncontrolled division of cells. Depending on their origin, these cells can be present as disseminated in body fluids or form solid tumors. In malignant tumors, the abnormal growth of cells is accompanied by invasion of neighboring tissue and spread of cancer cells to distant locations (metastasis). Cancers can arise from a wide range of cell types and organs, and the degree of malignancy varies both between cell types and within cancers arising from the same cell type. This variation is reflecting the underlying genetic abnormalities that cause cancer. A wide range of cancer-promoting abnormalities in the genetic material cells can cause cancer. Such abnormalities can occur both in single genes and in combinations of several genes, but are typically related to the cell's ability to replicate, its ability to avoid death, and its ability to interact with surrounding tissue.

Cancer is a major source of morbidity and mortality both nationally and globally. In 2008, global estimates included 12.7 million new cancer cases and 7.6 million cancer deaths (Ferlay 2010). Through organized efforts in cancer prevention and treatment, these numbers could be significantly reduced. Still, there is a large unmet medical need for earlier diagnosis, better risk prediction and treatment of cancer. Treatment options include surgery, radiation therapy and chemotherapy/hormonal therapy. Optimal treatment of the disease is important not only for individual patients but also for socio-economic reasons. In recent years, treatment has become increasingly personalized, meaning that the biologic features of individual cancers are taken into account when selecting treatment strategies.

Further understanding of the genetics of cancer will hopefully aid in development of new drugs targeting genetic abnormalities. Stratification of patients into increasingly smaller subgroups that can be managed and treated based on specific disease and risk profiles will also expectedly improve today's standards of cancer management.

1.2 Breast cancer

Worldwide, breast cancer is the most frequent cancer type in women, and causes more than 400.000 deaths per year. In Norway, approximately 2700 cases are diagnosed each year (Bray 2009). It is characterized by highly variable progression, from rapidly growing tumors with early distant metastases to slowly growing tumors that do not spread from the mammary gland. The prognosis has continuously improved through several decades, which could be associated with both the introduction of screening programmes and better treatment (La Vecchia C. 2010). In Norway, the 5-year survival without signs of relapse is more than 80% (Bray 2009). Still, breast cancer is a leading cause of lost life-years in women. The prognosis of the disease depends on the stage at the time point of diagnosis, and the 5-year survival in patients who are diagnosed with metastatic breast cancer is below 20% (Bray 2009). Thus, current research tends to focus on treatment options for the most aggressive forms of breast cancer.

1.2.1 Breast cancer classification

Breast cancer is a highly heterogeneous disease, and classification systems have been constructed to account for morphological, functional and molecular differences. In accordance with the theory of step-wise acquisition of malignant phenotype, breast cancer present in the range from dysplastic lesions to distal metastatic disease. Most malignant breast tumors are carcinomas, of which ductal and lobular carcinomas are the most frequent morphological subtypes. Breast cancer metastasis most frequently occur in axillary lymph nodes due to local lymphatic transport of tumor cells. Distant metastases show high affinity to bone, lung, brain and liver tissue.

Clinically, tumors are staged according to their size, lymph node involvement and metastasis status using the TNM (tumor, node, metastasis) system (Singletary 2003). Depending on these characteristics, breast tumors are classified as primarily operable or primarily inoperable.

Histological evaluation of breast tissue includes description of premalignant conditions such as lobular and ductal hyperplasia, where more than two cell layers are present in these structures. In addition, atypical features such as enlarged cell nuclei may be observed. If the hyperplastic lesions have high proliferative rate and high degree of atypic features, the lesion may be termed a ductal/lobular carcinoma *in situ*

(DCIS/LCIS). In these conditions, the cancer cells are confined to the ductal/lobular lumen. If cancer cells have penetrated the basal membrane, the lesions represent invasive breast cancer. The histological examination of breast cancer also includes an assessment of tumor grade, which depend on parameters such as cellular proliferation, variation in nuclear size and shape, and the degree of differentiation in the tumor tissue. High proliferation rate, poorly differentiated cells and large nuclear variation are associated with high tumor grade and indicate a poor prognosis.

1.2.2 Estrogen/progesteron receptor expression and HER-2 overexpression

In addition to anatomical and morphological classification, histopathological evaluation of breast cancer includes assessment of hormone receptor status and human epidermal growth factor 2 (HER-2) status. The presence or absence of estrogen receptor (ER), progesterone receptor (PgR) or HER-2 has consequences for choice of treatment, as hormone blocking therapy (tamoxifen, aromatase inhibitors) or HER-2-blocking antibodies (trastuzumab) should be administered only to patients that express these receptors.

Approximately 70-75% of all breast cancers express either estrogen receptor (ER) or progesterone receptor (PgR) (Osborne 1998). The importance of circulating estrogen levels in breast cancer was acknowledged in the 19th century, when ovariectomy was shown to induce regression of primary breast carcinomas (Beatson 1896). Activation of hormone receptors lead to transcription of a number of genes involved in cell proliferation (Osborne 2005). In patients with hormone-receptor positive tumors, endocrine therapy is therefore an attractive treatment strategy with proven efficacy and favorable side effect profile (Johnston 2010). Drugs used in endocrine therapy are designed to inhibit ER/PgR activity, either by reduction of circulating estrogen levels or by blocking the hormone receptors.

The epidermal growth factor receptor HER-2 is overexpressed in 20-30% of breast cancers. Activation of this receptor can trigger downstream signalling cascades resulting in effects on cancer cell proliferation, differentiation, adhesion and migration (Harries 2002). HER-2 overexpression is predominantly caused by

amplification of the *Her-2* gene, and is associated with poor prognosis. However, development of the anti-HER-2 antibody trastuzumab (Herceptin®) has provided an attractive treatment alternative for this subset of breast cancer patients (Slamon 1989).

1.3 Breast cancer treatment

The major clinical treatment decision in breast cancer is whether or not the tumor should be surgically removed. Therefore, the staging system plays an important role in breast cancer management. Depending on tumor stage, chemotherapy can be used to prevent cancer recurrence following surgery (adjuvant therapy), to shrink a tumor prior to surgery (neoadjuvant therapy) or to slow down the progress of inoperable disease. In Norway, treatment guidelines and algorithms for different scenarios are recommended by the Norwegian Breast Cancer Group (NBCG). Typically, several treatment modalities such as surgery, radiotherapy and adjuvant chemotherapy are combined for the best possible outcome.
Localized disease is always treated with curative intention. Surgical resection of the tumor and, if necessary, infiltrated lymph nodes, is the treatment of choice. This is usually combined with radiation therapy and/or adjuvant chemotherapy.

Approximately 10% of breast cancer patients are diagnosed with locally advanced breast cancer, due to large tumor size (T3-T4) or metastases to axillary lymph nodes (N"-N3) but no distant metastasis. These patients are defined as primary inoperable, and neoadjuvant chemotherapy is often considered. The intention of this treatment is to reduce the tumor size, thereby allowing surgical removal of the tumor. Currently, there is a trend to include patients with primary operable tumors in NAC regimens as well, in order to increase the possibility of performing breast conserving surgery instead of mastectomy.

NAC regimens have a long duration and there is a need for methods that allow early discrimination between responders and non-responders. Early identification of non-responders has several benefits: the patients can be rapidly re-assigned to new and potentially more effective treatment regimen. Discontinuation of ineffective

treatments also reduces the risk of adverse effects. Finally, rapid evaluation of treatments can reduce the use of expensive drugs, thereby reducing treatment costs for the healthcare services. Non-invasive therapy monitoring using medical imaging is a potentially useful tool for early therapy monitoring in cancer.

In breast cancer with distant metastasis, there is currently no available curative treatment. The treatment therefore aims at delaying the progression of the disease and to reduce symptoms with as little toxicity as possible. Chemotherapy is the treatment of choice, and the treatment is tailored to each patient's hormone receptor status and HET-2 expression. Radiotherapy is frequently added to the regimen.

1.4 Molecular subtyping of breast cancer

A recent contribution to understanding the diversity of breast cancer is subtyping based on gene expression profiling. First reported in 2000, this approach has been used to classify breast cancer into subtypes based on expression of subsets of genes (Perou 2000). Despite great molecular heterogeneity among breast cancers, clusters of genes ("molecular portraits") with coherent expression patterns were found to be associated with specific biological features such as variation in proliferation rates and receptor expression. Stratification by gene expression profiling subtype was later demonstrated to correlate with prognosis (Sorlie 2001). Initially, five subtypes were defined (Figure 1). Later, a new subtype, called claudin-low, has been proposed (Perou 2010).

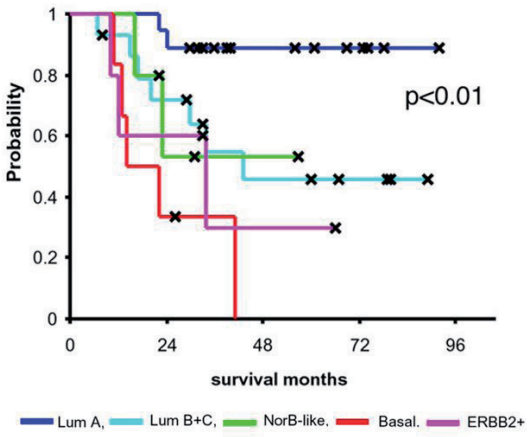

Figure 1 Survival analysis of breast cancer patients with different gene expression profiles.

Patients with luminal-like breast cancer have better long-term survival than patients with ERBB2-positive and basal-like breast cancer. Adapted from Sørlie *et al* (Sorlie 2001) with permission from the National Academy of Sciences, USA (Copyright 2001).

The main distinction between the subtypes is between tumors expressing genes characteristic of the luminal epithelial cells, and those that are negative for these genes. The incidence of the gene expression subtypes varies within patient subpopulations depending on patient age and ethnicity (Naume 2007; Yu 2010). The luminal-like subtypes constitute approximately 50-70 % of all cases, whereas the ErBB2+ (10 %) and basal-like (10-20%) subtypes have a lower incidence (Perou 2010). The incidence and clinical relevance of the normal-like and claudin-low subtypes remains unclear. The most common subtype, termed Luminal A, typically exhibits strong expression of ER, and is associated with a favorable overall prognosis. The Luminal B subtype has low to moderate ER expression and relatively high expression of proliferation genes (Loi 2009). The ErBB2+ subtype is characterized by amplification of the HER-2 gene and high expression of genes located adjacent to the HER-2 locus. The basal-like subtype has a gene expression profile similar to that of myoepithelial/basaloid epithelial cells, and is often associated with lack of ER/PgR

receptor expression and HER-2 amplification. This phenotype is often termed 'triple negative'. There is considerable, but not complete, overlap between the basal-like gene expression profile and the triple negative phenotype (Podo 2010). Triple negativity is a highly sensitive, but not specific, selection criterion for basal-like breast cancer. Inclusion of basaloid markers such as basal cytokeratins increases the specificity of immunohistochemical determination of basal-like gene expression profile (Rakha 2009). The claudin-low subtype is characterized by low expression of genes involved in cell-cell adhesion and high expression of mesenchymal cells, and is proposed to represent breast cancers originated from an early stage in mammary epithelial cell development. According to the same theory, basal-like cancers are proposed to represent cancers originated from epithelial progenitor cells, whereas luminal-like breast subtypes represent cancer originated from more differentiated mammary epithelium.

The biology of hormone receptor negative breast cancer confirms that these represent a separate disease entity. These tumors, constituting 20-40 % of all cases, with higher incidence in young patients, tend to be of high grade and are frequently carrying mutations in TP53 and BRCA1 (Shao 2004). Patients with triple negative breast cancer do not benefit from any available targeted therapy. This relative lack of treatment options and the aggressive behavior of the tumors result in poor prognosis for these patients.

1.5 Tumor morphology

As tumors co-evolve and communicate with their neighboring tissue, they do not consist of cancer cells alone. Various stromal components are also present, including vasculature, fibroblasts, inflammatory cells and an extracellular protein matrix. The cancer cells and the stromal cells interact dynamically as the tumor grows, creating a tumor microenvironment which ultimately promotes tumor growth and invasion. The cellularity of tumors is generally higher than in healthy tissue. In cases where the tumor microenvironment does not support cancer cell growth, for instance due to insufficient blood supply, necrotic areas filled with cellular debris may be formed.

1.5.1 Cancer vasculature and angiogenesis

Cancer cells can form avascular microscopic tumors, but their size is restricted to a diameter of 2-3 mm due to limited diffusivity of oxygen and nutrients (Folkman 1972). To grow beyond this size, tumors need to establish a vascular supply. Through paracrine signalling, cancer cells recruit new blood vessels in a process called angiogenesis. However, the resulting tumor vasculature is both structurally and functionally abnormal. Typically, tumors have distorted and dilated vessels with abnormal interconnections and defects in the basement membrane. The structural abnormalities cause spatial and temporal heterogeneity in blood flow, leading to a microenvironment with hypoxia and acidosis. The basal membranes of tumor capillaries are often leaky, allowing extravasation of plasma proteins. This in turn causes osmotic outflow of fluid from the vasculature. Tumors often have a relative lack of functional lymphatic vessels, impairing the drainage of extracellular fluid. The interstitial fluid pressure (IFP) of tumors is therefore high compared to normal tissue. The high IFP reduces convective flow out of tumor capillaries, limiting the extravasation of small molecules such as drugs and contrast agents.

1.5.2 Antiangiogenic therapy

Sustained angiogenesis is one of the original hallmarks of cancer (Hanahan 2000). As tumors depend on vascularization for growth, and as they can stimulate the formation

of new vasculature through paracrine signalling, the concept of antiangiogenic therapy was conceived in the 1970s (Folkman 1971). A large body of experimental evidence has demonstrated that tumor progression can be arrested by inhibiting formation of tumor vasculature, for example through blockade of vascular endothelial growth factor (VEGF) (Ferrara 2005; Gerber 2005). In addition to the effect on neoangiogenesis, treatment with VEGF inhibitors also changes the function of existing tumor vasculature. These changes include reduced macromolecular permeability, normalization of vessel morphology and increased blood flow. This normalization of vasculature improves oxygenation of the tumor tissue and reduces interstitial fluid pressure (Jain 2005). As a result, antiangiogenic drugs may enhance the efficacy of chemotherapy or radiation therapy (Dickson 2007; Segers 2006).

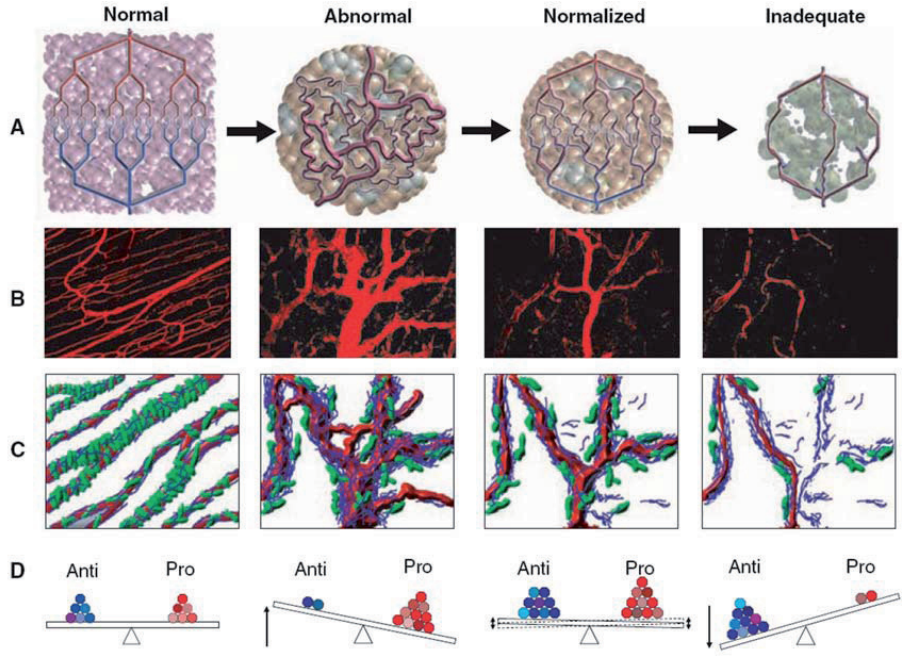

Figure 2 The morphology of tumor vasculature and its response to antiangiogenic therapy.

The figure illustrates the dilated, distorted and dysfunctional vasculature of solid tumors. Following antiangiogenic treatment, the vascularity is decreased and the vessels have a normalized appearance. Reproduced with permission (Copyright 2005) from the American Association of Advances in Science (Jain 2005).

The clinical role of antiangiogenic therapy remains somewhat unclear, as the survival benefits reported in large clinical trials have been smaller than anticipated (Hayes

The clinical role of antiangiogenic therapy remains somewhat unclear, as the survival benefits reported in large clinical trials have been smaller than anticipated (Hayes 2011). Identification of patient subgroups most likely to benefit from the treatment is needed to maximize the clinical usefulness of bevacizumab. There is an unmet need for biomarkers that can predict response to antiangiogenic therapy, and there is also a need for tailor-made treatment regimens that combine chemotherapy with antiangiogenic drugs in a rational manner (Jain 2009).

1.6 Cancer metabolism

One of the central hallmarks of cancer is the rapid and infinite cellular proliferation. In order to cope with increased requirements for cellular building blocks and energy, the metabolism of cancer cells is remarkably different from their normal counterparts. The alterations in metabolism allow cancer cells to sustain a high rate of proliferation while at the same time protecting against oxidative damage (King 2009). In order to divide, cancer cells both need to replicate their DNA and to synthesize large quantities of cell membrane constituents and proteins. The cancer-specific metabolic phenotype alters metabolic flux through key metabolic pathways such as glycolysis, glutaminolysis and fatty acid synthesis, to meet these needs. Although the aberrant glucose metabolism in cancer has been known for more than 80 years, its molecular background is still being elucidated. Interestingly, oncogenic signalling pathways that regulate cell proliferation are also linked to key metabolic pathways. Thus, abnormalities in these pathways both trigger cell growth and provide the necessary metabolic conditions at the same time. As cancer cells depend on altered metabolism for survival and proliferation, drugs targeting metabolic pathways are being pursued as anticancer therapies (Tennant 2009; Tennant 2010).

1.6.1 Glucose metabolism

A frequent abnormality of cancer is the altered glucose metabolism. Under aerobic conditions, normal cells use glucose as a substrate in oxidative phosphorylation to generate energy. Under anaerobic conditions, glucose is instead fermented to yield lactate, a process that generates 18-fold less energy in terms of ATP yield per invested

glucose molecule. In contrast, cancer cells convert glucose to lactate also under aerobic conditions, a phenomenon termed “the Warburg effect” (Warburg 1924). The reduced efficacy in energy production is compensated for through increased glucose uptake and glycolytic flux (Vander Heiden 2009). Increased aerobic lactate production is beneficial for cancer cells as it facilitates survival under hypoxic conditions, and as it generates energy without wasting carbon that is needed for synthesis of macromolecules. It has been proposed that the Warburg effect is an adaption to transient hypoxic conditions, providing the cancer cells with a biochemical tool for generating energy in the absence of sufficient oxygen to perform oxidative phosphorylation. However, it is also shown that leukemic cells, which are freely circulating and do not experience hypoxia, have abnormal glucose metabolism (Gottschalk 2004; Vander Heiden 2009). This is due to the specific effect of oncogenic mutations on the regulation of glycolytic enzymes. In most solid tumors, both direct oncogenic regulation and microenvironmental parameters dictate the glucose metabolism. The increased glycolytic flux and lactate production is exploited in characterization of cancer, both for diagnostic purposes and in therapy monitoring (Glunde 2010).

1.6.2 Choline metabolism

Phospatidylcholine (PtdCho) is an essential phospholipid and a major membrane constituent of mammalian cells. The rapid growth and proliferation of cancer cells require continuous rearrangement of cell membranes, and abnormalities in the synthesis and degradation of PtdCho is a typical biochemical alteration observed in cancer (Glunde 2006).

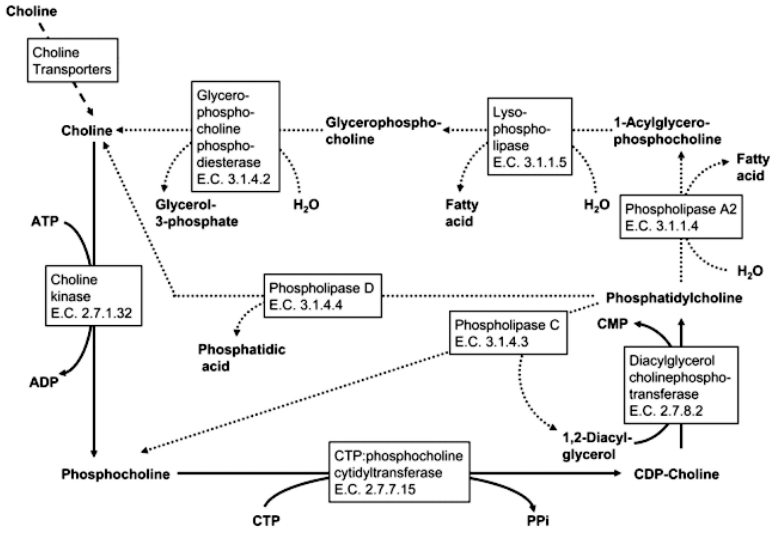

Figure 3 Choline metabolism

Biosynthetic (solid lines) and catabolic (dashed lines) enzymatic reactions in phosphatidylcholine metabolism. In cancer, the levels of choline, phosphocholine and glycerophosphocoline are often increased. Reproduced with permission (Copyright 2004) from American Association of Cancer Research (Glunde 2004).

Cancer cells frequently have increased concentration of choline-containing compounds (CCCs), including choline (Cho) and phosphocholine (PCho), which are precursors in the synthesis of PtdCho. The levels of these metabolites may decrease following successful treatment of tumors (Gillies 2005). CCCs are therefore useful biomarkers in diagnosis and management of cancer. The abnormalities in choline metabolism may be related to increased turnover of cell membranes during cancer cell proliferation, but it has also been suggested that oncogenic signaling pathways are directly linked to the PtdCho metabolism (Al-Saffar 2010; Beloueche-Babari 2006; Yalcin 2010). Drugs inhibiting phosphocholine synthesis have been shown to have antitumor activity (Lacal 2001).

1.7 Animal models of breast cancer

Several features of breast cancer can be studied using cancer cell cultures, including cell signalling, gene expression, metabolism and the effect of anticancer drugs. However, the heterogeneity of solid tumors, the impact of microenvironmental factors and interactions between cancer cells and stromal components are highly relevant parameters in cancer research. Through use of animal models of breast cancer, the interactions between cancer cells and their surroundings and the association between microenvironment and cancer cell phenotype can be studied. Breast cancer is a heterogeneous disease, and a variety of animal models have been established. In the context of multistage initiation and progression of breast cancer, these models have different strengths and limitations. No single animal model can mimic all aspects of the disease. Instead, optimal choice of model depends on the objective of the research. Breast cancer animal models are traditionally based on cultured human cancer cell lines (Lacroix 2004). Models based on breast cancer cell lines have provided a wealth of information about gene expression, signalling pathways and cancer cell proliferation. Established cell lines are easily cultivated, can be grown as xenografts in immunocompromised animals, and generally yield reproducible and quantifiable data. These cell lines are considered relevant to human disease as they are derived from human cancers. Although no single cell line is truly representative of human breast cancer, panels of cell lines can be used to model the heterogeneity of breast cancer. A limitation of such models is their monoclonal nature, as human breast cancers consist of a multitude of genetically distinct subpopulations of cells. Furthermore, only cell clones that have adapted to artificial culture conditions are represented. It should also be noticed that the most frequently used breast cancer cell lines are derived from advanced human cancers or metastatic tumors, and that they may not represent the most common types of breast cancer.

In order to establish more relevant models of cellular breast cancer heterogeneity, models based on transplanted primary patient tumor tissue (PPTT) have been established. Such models evidently bridge the gap between the original patient tumor and the *in vivo* model. It has been shown that these models maintain many key features of the primary patient tumor, including morphology and the molecular

signature (Bergamaschi 2009; Marangoni 2007). In contrast to models based on cultured cell lines, the response to therapy in PPTT-based models is closely correlated to the response of the parent tumor (Boven 1992). However, the transplantation efficiency is low, and the more aggressive breast cancer subtypes may be overrepresented in panels of PPTT-based xenografts (Marangoni 2007). A limitation of both cell line based and PPTT-based xenografts are the use of immunodeficient host animals, as the impact of the immune response on tumor progression is lost in these models.

For detailed examination of oncogenic transformation and tumorigenesis, genetically engineered mouse models (GEMM) have also proven valuable. Although cancer arising from mouse cells cannot recapitulate all aspects of human breast cancer, GEMM allow studies of relationships between oncogenic signalling and tumor initiation and progression. Initially, transgenic models were used to study inherited cancer syndromes, but development of more sophisticated multiallelic models mimicking spontaneous tumorigenesis has allowed more detailed examination of multi-step oncogenic transformation. However, such models have been difficult to adapt to translational cancer research due to long timelines and difficulty in establishing large cohorts (Heyer 2010). One possible advantage of GEMMs is that they are directly applicable to preclinical development of molecularly targeted drugs. The main disadvantage is the fact that although mice and humans develop cancer through similar mechanisms, species-specific phenotypes are frequently observed. Despite advances in genetic engineering, the most common subtypes of breast cancer are difficult to recapitulate in GEMMs (Vargo-Gogola 2007).

1.8 Magnetic resonance in biomedicine

The principles of nuclear magnetic resonance were discovered by Rabi, Purcell and Bloch in the 1940s, and have later found widespread use in modern medicine (Bloch 1946; Purcell 1946; Rabi 1938). Initially, the interaction between nuclei with spin angular momentum and a magnetic field was investigated as a physical phenomenon. During the 1950s, the methods had developed to allow studies of biological material. Using increasingly sophisticated methods, nuclear magnetic resonance has become a fundamental factor in modern medicine and biomedical research. Not only anatomical, but also functional and biochemical properties of biological specimens can be assessed due to the inherent versatility of the technique.

1.8.1 Principles of nuclear magnetic resonance

In a strong magnetic field, nuclei in possession of a spin angular momentum will align either with or against the magnetic field. The energy levels of these two orientations are slightly different, and at equilibrium the nuclei will have a magnetic moment proportional to the strength of the magnetic field and spin properties of the nuclei. The magnetic moment of the nuclei precess around the axis of the magnetic field with a frequency (ω_0) proportional to their gyromagnetic ratio (γ) and the magnetic field strength (B_0) according to equation (1), and this frequency is called the Larmor frequency.

$$\omega_0 = \gamma B_0 \qquad (1)$$

This aligned equilibrium can be perturbed by employing an additional magnetic field perpendicular to the static magnetic field (typically through a radiofrequent (RF) electromagnetic pulse). If the additional magnetic field oscillates with the same frequency as the Larmor frequency, the nuclei will be exited and their magnetic moment will change direction according to the properties of the RF pulse, while retaining its rate of oscillation. This phenomenon represents the “resonance” property of magnetic resonance spectroscopy and imaging. Following the excitation pulse, the magnetization will return to equilibrium through a process called relaxation. During

relaxation, the net magnetic moment gradually returns to its position aligned with the static magnetic field, and this process induces an electric current in a receiving electric coil. This electric current is the signal received in magnetic resonance experiments, and the amplitude, duration and shape of the signal depends on the properties of the exited sample. By mathematically resolving the signal, information about the composition of the sample can be extracted.

1.8.2 Magnetic resonance spectroscopy (MRS)

Due to minuscule field inhomogeneities caused by the local chemical environment, the resonance frequency is not identical for all the nuclei. Importantly, shielding electrons in the environment reduce the magnetic field experienced by the nuclei, thereby reducing the resonance frequency. Nuclei located in various positions in biomolecules resonate at different frequencies, providing information on the chemical content of a sample. This phenomenon is known as chemical shift. Closely located nuclei also influence each other through spin couplings, resulting in the splitting of a signal into multiple peaks, in characteristic patterns depending on the nature of the coupling interactions. These patterns provide highly specific structural information. The combined effects of chemical shift and coupling constants allow identification of different chemical entities in biological specimens using magnetic resonance spectroscopy (MRS). As signal strength is proportional to the number of protons that were excited by the RF pulse, quantification of metabolites in the spectra may be possible provided that a suitable internal or external calibration standard is used. In biomedicine, the most commonly studied nucleus is ^{1}H, due to its high natural abundance in biological specimens and its inherent high magnetic resonance sensitivity. A wide range of biomolecules can be detected using ^{1}H MRS. However, other nuclei such as ^{13}C, ^{15}N, ^{19}F and ^{31}P may also be utilized for special applications. The use of such heteronuclei depends on the same physical phenomena, but requires customized experimental protocols that are adapted to the inherent magnetic resonance sensitivity and Larmor frequency of the nuclei.

Ex vivo magnetic resonance spectroscopy

In order to improve the spectral resolution in MRS of biological tissues, biopsies may be sampled and analyzed in high-field spectrometers. The better sensitivity, higher field strength and improved field homogeneity is improved compared to *in vivo* MRS. However, anisotropic interactions are still present. By spinning the sample at an angle of 54.7° (the magic angle) to the static magnetic field, these interactions are averaged out, producing signal lines comparable to those achieved in *in vitro* MRS of solutions. This method has been termed high resolution magic angle spinning MRS (HR MAS MRS) and is a useful tool for analysis of intact tissue specimens. The method has been widely applied in studies of cancer metabolism, as information on a large number of metabolites can be obtained. In addition, the simple sample preparation and the availability of the sample for subsequent analyses are advantages of HR MAS MRS (Moestue 2011b).

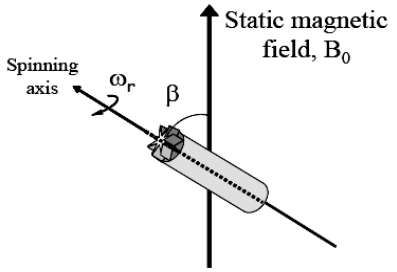

Figure 4 Schematic presentation of Magic Angle Spinning.

The rotor is oriented at an angle (β) of 54.7° to the static magnetic field (B_0). The rotor spins around its own axis with a spin rate of ω_r. Reproduced with permission from Beathe Sitter, MR Cancer Group, NTNU.

In vivo magnetic resonance spectroscopy

In magnetic resonance spectroscopy of homogenous biological specimens such as cell extracts or intact cultured cells, information on the localization of the different metabolites is not needed. However, when MRS is performed in living subjects, it is frequently of interest to obtain metabolic information from a distinct organ or other tissue of interest, such as a solid tumor. Localized excitation of nuclei is therefore the most frequently used approach in *in vivo* MRS. This can be achieved using the principles of magnetic resonance imaging, where spatial information is added to the data through use of magnetic field gradients. By applying gradients to the static

magnetic field, the Larmor frequency becomes a function of localization in the field. This allows localized excitation of nuclei through specialized, spatially selective pulse sequences such as the PRESS sequence (a 90° RF pulse followed by two 180° RF pulses, all along perpendicular axes). The localization techniques can be used to delineate one well-defined voxel (single-voxel MRS) within the tissue of interest. Alternatively, multiple voxels can be defined in single or multiple slices. This allow spectroscopic mapping of the tissue of interest, and is referred to as MR spectroscopic imaging (MRSI) or chemical shift imaging (CSI).

In order achieve a high spectral resolution in *in vivo* MRS, it is important with a highly homogenous static magnetic field. High field strength also improves the separation of metabolites, as the difference in resonance frequency is proportional to field strength. Still, the spectral resolution *in vivo* typically allows identification of a limited number of metabolites.

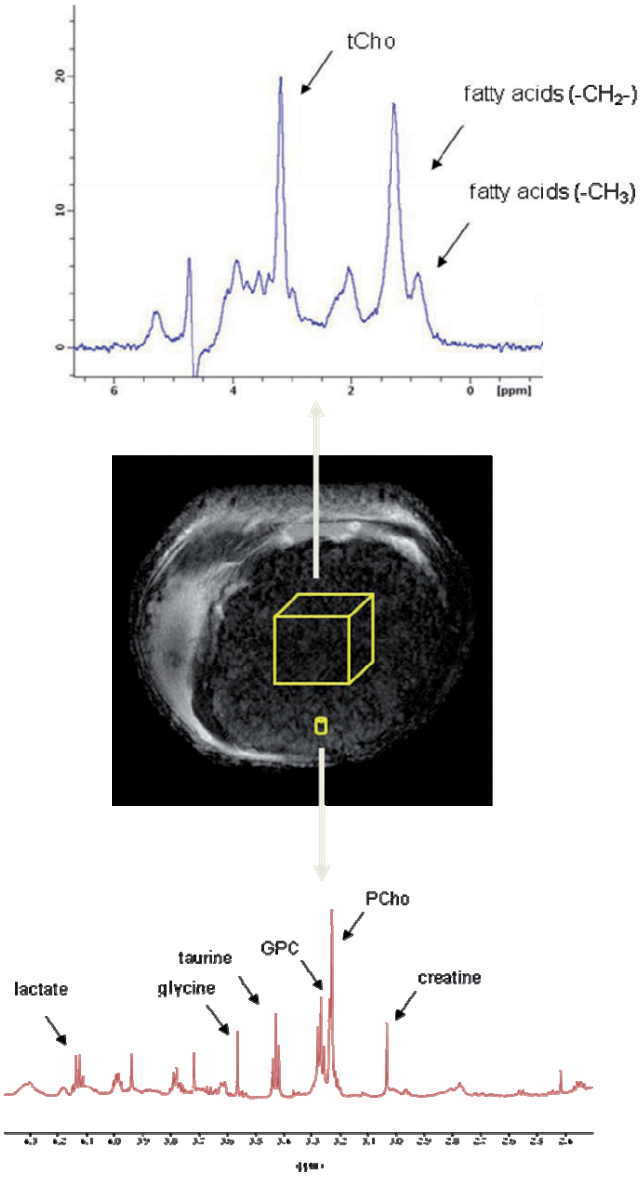

Figure 5 Spectral resolution in *in vivo* and *ex vivo* MR spectroscopy

Following the acquisition of an anatomic MR image (middle), a localized volume of interest for spectroscopic assessment can be defined within the tumor (represented by the yellow voxel). The *in vivo* MR spectre (top) represents the signal obtained from this voxel. Harvesting a biopsy (represented by the yellow cylinder) from this tumor allows acquisition of an *ex vivo* spectrum at higher field strength (bottom). Image and spectra were obtained in a xenograft model of luminal-like breast cancer (MAS98.06). The *in vivo* spectrum was obtained in a 7T small animal scanner (PRESS sequence, voxel size: 3 x 3 x 3 mm, scan time: ca 6 min). The *ex vivo* spectrum was obtained from a 15-mg biopsy from the same tumor, analyzed using HR MAS MRS on a 14.1T spectrometer (CPMG sequence, scan time: ca 6 min). Some typical metabolites are identified in both spectra. Reproduced with permission from Moestue *et al* Mol Oncol 2011; 5 (3); 224-241.

Analysis of MRS data

In order to use MRS data, the signal at different resonance frequencies has to be assigned to the correct biomolecules. Analyses of reference standards in solutions can be used to generate a library of spectra representing candidate molecules. Careful matching of reference spectra with spectra from biological samples is used to identify the peaks. In some cases, multidimensional spectroscopy is needed to confirm the identity of metabolites which resonate with similar frequency.

The MRS signal is proportional with the metabolite concentration (taking the number of protons in each metabolite into account). Therefore, the metabolite concentrations can be quantified. The first step in this process is determination of the area under each metabolite peak. Due to variation in peak width between spectra, the peak area is a more accurate measure of metabolite concentration than the peak height. This can be done using polynomial regression or other approaches that translate the peaks of the spectre into a mathematical function.

Analyzing the ratios between different peak areas can provide valuable information. In *in vivo* MRS, this is the most commonly used method for analyzing the spectra. For absolute quantification of metabolite concentration it is more common to use a reference with known concentration. A commonly used approach is to determine the area of the water peak in the spectre and then experimentally determine the water content of the tissue. Assuming that the water content in tissue is constant, this method has been applied to *in vivo* MRS. *Ex vivo* and *in vitro*, an external reference standard can be added to the sample in known concentration before analysis. Recently, a method for introducing an electronic reference signal into the spectra has been introduced (ERETIC) (Barantin 1997). Calibrating this reference signal to reference standards allow direct quantification of metabolite concentrations. Finally, if the stability of the spectrometer is high enough, the peaks in the spectra can be assumed to be directly proportional to the metabolite concentration as long as the acquisition parameters remain constant. Thus, the areas can be directly calculated based on a calibration standard curve obtained from a reference standard solution (Pulcon) (Wider 2006).

1.8.3 Magnetic resonance imaging (MRI)

As magnetic resonance signal strength depends on the composition of a biological specimen, reconstruction of magnetic resonance data into images representing anatomy is a widely used modality in medical imaging. Magnetic resonance imaging (MRI) requires the use of magnetic field gradients in at least three directions (often termed the x-, y- and z-axis, where the z-axis is parallel to the static magnetic field B_0), allowing spatial encoding of the emitted signal. By superimposing a field gradient parallel to the static magnetic field B_0, the resonance frequency of the protons becomes a function of their position along the field. This allows selective excitation of a tissue slice, defined by the frequency of the RF-pulse. Application of a phase encoding gradient and a readout gradient along the x- and y- axis give the relaxing protons a phase shift depending on their location along the x-axis and a frequency depending on their location along the y-axis. The detected signal is complex and can be expressed as a function of spatial frequencies in the x,y-plane. The longitudinal magnetization in each position of the exited slice can be calculated through Fourier transformation, allowing reconstruction of an image.

By taking the magnetic properties of protons into account in the excitation sequence, images with different type of contrast can be acquired. Both the proton density, the longitudinal relaxation rate (*T1*) and the transversal relaxation rate (*T2*) are tissue-dependent parameters. In *T1* and *T2*-weighted images, the contrast represents differences in *T1* and *T2* in the imaged tissue, respectively. *T1* and *T2* can be modulated using contrast agents, further increasing the ability of MRI to differ between various tissues. Some contrast agents, including gadolinium complexes, cause concentration-dependent reduction of *T1*. This leads to higher signal intensity in tissue with high concentration of contrast agent. Other contrast agents, such as iron oxide particles, cause concentration-dependent reduction in *T2* and lower signal intensity in tissues with high concentration of contrast agent. In both cases, differences in contrast agent concentration between tissues increase the contrast in MR images.

Besides anatomical imaging, MRI can also be used to visualize functional properties of tissue. In cancer, diffusion-weighted MRI (DW-MRI) and dynamic contrast-enhanced MRI (DCE-MRI) are the most frequently used techniques.

DW-MRI

Diffusion-weighted MR imaging is a technique that allows measurement of random thermal movement of water molecules (diffusion). As diffusion depends on the amount of macromolecular barriers (cell membranes, stromal macromolecules), DW-MRI provides information on the cellular density of tissues. This information is relevant in medical imaging, as the water diffusivity in pathologic tissue may differ from normal tissue. Tissue with high cellular density (and therefore low water diffusivity) is frequently observed in solid tumors. Response to treatment may cause changes in diffusivity, allowing the use of DW-MRI both in diagnosis and treatment monitoring of cancer (Padhani 2009; Padhani 2011). As the signal in MRI depends on the location of protons, carefully designed pulse sequences can be used to indirectly measure the diffusivity of water. These sequences utilize a pair of bipolar gradients, often termed Stejskal-Tanner gradients, which sensitizes the signal to net displacement of water molecules during the imaging sequence (Stejskal 1965). The gradients are applied before and after the 180° pulse in a spin-echo sequence. Protons that move in the interval between these gradients will gain a net phase shift, causing a loss of signal. The signal loss depends on the strength and duration of the diffusion gradients, and the time interval between the gradients. The accumulative effect of these parameters is reflected in the *b*-value. The relationship between the *b*-value and the signal intensity (SI) is defined as:

$$\mathrm{SI} = \mathrm{SI}_0 \cdot \mathrm{e}^{-\mathrm{b}\cdot\mathrm{ADC}} \tag{2}$$

where SI_0 is the signal intensity without application of diffusion gradients and ADC is the apparent water diffusivity. By performing experiments with variable *b*-values, the ADC can be calculated through exponential curve fitting of the resulting signal intensities. The diffusion gradients are usually applied in three orthogonal directions, to average out potential anisotropy. In tissues where water molecules diffuse freely,

the movement causes a signal loss and the tissue appears with low signal intensity in the diffusion-weighted images. Conversely, densely packed tissue has low ADC and appears with high signal intensity.

DCE-MRI

In dynamic contrast enhanced MRI a series of images with identical geometrical orientation is acquired before and after intravenous injection of a contrast agent. Following injection, the distribution of contrast agent depends on tissue perfusion and the rate and extent of contrast agent extravasation. Contrast agents in clinical use are often based on paramagnetic elements such as gadolinium or manganese. Gadolinium shortens *T1* relaxation time and increases signal intensity in *T1*-weighted MR images, but gadolinium ions are highly toxic. When complexed or bound to a carrier molecule, the magnetic properties are retained whereas toxicity is minimized. Most commercial gadolinium-containing contrast agents have similar pharmacokinetics, with rapid distribution to extracellular (but not intracellular) fluid and renal excretion of the contrast agent. Several different imaging sequences can be used in DCE-MRI, all with different advantages and disadvantages. The spin-echo sequence is time-consuming but has the advantage of a linear contrast agent concentration/signal intensity relationship (Larsson 1990). The signal intensity (SI) for a spin-echo sequence follows equation (3):

$$SI \propto \rho \cdot \left(1 - e^{\frac{-TR}{T1}} \right) \cdot e^{\frac{-TE}{T2}} \tag{3}$$

where ρ is the proton density, TR the repetition time, TE the echo time, and *T1*/*T2* are the longitudinal and transverse relaxation times, respectively. By choosing a short echo time, the sequence will be *T1*-weighted and the signal intensity will be strongly dependent on contrast agent concentration. The *T1* relaxation rate is related to the contrast agent concentration (C) and relaxivity (r_1), according to equation (4):

$$\frac{1}{T1} = \frac{1}{T10} + r_1 \cdot C \tag{4}$$

where *T10* is the longitudinal relaxation time in the absence of contrast agent. The pre-contrast longitudinal relaxation time therefore has to be measured prior to the DCE-MRI acquisition, for example by varying the repetition time in a spin-echo sequence.

The change in contrast agent concentration over time is reflected in the series of MR images. This allows analysis of temporal and spatial components of contrast agent distribution between tissue compartments. In solid tumors, blood vessels are typically leaky, allowing rapid extravasation compared to surrounding tissue. In breast cancer, it was early demonstrated that DCE-MRI can differentiate between benign and malignant lesions, and that tumor size measured using DCE-RMI correlates well to pathologic tumor size (Gribbestad 1992). The use of DCE-MRI in breast cancer management has later expanded to include staging, screening of patients at high risk, monitoring of treatment response, and follow-up after surgery and radiotherapy (Turnbull 2009).

Analysis of DCE-MRI data

Signal intensity/time curves obtained from DCE-MRI acquisitions can be evaluated both empirically and numerically. Empirical methods are simple and robust, whereas numerical methods often can provide additional functional information. Due to their simplicity, empirical methods are frequently used in the clinic. Parameters derived from signal intensity/time curves include area under the signal intensity curve (AUC), relative signal intensity (RSI) and time to peak concentration (TTP).

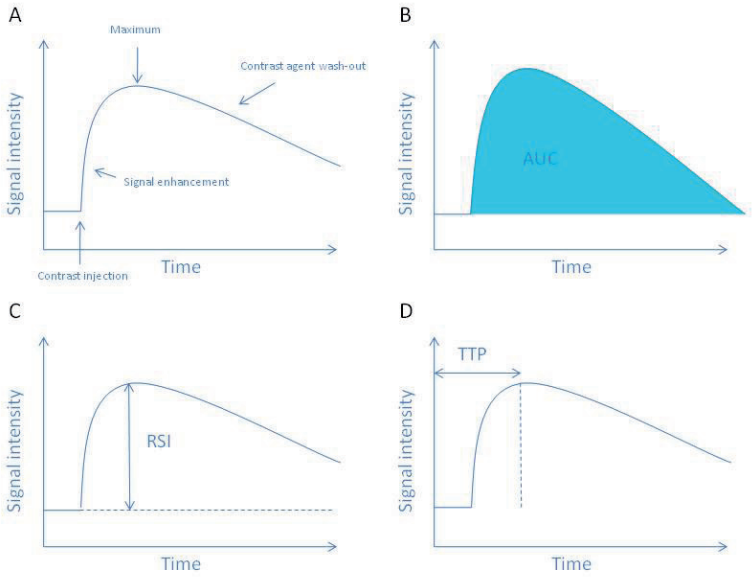

Figure 6 Empirical analysis of signal enhancement curves

Signal enhancement curves from DCE-MRI consist of several phases (A). The area under the curve (AUC) is illustrated in (B). Partial AUCs can also be calculated. In (C), the signal increase relative to baseline (RSI) is illustrated. It can also be calculated at a fixed time point. Time to peak (TTP) is the time to reach the intensity maximum from the time point of injection (D).

High AUC and RSI values combined with short TTP indicate rapid and extensive extravasation of contrast agent, suggestive of malignant disease. In addition, the curve shape in each voxel can provide information on the aggressiveness of the tumor. A rapid increase and decline in contrast agent concentration is frequently associated with aggressive disease, whereas slow and persistent increase is a typical feature of necrosis and benign breast lesions.

Through pharmacokinetic modelling of the contrast agent concentration, the vascular function of tumors can be quantitatively evaluated. By fitting a mathematical model to the signal intensity/time curve, the rate and extent of contrast agent transport from the blood and into the extravascular extracellular space (EES) can be estimated. Gadolinium complexes are extracellular tracers, and the contrast agent is therefore restricted to the plasma volume and the EES. Immediately following injection, it is

assumed that the contrast agent is evenly distributed throughout the entire plasma volume. Then, it is rapidly distributed into the EES, reaching a distributional equilibrium. Finally, a slower decline in plasma contrast agent concentration due to renal excretion is observed. The association between arterial and tissue concentration of contrast agent over time is shown in Figure 7.

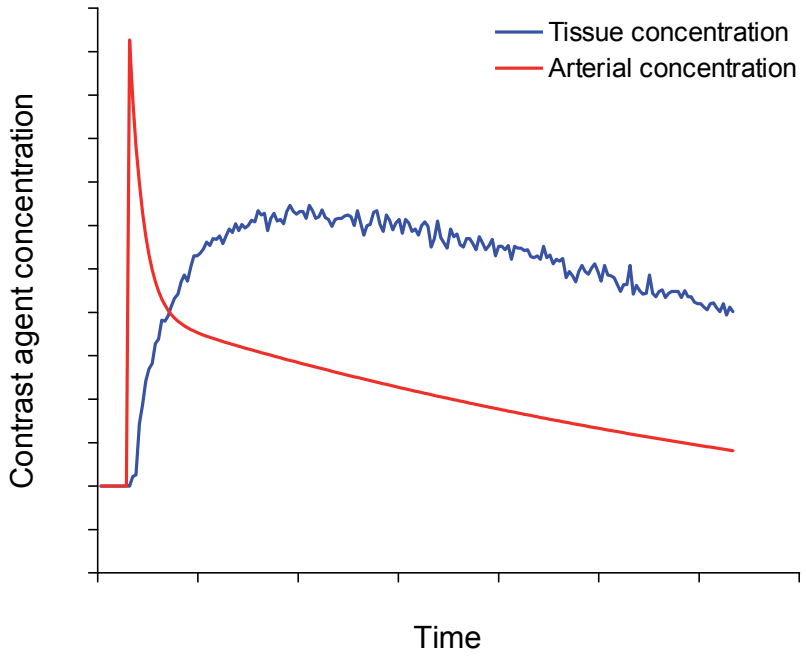

Figure 7 Arterial and tissue contrast agent concentrations.

It is assumed that the contrast agent mixes into the entire plasma volume immediately after injection. The contrast agent then distributes into tissue at a rate determined by blood flow and extraction fraction. Later, the contrast agent is renally eliminated from the blood, which is reflected in declining tissue contrast agent concentration.

The rate of contrast agent transfer (K^{trans}) between the plasma volume and the EES depends on the concentration difference between these two compartments, the blood flow and the permeability surface product of the vascular bed, and is described by equation (5):

$$K^{trans} = E \cdot F \cdot \rho \cdot (1 - Hct) \tag{5}$$

where E is the extraction fraction, F is blood flow, ρ is tissue density and Hct is the hematocrit. The two-compartment pharmacokinetic model for contrast agent concentration also requires knowledge about the amount of contrast agent that is supplied to the tissue of interest, also known as the arterial input function (AIF). The plasma concentration of extracellular contrast agents over time is typically described by a biexponential function:

$$C_p(t) = D \cdot (A \cdot e^{-at} + B \cdot e^{-bt}) \tag{6}$$

where D is the contrast agent dose, A and B are the amplitudes of each exponential component, and a and b are their respective rate constants. For accurate estimation of contrast agent pharmacokinetics, the AIF should ideally be measured in an artery supplying the tumor in each individual subject during DCE-MRI acquisition. However, this is not always achievable, and an AIF representative for the entire study population is often used instead. The total tissue concentration of contrast agent (C_t) can be expressed as a function of time (t) (6):

$$C_t(t) = v_p C_p(t) + K^{trans} \int_0^t c_p(t') \cdot e^{K^{trans}(t-t')/v_e} dt \tag{7}$$

where v_p is the volume fraction of blood plasma, C_p is the concentration of contrast agent in the blood plasma, K^{trans} is the volume transfer constant between plasma and EES and v_e is the volume fraction of EES (Tofts 1999). Taking the AIF into account, this model allows calculation of contrast agent concentration in the vascular space and the EES, as well as the rate of transfer between the two compartments.

1.9 MR in breast cancer

As MRI and MRS can provide both anatomical and functional information, these techniques are useful tools both in basal breast cancer research and for clinical breast cancer management. Morphology, vascular function and cellular density of breast tumors can be evaluated using MRI, whereas MRS has been widely used for assessment of breast cancer metabolism. In the following section, the clinical role of MRI and MRS in breast cancer is discussed, as well as the most common applications of MRI and MRS in preclinical cancer research.

1.9.1 Current clinical status of MR in breast cancer

The use of MRI in breast examinations is rapidly increasing, despite a lack of clear evidence of its value in preventing breast cancer deaths. MRI using low-molecular Gd-based contrast agents is currently the most used method in breast MR examinations. This is a sensitive, but only moderately specific method. However, the performance of MRI in various clinical settings has been thoroughly examined, and its current clinical use in screening of high-risk populations and in preoperative treatment planning is therefore justified. Future use of MRI and MRS in breast cancer management is likely to include a combination of several different methods in each patient examination. This allows both morphological and functional assessment of the pathology, which in general has been shown to increase sensitivity and specificity of the examination (Sardanelli 2011).

1.9.2 MRI in breast cancer

Diagnosis and staging

Contrast-enhanced MRI is a more sensitive method for detection of breast tumors, including DCIS and multifocal tumors, than X-ray mammography (XRM) (Sardanelli 2010; Schnall 2005). Based on this, MRI is used for staging and treatment planning of newly diagnosed breast cancer. Overall, MRI has been reported to have a positive impact on the choice of surgical procedure in approximately 10% of cases (Sardanelli 2010). Population-wide screening for breast cancer is currently performed using

XRM, and MRI is not considered to be cost-effective enough to be used for this purpose. However, in high-risk populations, MRI is increasingly used in screening for lesions. MRI has high diagnostic sensitivity compared to other imaging modalities, and it is recommended that carriers of BRCA1/BRCA2 mutations or first-degree relatives of carriers should undergo annual MRI screening (Mann 2008; Norsk bryst cancer gruppe (NBCG) 2011). Contrast-enhanced MRI has also been suggested for evaluation of response to neoadjuvant therapy (NAC). In this setting, the aim is to downstage the tumor from inoperable to operable, or from a size that dictates radical mastectomy to a size that allows breast-conserving surgery. MRI is useful in surgery planning following completion of NAC, but may also be considered for early prediction of response to NAC and prediction of survival. Response monitoring in NAC may be an important application for MRI, as 10 - 20% of patients (depending on treatment regimen and response criteria) are classified as non-responders (Buchholz 2003). Rapid monitoring of treatment effect would allow discontinuation or change of treatment regimen or re-planning of surgical treatment. MRI is a more accurate tool for monitoring effect of NAC than XRM or ultrasound, and provides a better basis for surgical planning than these modalities (McLaughlin 2011a). The utility of MRI in early assessment of response to NAC and on long-term outcome needs to be further investigated, as the heterogeneity of breast cancer and the variety of drugs used in NAC regimens are not yet fully accounted for (Sardanelli 2010). As an example, it has been reported that MRI following bevacizumab-containing NAC in HER-2 negative breast cancer causes underestimation of the residual tumor mass (Chen 2008).

DW-MRI

The majority of MRI examinations are performed using contrast-enhanced T1-weighted imaging. However, several studies have demonstrated that DW-MRI also can detect malignant breast cancer lesions. More interestingly, addition of DW-MRI to the imaging protocol has been demonstrated to increase the diagnostic value of breast MRI (Ei Khouli 2010; Kul 2011; Partridge 2009). As benign lesions in general have higher ADC values than malignant lesions, DW-MRI tends to increase the specificity of breast MRI examinations. It has also been demonstrated that morphological changes after NAC are preceded by increased ADC values (Ei Khouli

2010; Pickles 2006). This suggests that ADC may have potential role as an early marker for response to NAC. It has also been reported that pre-treatment ADC values may have predictive value (Park 2010). In animal xenograft models of breast cancer, DW-MRI has been used to demonstrate efficacy not only of classical chemotherapeutics, but also by molecularly targeted drugs (Aliu 2009; Kim 2008).

DCE-MRI

As breast cancer MRI examinations generally depend on Gd-chelate based contrast agents for tumor delineation, a DCE-MRI protocol can be included with relative ease. However, care must be taken to balance the need for both high temporal resolution and high spatial resolution. The choice of protocol dictates how the data should be analyzed. In order to perform pharmacokinetic modelling of the contrast enhancement, high temporal resolution is generally needed. Semiquantitative methods are less dependent on temporal resolution, and can contribute positively to increased sensitivity and specificity in lesion detection and differentiation. The trade-off between spatial and temporal resolution has been studied by Kuhl et al by direct comparison of two different DCE-MRI protocols in the same patient cohort (Kuhl 2005). This study demonstrated that a low temporal resolution caused loss of diagnostically relevant information. However, the protocol with high spatial resolution had a significantly better diagnostic performance, suggesting that that delineation of tumor margins and visualization of internal tumor architecture was important factors for the readers of the images. It has also been suggested that DCE-MRI increases the performance of staging examinations due to its ability to detect small lesions and intraductal spread (Hata 2004). However, despite the number of studies demonstrating that DCE-MRI increases diagnostic accuracy in small patient populations, a multicentre trial including 1623 women with newly diagnosed breast cancer demonstrated that inclusion of DCE-MRI to the diagnostic regimen did not have a measurable impact on the number of re-operations needed (Turnbull 2010). This suggests that DCE-MRI should be used as an additional examination in carefully selected cases rather than as a standard method for staging of tumors.

DCE-MRI may also be used in assessment of response to NAC. In addition to tracking anatomical and morphological changes, functional indicators for early response monitoring have been evaluated in clinical trials. The response may be

predicted based on the pre-treatment MRI examination, or based on changes between pre-treatment and early post-treatment MRI examinations (Heldahl 2010; Pickles 2005; Pickles 2009).

Breast cancer with rapid wash-out of contrast agent in the pre-treatment MRI examination is associated with positive response to NAC (Heldahl 2010). It has also been found that breast tumors with high levels of perfusion and vessel permeability before NAC are associated with shorter overall survival (Pickles 2009). Reduction of tumor volume determined by early post-treatment DCE-MRI has been found to predict response to NAC (Heldahl 2010; Padhani 2006). Semi-quantitative analysis of contrast agent pharmacokinetics has also been investigated, and a reduction in mean RSI has been described in responders (Johansen 2009). Several studies using compartmental modeling of DCE-MRI data have demonstrated that decrease in K^{trans} and the amplitude of signal enhancement is associated with a favorable response to therapy (Pickles 2005; Turnbull 2009). The optimal time-point for performing follow-up DCE-MRI is still debated (McLaughlin 2011b).

Antiangiogenic treatment

As DCE-MRI measures vascular function, there has been particular interest in assessment of response to antiangiogenic therapy. A reduction in neoangiogenesis caused by bevacizumab or other antiangiogenic agents should produce fewer and less leaky tumor blood vessels, which would be reflected in the contrast enhancement pattern observed by DCE-MRI. Two different studies have demonstrated reduced K^{trans} or AUC_{1min} after bevacizumab therapy, an effect that has been shown to be additive to concomitant administration of docetaxel (Baar 2009; Wedam 2006). The reduction in contrast enhancement mostly occurred during the first cycles of NAC, and was not correlated to clinical or pathological response.

1.9.3 MRS in breast cancer

Abnormal choline metabolism is found in breast cancer as well as in several other cancers, and MRS can be used to detect the presence of the choline-containing compounds glycerophosphocholine (GPC), phosphocholine (PCho) and choline. In clinical MRS examinations, the signal from these metabolites overlap considerably

and the readout parameter is therefore their cumulated signal at 3.2 ppm, denoted total choline (tCho). In healthy breast cancer tissue, a tCho peak is normally not found. In benign lesions, tCho is also absent or very low. A high tCho peak is therefore associated with malignant disease (Gillies 2005). A meta-analysis of five studies, including 100 malignant and 53 benign lesions demonstrated a sensitivity of 83% with a specificity of 85%, suggesting the possible utility of MRS as a diagnostic tool (Katz-Brull 2002a). However, MRS performance is associated with tumor size, and for small lesions the sensitivity of the method is significantly decreased (Tozaki 2009). This is considered to be related to the sensitivity of MRS at 1.5 T rather than an intrinsic metabolic property of small tumors (Katz-Brull 2002a). The low sensitivity is also thought to be a problem for reliable use of MRS in monitoring response to NAC (Haddadin 2009). Accurate therapy monitoring is also complicated due to the complex changes that are observed in individual choline-containing metabolites, which depend on both the tumor type and the treatment (Beloueche-Babari 2010b). Technical improvements, including MRS at 3 T or MRSI examinations may increase specificity, but the role of MRS in breast cancer examinations remains unresolved (Jagannathan 2009).

1.9.4 MRI in preclinical cancer research

The applications for MRI and MRS in cancer are continuously being extended and improved through the use of animal models. In particular, MR is used in order to understand the biology of tumors and to describe various biological characteristics. Using parametric maps, microenvironmental features such as necrosis, hypoxia and intratumoral fluid pressure can be mapped using MRI (Bhujwalla 2002; Egeland 2009; Gulliksrud 2009). Knowing how these microenvironmental parameters differ between various cancer subtypes, it has been suggested that MRI holds the potential to discriminate between different cancer subtypes or to predict tumor aggressiveness (Bhujwalla 2001; Wu 2009). One of the fields that have received most attention is how DCE-MRI can be used to monitor changes in vascular function following various interventions. Performing DCE-MRI in animal models may be technically challenging due to motion artefacts and small lesions, but on the other hand it offers advantages in terms of reproducibility and flexibility and the possibility to use contrast agents that

are not clinically available. The vascularization of xenografted tumors may in some aspects differ from that of human tumors, but the responses to therapy observed in animal models may still be clinically relevant.

The effect of chemotherapy and radiotherapy in xenograft models can be monitored using DCE-MRI, supporting the use of this technique in monitoring response to therapy (Jensen 2010; Rofstad 2009). Efforts have also been made to co-register DCE-MRI data with histological data or functional *in vivo* measurements in order to understand how tumor biology is reflected by the DCE-MRI parameters (Ellingsen 2009; Ellingsen 2010; Gulliksrud 2011). In the last decade, DCE-MRI has been used for monitoring response to antiangiogenic drugs, thereby contributing to increased understanding of the effects of these drugs. The importance of angiogenesis in cancer was first suggested in the 1970's (Folkman 1971). It took nearly 20 years before the angiogenic growth factor VEGF was described, but this lead to an explosive interest in this as a druggable anticancer target (Leung 1989). This has culminated in the development of several clinical angiogenesis inhibitors such as the specific anti-VEGF antibody bevacizumab and receptor tyrosine kinase inhibitors such as sorafenib and sunitinib (Levitzki 2010). Bevacizumab as well as numerous new drug candidates either inhibiting angiogenesis or causing disruption of newly formed blood vessels (vascular disrupting agents) have been evaluated in animal models of cancer. Through the use of macromolecular contrast agents, microvascular leakiness and fractional plasma volume are readily assessed. Such contrast agents are too large to leak out of normal capillaries, but can cross the endothelial lining of immature tumor blood vessels. Following antiangiogenic therapy, the transfer of macromolecular contrast agents from the vasculature to the interstitial space is greatly reduced. Although these contrast agents are not approved for clinical use, they are useful tools in evaluating the biological activity of potential antivascular drug candidates (Padhani 2003). Using this approach, the effect of bevacizumab has been studied in several different cancer models (Preda 2004; Turetschek 2004). In addition, drugs targeting other molecular pathways may also indirectly inhibit angiogenesis. As an example, drugs inhibiting the PI3K/Akt/mTOR axis have been shown to both reduce proliferation of cancer cells and to reduce neoangiogenesis, possibly due to inhibition of downstream targets such as HIF-1 (Lane 2009; Schnell 2008; Schwartz 2010). The effect of vascular

disruption agents such as combretastatin A4 phosphate can also be monitored using DCE-MRI. These agents typically cause a rapid (within a few hours) decline in K^{trans} due to a decrease in the number of functional blood vessels and reduced blood flow (Galbraith 2003).

1.9.5 MRS in preclinical cancer research

Breast cancer typically exhibits most characteristics of a cancer-specific metabolic phenotype, with abnormal glucose metabolism and elevated levels of CCCs. Therefore, the metabolism of breast cancer has been extensively studied using both *in vitro*, *ex vivo* and *in vivo*. This is in part due to the potential use of metabolites as prognostic or predictive biomarkers, or in assessment of response to therapy. Another reason for the interest in the abnormal metabolism is the direct link between oncogenic signalling and regulation of metabolic pathways, suggesting that metabolic pathways may contain potential new drug targets.

Initial studies in animal models used ^{31}P MRS to demonstrate the differences between tumors and normal tissue with respect to phosphorous-containing metabolites (Griffiths 1982). These experiments suggested that MRS indirectly can describe the microenvironment of tumors. By determining the chemical shift of inorganic phosphorous, the tumor pH can be determined. The presence of high phosphomono- and -diesters was also noticed. Through ^{1}H MRS of cultured breast cancer cells it has been shown that malignant transformation is strongly associated with high concentrations of phosphocholine (PCho) (Eliyahu 2007b; Glunde 2004). The metabolic flux in the choline pathway has also been studied *in vitro* using ^{13}C-enriched choline as a tracer, demonstrating that choline uptake and conversion of choline into PCho is upregulated in breast cancer. Conversion of PCho to PtdCho is not upregulated, suggesting that the abnormal choline metabolism does not contribute to increased synthesis of cell membrane constituents (Katz-Brull 2002b). In fact, PtdCho catabolism by phospholipase C contributes to increased PCho concentration in breast cancer cells but not in immortalized human mammary epithelial cells. However, substantial GPC contributions to the tCho signal have been observed both in xenograft models and in human biopsies analyzed *ex vivo*, suggesting that microenvironmental or genetic/epigenetic factors are likely to be important factors in

determining the choline metabolite pattern (Moestue 2010; Sitter 2006). This is also illustrated by discrepancies between studies using the same breast cancer cell lines, suggesting that experimental conditions may have a large impact on the choline metabolism *in vitro*. The abnormal choline metabolism has traditionally been linked directly to the increased proliferation rate of cancer cells (Podo 1999). However, recent studies have also suggested a close relationship between oncogenic signalling pathways and the regulation of the PtdCho cycle, suggesting that choline metabolites under given conditions may function as oncometabolites (Yalcin 2010).

Although the regulation of choline metabolism *in vivo* is not completely understood, tCho has been suggested a clinically relevant biomarker for response to treatment both with anticancer drugs and radiotherapy. This is predominantly thought to be caused by a reduction of PCho concentrations following successful treatment. Studies of animal models and cultured cancer cells have suggested that choline metabolite responses to therapy are complex. First, the contribution of GPC to the tCho signal should be taken into account. Following treatment with antimicrotubule drugs, a marked increase in GPC concentrations has been demonstrated (Sterin 2001). Increased GPC concentrations have also been demonstrated after treatment with the heat shock protein 90 inhibitor 17-AAG, the Bcr-Abl inhibitor imatinib and the PI3K inhibitor LY294002 (Beloueche-Babari 2006; Beloueche-Babari 2010a; Gottschalk 2004). A treatment-induced increase in GPC concentration could lead to misinterpretation of changes in the tCho levels in cancers where GPC concentrations are in the same order of magnitude as PCho. Second, PCho concentrations have been shown to increase following treatment with 17-AAG or histone deacetylase inhibitors such as SAHA or LAQ824 (Chung 2003; Chung 2008; Sankaranarayanapillai 2006). Based on the data obtained *in vitro* and in animal models it is therefore not necessarily appropriate to associate a favorable treatment outcome with decreased tCho signal intensity.

MRS has also been used to study glucose metabolism in various model systems. Using ^{13}C-enriched glucose as tracer, regulation of both glucose and glutamine metabolism in cancer has been studied (Portais 1996). This allows both *in vitro* and *in vivo* studies of how various anticancer treatments reduce the rate of glucose utilization

(Gottschalk 2004; Neeman 1989). Using *ex vivo* MRS, the improved sensitivity and spectral resolution allows detailed analyses of ^{13}C-labeled tracers and their downstream metabolites. Regular ^{13}C MRS has too low sensitivity to be directly translated to clinical applications. However, using a process called dynamic nuclear polarization (DNP), tracers may be hyperpolarized prior to injection, resulting in more than 10.000-fold in sensitivity. This allows dynamic magnetic resonance spectroscopy imaging, which has been used to study the reaction rates of key metabolic steps in cancer. The most widely used tracer is [1-^{13}C] pyruvate, which is converted to [1-^{13}C] lactate by the enzyme lactate dehydrogenase (LDH). In cancer, this conversion typically takes place at a higher rate than in normal tissue, and the rate of lactate production can therefore be used as a diagnostic tool or to monitor response to therapy (Brindle 2008; Golman 2006). This method is considered clinically applicable and may prove highly useful for detection and characterization of cancer in the future.

2 Objectives

The main objectives of the research presented in this thesis were to:

- characterize orthotopic xenograft models of luminal-like and basal-like breast cancer using MRI and MRS.

- identify MR-derived parameters associated with breast cancer aggressiveness using the xenograft models.

- examine the relationship between metabolite profiles and expression of genes involved in regulation of metabolic pathways.

- examine the relationship between histopathological analyses of vascularity and contrast agent kinetics in luminal-like and basal-like xenografts.

- use MRI to assess changes in vascular function after antiangiogenic treatment.

3 Materials and methods

3.1 Animal model

The MAS98.12 and MAS 98.06 orthotopic xenograft models were previously established by surgical implantation of primary breast carcinomas in to the mammary fat pad of immunodeficient mice, as described in (Bergamaschi 2009). Serial transplantation of xenografts was performed at Oslo University Hospital, Radiumhosptitalet, and animals were transported from Oslo to Trondheim prior to the experiments. The tumors have a basal-like (MAS98.12) and luminal-like (MAS98.06) gene expression profile. The molecular characterization is described in (Bergamaschi 2009). The gene expression profiles are similar to that of the parent tumors, and have been stable over several passages. The animals were kept in pathogen-free conditions (individually ventilated cages, sterilized bedding). Room temperature (19-22°C), humidity (50-60%) and light dark/cycle (12/12h) were continuously monitored. The mice were given standard diet and sterilized water supplemented with 4 μg/ml 17-β-estradiol *ad libitum*. In Paper II, III and IV, experiments were performed using isoflurane anesthesia (delivered at a dosage of 5% for induction, 2% for maintenance anesthesia, in 67% N_2 and 33% O_2).

All animal experiments were approved by the National Animal Research Authority.

3.2 MR protocols

In Paper I and II, HR MAS MRS was used for analysis of xenograft tissue samples (Bruker AVANCE DRX600 spectrometer). In paper I, the metabolite peak areas in the HR MAS MRS spectra were calculated by curve fitting (PeakFit, SeaSolve, San Jose, USA) and the metabolite concentrations were quantified using the ERETIC method, taking biopsy weight into account (Barantin 1997). The metabolite concentrations were compared between xenograft models using a two-sided t-test with a significance level of $p < 0.05$. In paper II, the spectra were converted to ASCII files and preprocessed to allow multivariate analyses (MATLAB, MathWorks, Natick, USA). Differences between the xenografts were analyzed using principal component analysis (Unscrambler, Camo, Oslo, Norway). The presence of ^{13}C-labelled

metabolites was determined by comparing natural abundance spectra with spectra from animals which received ^{13}C glucose. For comparison of glucose metabolism between the xenograft models, the peak area ratios between the observed metabolites were used.

In paper III and IV, the animals were imaged using a 7T Bruker Biospec Avance 70/20 small animal scanner (Bruker Biospin, Ettlingen, Germany). A 72 mm volume coil was used for transmission and an actively decoupled quadrature mouse head surface coil was used for receiving. The animals were imaged using T1-weighted DCE-MRI with gadodiamide, and DW-MRI. In addition, high-resolution T2-weighted (pre-contrast) and T1-weighted (post-contrast) images were obtained to support slice orientation and to evaluate the final distribution of contrast agent in the tumors. The imaging setup is presented in Figure 8.

Figure 8 Imaging set-up

A) The animal bed. The green tube delivers heated air and the coil is immersed in the bed. B) An anesthetized mouse placed on an adapter with the tumor freely hanging down into the coil. C) The Biospec animal scanner with the bed positioned so that the tumor is located in the isocenter. Reproduced with permission from Else Marie Huuse, FUGE MIC, NTNU.

Technical details are presented in Table 1 and Table 2. The DWI-MRI and DCE-MRI data were analyzed using in-house software developed in MATLAB (MATLAB, MathWorks, Natick, USA). The pre-contrast T_1 values were obtained from a series of images with varying TR and used to calculate a contrast agent concentration/time curve for each voxel in the dynamic imaging series. The generalized compartment model proposed by Tofts *et al* (Tofts 1999) was then fitted to each voxel. Voxels without post-contrast signal enhancement ($RSI_{1min} < 1$ or $AUC_{1min} < 0$) were excluded from the pharmacokinetic modeling. The median K^{trans}, v_e and v_p values were determined in all defined ROIs and compared across xenograft model and treatment using a two-sided t-test with a significance level of $p < 0.05$. ADC maps were calculated using a monoexponential fit of voxel signal intensities versus b-values (100, 300, 600 and 1000 s/mm^2) and the median ADC values were calculated for each tumor.

Table 1 Detailed HR MAS MRS parameters used in Paper I and Paper II

	Paper I		Paper II	
			Xenografts	
	Xenografts	Human tissue	^{1}H	^{13}C
Sequence	single pulse (ereticpr.drx)	cpmg (cpmgpr.drx)	single pulse	single pulse
Spin rate (kHz)	5	5	5	5
Temperature (°C)	4	4	4	4
Water suppression	yes	yes	yes	NA
Flip angle	60°	90°	90°	60°
Echo time (ms)	NA	285	NA	NA
Sweep width (ppm)	16.7	16.7	12	210
Acquisition time (s)	3.28	1.64	4.6	0.5
No. averages	128	128	128	26000

NA: not applicable

Table 2 Detailed MRI parameters for sequences used in Paper III and Paper IV

DCE-MRI		
	T1-map	RARE
	RARE-factor	2
	TR (ms)	150, 750, 1500, 2500, 4500, 12000
	TE (ms)	7
	Dynamic series	
	RARE-factor	4
	TR (ms)	300
	TE (ms)	7
	Temporal resolution (s)	4.8
	Number of repetitions	200
	Contrast agent injection	
	Contrast agent	Gadodiamide
	Dose (mmol/kg)	0.3
	Precontrast images	10
	Injection duration (s)	4
	Geometry	
	Field of view (mm^2)	22 x 22
	Matrix	64 x 64
	In plane resolution (mm)	0.34
	Slice thickness (mm)	0.6
	Number of slices	5
Post-contrast T1-weighted image		
	Sequence	FLASH
	TR (ms)	300
	TE (ms)	5.4
	Field of view (mm^2)	16 x 16
	Matrix	256 x 256
	In plane resolution (mm)	0.078
	Slice thickness (mm)	0.5
DW-MRI		
	Sequence	Diffusion sensitized EPI
	b-values (s/mm^2)	0, 100, 300, 600, 1000[1]
	TR (ms)	3000
	TE (ms)	35
	Field of view (mm^2)	15 x 15
	Matrix	64 x 64
	In plane resolution (mm)	0.23
	Slice thickness (mm)	1
	Number of averages	6

RARE - rapid acquisition with refocused echoes; TR - repetition time; TE - echo time; EPI – echo planar imaging

[1] Images obtained with b = 0 were not included in calculation of ADC values

3.3 Gene expression

Gene expression analyses were performed on xenograft tissue from both models, and the expression of selected genes was combined with the metabolic profiles obtained by HR MAS MRS in Paper I and II. The expression of genes reported in these two studies was obtained from the same set of global gene expression profiles. The gene expression analyses were performed with support from the Dept. of Genetics, Institute for Cancer Research, Oslo University Hospital, Radiumhospitalet.

After extraction from fresh frozen xenograft tissue, mRNA was hybridized to 44k microarrays (Agilent Whole Human Genome Oligo Microarrays, Agilent Technologies Inc, Santa Clara, USA). After processing of the raw signals, the expression data for genes listed in the glycerophospholipid (hsa:00564) and glycolysis (hsa:00010) pathways in KEGG (Kanehisa 2000) or otherwise known to be relevant for the choline and glucose metabolism was retrieved from the microarrays. The selected genes were tested for differential expression between the xenograft models using t-tests with correction for multiple testing. The global gene expression profiles have been deposited in NCBI's Gene Expression Omnibus (GEO) and are available to the public through GEO Series accession number GSE25915 (Edgar 2002).

3.4 Histopathology

All histopathological examinations were performed in collaboration with the Dept. of Laboratory Medicine, Children's and Women's Health, NTNU. In addition, samples from Paper III and a subset of samples from Paper IV were stained and read at The Gade Institute, Section for Pathology, University of Bergen.

In all studies, tumor tissue was harvested at the end of the experiment and fixed using neutral buffered formalin. The samples were subsequently embedded in paraffin and 4µm tissue slices were cut. These sections were then stained with HES according to the standard procedures of the department. HES-stained slices were examined under light microscope in Paper I and Paper II in order to verify the presence of viable cancer cells. In Paper III and IV, hypoxia was assessed by immunohistochemistry using the *in vivo* marker pimonidazole (Natural Pharmacia International Inc., Burlington, USA), which was injected intravenously prior to sacrifice of the animals. The stained sections were imaged at 2x magnification (Nikon Eclipse 80i microscope, Nikon Digital Sight DS-U1 camera, NIS-elements F3.0 software) using enough exposures to cover the entire tumor slice. Images were merged in Photoshop Elements 6.0 (Adobe Systems Inc., San Jose, USA), converted to 32 bit b/w and the degree of hypoxia determined. ROIs enveloping the necrotic areas and the total tumor slice area were defined manually, and the hypoxic fraction was defined as the percentage of the stained area relative to the total area of the slice (ImageJ, National Institute of Health, USA). The mitotic activity of the tumors was assessed through the phosphohistone H3 (PPH3), and reported as the number of mitotic cells per 10 FOVs. Staining of tumor vasculature was performed using CD34 and Ki67. All examinations of these samples were performed by an experienced pathologist. The stained sections were used to determine the mean microvessel density (MVD, CD34-positive counts/mm^2) and the proliferative MVD (CD34+Ki67-positive counts/mm^2).

4 Results

4.1 Paper I

Distinct choline metabolic profiles are associated with differences in gene expression for basal-like and luminal-like breast cancer xenograft models.

The purpose of this study was to compare the choline metabolic profiles of a luminal-like and a basal-like breast cancer xenograft model. In addition, the expression of genes involved in choline metabolism was compared between the models. Finally, the association between gene expression and metabolite profile was studied.

The study was performed in luminal-like (MAS98.06) and basal-like (MAS98.12) orthotopic breast cancer xenograft tumors. These models have previously been established by direct transplantation of human primary tumor tissue, and are now serially propagated in SCID mice. The xenografts have maintained the gene expression profiles and hormone receptor status from the primary tumors. Quantitative metabolic profiles were obtained in fresh frozen tissue using HR MAS MRS, and the expression of genes involved in choline metabolism was retrieved from whole genome expression microarray analyses. The metabolite profiles from the xenografts were compared with corresponding profiles from human breast cancer, sampled from patients with estrogen/progesterone receptor positive (ER+/PgR+) or triple negative (ER-/PgR-/HER2-) breast cancer.

In the basal-like xenografts, glycerophosphocholine (GPC) concentrations were significantly higher than phosphocholine (PCho) concentrations. This pattern was reversed in luminal-like xenografts. These differences could be explained by lower expression of choline kinase alpha/beta, as well as higher PtdCho degradation mediated by higher expression of phospholipase A2 group 4A (PLA2G4A) in the basal-like model. The glycine concentration was also significantly higher in the basal-like model. Although glycine could be derived from energy metabolism pathways, the gene expression data suggested a metabolic shift from PtdCho synthesis to glycine

formation in basal-like xenografts. In agreement with results from the xenograft models, tissue samples from triple negative breast carcinomas had higher GPC/PCho ratio than samples from ER+/PgR+ carcinomas.

In this study, we demonstrated that differences in choline metabolite concentrations corresponded well with differences in gene expression. Using HR MAS MRS, we found distinct metabolic profiles in the xenograft models representing basal-like and luminal-like breast cancer. The same choline metabolite profiles were also observed in patient material from ER+/PgR+ and triple-negative breast cancer, suggesting that the xenografts are relevant model systems for studies of choline metabolism in luminal-like and basal-like breast cancer.

4.2 Paper II

^{13}C High Resolution Magic Angle Spinning MRS reveals differences in glucose metabolism between two breast cancer xenograft models with different gene expression patterns

The purpose of this study was to examine the glycolytic activity in a luminal-like and a basal-like breast cancer xenograft model. This was accomplished by intravenous administration of [1-^{13}C] glucose. Using HR MAS MRS, the levels of the parent tracer and its downstream metabolites was assayed. In addition, the expression of genes involved in glycolysis was compared between models. Finally, the relationship between glucose metabolism and gene expression was evaluated.

The study was performed in luminal-like (MAS98.06) and basal-like (MAS98.12) orthotopic breast cancer xenograft tumors. Tumor tissue was collected both from untreated mice and mice that received an injection of 29 mg [1-^{13}C] glucose 10 or 15 minutes before harvesting of tumor tissue. Glucose and its downstream metabolites lactate and alanine were determined by ^{13}C HR MAS MRS, and the expression of genes involved in glycolysis was retrieved from whole genome expression microarray analyses.

Both in natural abundance spectra (untreated animals) and in spectra from mice receiving [1-^{13}C] glucose, the glucose/lactate and glucose/alanine ratios were found to be lower in luminal-like than basal-like xenografts. [3-^{13}C] lactate and [3-^{13}C] alanine were the predominant metabolites observed after [1-^{13}C] glucose administration. [4-^{13}C] glutamate was identified in most luminal-like samples, but no other metabolites downstream of [1-^{13}C] glucose were observed. The gene expression analyses demonstrated that most genes involved in glucose transport and glycolysis were higher expressed in the luminal-like than the basal-like xenografts.

The study demonstrated that only a minimal fraction of the injected [1-^{13}C] glucose was shunted to the TCA cycle for oxidative phosphorylation. The rate of lactate production in luminal-like xenografts was higher than in basal-like xenografts. The *in*

vivo growth rate of basal-like xenografts is significantly higher than luminal-like xenografts. Therefore, the study has shown that glycolytic activity and lactate production not directly reflect tumor growth rate. Microenvironmental factors such as hypoxia may stimulate to lactate production beyond the metabolic requirements for cellular proliferation and tumor growth.

4.3 Paper III

In vivo magnetic resonance imaging and histopathological assessment of tumor microenvironment in luminal-like and basal-like breast cancer xenografts

The purpose of this study was to explore tumor characteristics related to tumor microenvironment by in vivo MRI and histopathological markers, using two orthotopic breast cancer xenograft models reflecting luminal-like (MAS98.06) and basal-like (MAS98.12) gene expression profiles. Alterations associated with tumor growth and response to estradiol withdrawal were monitored by MRI and compared to histopathological measures of vascularization, hypoxia and markers of VEGF activation.

Luminal-like (n=14) and basal-like (n=12) tumors (volume 200 - 600 mm^3) were examined twice by dynamic contrast enhanced (DCE) and diffusion weighted (DW) magnetic resonance imaging (MRI), to monitor the effect of one week tumor growth or estradiol withdrawal. The impact of tumor size was investigated using large basal-like tumors (n=7, volume >1400 mm2). The transfer constant (K^{trans}) reflecting vascular permeability and perfusion, extracellular and extravascular volume fraction (v_e) and blood plasma volume fraction (v_p) were estimated using two-compartment modelling of the contrast agent uptake in the tumor. The apparent diffusion coefficient (ADC) of water in the tumor was calculated from the DW-MRI data.

K^{trans}, v_p and ADC were significantly higher in basal-like compared with luminal-like tumors (all $P<0.01$). The histopathologically measured vascular proliferation index (VPI) confirmed these findings, showing twofold higher values among the basal-like tumors. No changes in MRI extracted parameters were found after 6 days of tumor growth. Estradiol withdrawal induced a significant increase in K^{trans}, v_e and ADC (all $P<0.05$) in luminal-like xenografts, corresponding with an increase in VEGFR2 activation, which is likely to cause increased tumor vessel permeability.

The study confirmed the potential of functional MR methods to map changes in tumor vasculature and microenvironment in vivo, and demonstrated significant differences

in tumor architecture and vascular function between the luminal-like and basal-like xenografts.

4.4 Paper IV

Low-molecular contrast agent DCE-MRI and DW-MRI in early assessment of bevacizumab and doxorubicin therapy in breast cancer xenografts

The main purpose of this study was to assess vascular responses to the antiangiogenic agent bevacizumab in luminal-like (MAS98.06) and basal-like (MAS98.12) breast cancer xenografts using DCE-MRI and DW-MRI. To increase the clinical relevance of the study, a low-molecular Gd-based contrast agent (Omniscan®) was used. Animals were also treated with doxorubicin, in order to identify the effects specifically associated with antiangiogenic treatment.

Animals carrying luminal-like (MAS98.06) or basal-like (MAS98.12) xenografts were treated with bevacizumab (5 mg/kg ip.), doxorubicin (8 mg/kg iv.) or a combination of both drugs. The animals were imaged on a 7T animal scanner before and 3 days after treatment. Signal intensity curves obtained using DCE-MRI were assessed voxel-by-voxel using nonparametric and parametric methods. The spatial variation in tumors was assessed by defining ROIs both in central and peripheral regions of the tumors. Histopathological vascularization analyses were performed in order to correlate MRI findings with changes in vascular architecture and function. In addition, changes in hypoxic fraction and mitotic activity were determined.

In all treatment groups, a response to therapy was demonstrated using DW-MRI. Treatment-related increases in ADC were found both in central and peripheral regions of the tumors. DCE-MRI data demonstrated marked differences between pre-treatment and post-treatment signal intensity curves in bevacizumab-treated animals or animals receiving combination therapy. Doxorubicin treatment had little impact on contrast agent kinetics, except a late signal enhancement in basal-like xenografts indicative of necrosis. Increased RSI_{1min} was observed in all animals receiving bevacizumab or combination therapy. In addition, increased v_e was seen in basal-like xenografts whereas increased v_p was seen in luminal-like xenografts. The change in DCE-MRI parameters was more prominent in central tumor regions. In vascular histopathological analyses, both the total number of microvessels (MVD) and the

number of proliferating vessels (VPI) were decreased in basal-like xenografts after treatment with bevacizumab or combination therapy. A similar trend was seen in luminal-like xenografts.

The study demonstrated that DCE-MRI using a clinically available low-molecular contrast agent could detect changes in tumor vascular function after antiangiogenic treatment. Both bevacizumab and combination therapy caused increased contrast agent uptake in central regions of the tumor. Doxorubicin alone did not cause significant changes in vascular function. The changes suggested improved perfusion or reduced interstitial fluid pressure, consistent with transient normalization of tumor vasculature following antiangiogenic therapy. Histopathological analyses verified the antiangiogenic effect of bevacizumab and that changes in DCE-MRI parameters were related to vascular function rather than the number of blood vessels.

5 Discussion

The main objective of this thesis was to evaluate how MRI and MRS can be used to describe architectural, functional and molecular differences between two genetically and biologically different breast cancer xenograft models. The two models represent basal-like (MAS98.12) and luminal-like (MAS98.06) subtypes of breast cancer, and are associated with poor and good prognosis, respectively. It is therefore possible to determine how MRI and MRS parameters are associated with tumor growth rate, histopathological features, microenvironmental factors and the genetic background of two xenograft models representing different breast cancer subtypes. Characterization of the basal-like and luminal-like xenografts, both with respect to their biology and MRI/MRS parameters is an important step in establishing the xenografts as relevant model systems for human breast cancer. The models are representative of clinical luminal-like and basal-like breast cancer both with respect to vascularization and choline metabolism (Moestue 2010; Nalwoga 2011), and may therefore be valuable in evaluation of new drugs. In this context, understanding the biology of basal-like breast cancer and its response to treatment is particularly important, as this disease is associated with poor prognosis and currently lacks targeted alternatives for pharmacotherapy. Understanding the regulation of key metabolic pathways is an independent objective of the thesis. Both choline metabolism and glycolysis are considered to contain potential targets for anticancer therapy, but the regulation of these pathways is predominantly studied *in vitro* and the association between breast cancer subtypes and metabolic profiles is not previously studied. Finally, the thesis illustrates how a wide range of MR protocols can be used to characterize cancer subtypes. The versatility of the MR technology allows evaluation of several different aspects of tumor biology, increasing the possibility of identifying clinically relevant biomarkers.

5.1 Animal models

In contrast to cell cultures or other *in vitro* methods for studying the growth of cancer cells, xenograft tumors mimic the entire tumor system. It is widely recognized that tumors consist of several tissue types, including both stromal components and

vascular tissue, which have reciprocal effects on each other and generate a model-specific tumor microenvironment. Studies of cancer using xenograft models enable control of factors that affect tumor progression and response to treatment in a physiologically relevant context. However, the influence from vascular and stromal components and the tumor microenvironment must be taken into account when interpreting data from xenograft studies. Parameters such as hypoxia, perfusion and interstitial fluid pressure have impact on both tumor metabolism and response to therapy, and the results from MRI/MRS studies can therefore be used to evaluate the impact of microenvironmental parameters.

All studies included in the thesis are performed using the same breast cancer xenograft models. These models are established directly from primary carcinomas of breast cancer patients, and represent basal-like and luminal-like breast cancer. The xenografts grow orthotopically. This is considered to increase the clinical relevance as both tumor-stroma interactions and vascularization depend on the location of the xenograft (Vargo-Gogola 2007). The xenograft models have in general maintained both the gene expression profile and phenotype/receptor expression of the parent tumors. However, although the subtyping of breast cancer include both a luminal A and a luminal B subtype (Perou 2000), the exact subtype of the luminal-like xenograft model remains unknown. The clinical features of the luminal-like xenograft (estradiol-dependent growth, ER+/PgR+ phenotype) can be associated with the luminal-A subtype. However, the gene expression clustered tightly with the luminal-B subtype (Bergamaschi 2009). Expression profiles from the extracellular matrix clustered with the luminal-A subtype for the primary tumor. In the xenografts, where the extracellular matrix predominantly is of murine origin, this profile was shifted to a luminal-B-associated profile. This illustrates the complexity of subclassification of xenografts based on gene expression profiles. The luminal A subtype is generally associated with a more favorable outcome than the luminal B subtype (Sorlie 2001). Subtyping of xenografts based on gene expression profiling should be interpreted with caution, as the human stromal components are replaced with stromal components from the mice. In microarrays based on human genes, the expression of stromal genes from the mouse generally cause signal loss which in turn leads to underestimation of genes associated with the extracellular matrix.

Generally, establishing breast cancer from primary patient tumors is challenging, with a success rate of around 10%. Establishing ER+/PgR+ xenografts is especially difficult, as demonstrated by Marangoni *et al*, who obtained 25 xenograft models from 200 clinical tumor samples (Marangoni 2007). Of these 25, only one model was ER+, reflecting the strong selection bias toward aggressive tumors. However, xenograft models based on primary tumors offers an advantage compared to models based on cultured cell lines. The transplanted xenograft tumors contain numerous cell clones representing the diversity of cells present in human breast carcinomas. The cells in the xenografts are to some extent differentiated, and stromal components from the primary tumors may be carried along together with the cancer cells. In contrast, cultured cells generally have been selected for their ability to grow in artificial media and represent highly homogeneous cell populations. The xenografts are grown orthotopically, in the mammary fat pad. Compared to subcutaneously grown tumors, the mammary fat pad is considered to provide a more relevant microenvironment for breast tumors. Despite the controversy regarding the molecular subtype of the luminal-like xenograft, it is less aggressive than the basal-like xenograft. The slower tumor growth rate and lower level of angiogenesis, in addition to the profound addiction to a dietary estradiol supplement, distinguishes it clearly from the basal-like xenograft. Thus, the models are considered clinically relevant representations of human breast cancer heterogeneity, as they describe extremes in animal models of breast cancer with respect to aggressiveness.

To explore similarities in metabolic profile between the xenograft models and human breast cancer of corresponding subtype, spectra from patients with triple-negative breast cancer were compared with spectra from the basal-like xenografts. Although there is general consensus that these two entities overlap to a significant degree, the relationship between triple-negative and basal-like breast cancer is a topic of debate (Badve 2011a). Triple-negativity is a phenotype determined from receptor expression whereas basal-like breast cancer is determined from gene expression analysis. There is no internationally accepted definition for basal-like breast cancer. Using gene expression microarrays, a basal-like gene signature has been proposed (Perou 2000). However, classification of biopsies according to this gene signature may be difficult.

Cancers with basal-like gene expression may have significant variation in their morphological features. In general, they lack or have low ER/PgR levels, lack HER-2 amplification and express proteins usually found in the basaloid cells of the normal breast. In contrast, there is little controversy regarding the definition of triple-negative breast cancer. Still, different pathology laboratories may have different thresholds for scoring ER/PgR expression. Some laboratories require more than 10% ER-positive cells in order to classify a sample as ER positive, whereas other laboratories score samples as ER+ in the presence of >1% positive cells (Gown 2008). Some laboratories count only cells with nuclear staining whereas others also define cytoplasmic staining as a positive finding. Due to the numerous similarities between the two terms, basal-like breast cancer and triple negativity has often been used interchangeably (Rakha 2009). In general, however, it has been shown that tumors with triple-negative phenotype are classified as basal-like in more than 90% of cases (de Ronde 2010; Kreike 2007). It should be noted that the fraction of basal-like tumors exhibiting non-triple-negative phenotype in general is as high as 20-30% (Badve 2011b). The existing knowledge suggests that triple negative phenotype may be a valid surrogate marker for basal-like molecular subtype, whereas basal-like subtype is not a valid surrogate marker for triple negative phenotype.

5.2 Experimental protocols

5.2.1 HR MAS MRS

The metabolic profiles of the basal-like and luminal-like xenografts were studied using ^{1}H HR MAS MRS and ^{13}C HR MAS MRS. Due to its reproducibility and high spectral resolution, ^{1}H HR MAS MRS has become an important tool in metabolic profiling of cancer. In contrast to destructive MRS methods, HR MAS MRS allows subsequent analyses of intact tissue specimens. Histopathological evaluation of tissue samples after MRS analysis can ensure that the metabolic profile is obtained in viable cancer tissue. In paper II, we use ^{13}C HR MAS MRS for tracing ^{13}C-labeled glucose and its downstream metabolites. Although the sensitivity is a limitation, this method allows functional studies of metabolic processes. Such knowledge may be important for future studies of hyperpolarized tracers.

The metabolite concentrations in Paper I were quantified using the ERETIC method. The performance of the method has been evaluated using calibration standards and comparing with the commonly used internal standard TSP (Sitter 2010a). This demonstrated that the precision and accuracy of ERETIC is good, with a maximum relative error of 8.4%. This suggests that the variability in metabolite concentrations (relative standard deviation 25-66%) in the xenografts is due to intersubject variation rather than analytical inaccuracy. Such variation may reflect heterogeneous microenvironmental conditions within the tumors.

In Paper II, the main objective was to detect [1-^{13}C] glucose and any downstream metabolites. Quantification of metabolites was not performed, and metabolite ratios were instead used for evaluation of metabolic activity. However, comparing metabolite ratios at two different time points suggested that the luminal-like xenografts had higher glycolytic rate. This hypothesis was corroborated using gene expression profiling.

In both Paper I and Paper II, it was decided to perform HES staining and score the amounts of viable tumor tissue, necrosis and adipose/other tissue using light microscopy. Although xenograft tumors are more homogenous than human tissue samples, this allows the elimination of samples that are not representative due to extensive necrosis or the presence of non-tumor tissues. However, the histopathological examinations demonstrated that all samples predominantly consisted of viable tumor tissue, indicating that the results are not influenced by errors in tissue sampling. This serves as a quality control of the data, in contrast to destructive methods such as extraction procedures, which do not allow post-analysis evaluation of the specimens.

5.2.2 DCE-MRI and DW-MRI

DCE-MRI is a widely used method for *in vivo* characterization of tumor vasculature. As described in the introductory sections, tumor vasculature is chaotic, immature and leaky. Therefore, kinetic analysis of contrast agent disposition can distinguish tumor

vasculature from that of neighboring tissue. In Paper III and IV, a spin-echo sequence (MSME, Bruker Paravision 3.0) was used to acquire the dynamic image series. The sequence was accelerated using the RARE-method, with an acceleration factor of 4. This resulted in a temporal resolution of 4.8 seconds with a voxel size of 0.34 x 0.34 x 0.60 mm. The high temporal resolution allowed pharmacokinetic modelling of a clinically available, low-molecular contrast agent (gadodiamide, Omniscan®). Macromolecular contrast agents have slower pharmacokinetics and DCE-MRI can be performed with lower temporal resolution. However, such agents are not available for routine clinical use, which encouraged the use of gadodiamide. Due to its size, gadodiamide is not a freely diffusible tracer. Instead, its translocation from blood vessels to extravascular space is restricted both by perfusion and vessel permeability. This must be taken into account when the DCE-MRI data are interpreted. For perfusion measurements, freely diffusible tracers are more suitable as they leak rapidly into the EES. When equilibrium in contrast agent concentration between the blood pool and the EES is reached immediately, K^{trans} represents only the tissue perfusion. For macromolecular contrast agents, extravasation depends on the tumor vessel permeability, and K^{trans} is then a measure of the permeability. Using gadodiamide, changes in K^{trans} reflect both changes in perfusion and permeability. Its physiological meaning can therefore vary both between model systems and during tumor progression. Changes in interstitial fluid pressure may also influence the K^{trans} value (Gulliksrud 2009) due to changes in intratumoral conductivity. The DCE-MRI data (Paper III and Paper IV) were analyzed both using two-compartment kinetic modelling and empirical methods. If these two approaches can extract similar information from the experimental system, empirical methods are preferred in the clinical setting due to their simplicity and methodological robustness. When these two approaches provide coherent data, the empirical methods may also be considered an internal quality control of the pharmacokinetic modelling. To allow comparison of the pharmacokinetic parameters with other studies, Tofts' consensus model was used (Tofts 1999). To ensure compliance with the requirements of the two-compartment model, voxels without signal enhancement after injection of contrast agent (RSI_{1min}<1 or AUC_{1min} <0) were excluded from the modelling. In tumor xenografts, such voxels are typically associated with necrotic tissue, and trying to fit the 2-compartment model to such voxels often results in poor fit and unphysiological model parameters.

In individual tumors, from 10 to 25% of voxels were typically filtered out using this approach. The fraction of voxels with no signal enhancement 1 minute after administration of contrast agent was significantly reduced in animals treated with bevacizumab (Paper IV), suggesting that the fraction of filtered voxels may serve as a biomarker for altered vascular function.

An averaged population AIF was used in both Paper III and Paper IV. Ideally, an individual AIF should be obtained for all study subjects in order to improve the model fit. However, this is difficult to obtain as it requires a high spatial resolution in order to avoid partial volume effects and a global excitation pulse to avoid flow artifacts. In addition, a large blood vessel must be present in the FOV. It is in general difficult to separate individual biological variation from variation induced by measurement uncertainty. Orthotopic breast cancer xenografts are not fed by a single blood vessel, but by a number of different vessels that have been recruited from the mammary fat pad. The blood supply to the tumor depends on its ability to recruit these vessels and individual variation in the perfusion must be expected. Therefore, determining the AIF in a large vessel distant to the tumor on an individual basis may not necessarily reflect the actual arterial input function of the tumor. Due to the difficulty of obtaining an adequate individual AIF, it is generally accepted to use a relevant population AIF. When the appropriate precautions are taken, there is good correlation between the DCE-MRI pharmacokinetic parameters calculated from population and individual AIF (Loveless 2011). A population AIF should, as far as practically possible, be obtained in the same strain of animals and under identical experimental conditions as in the main experiment. In this work, an AIF modeled in-house in a similar strain of mice was used, potentially reducing the accuracy of the pharmacokinetic modeling.

DW-MRI is evolving into a tool for both tumor detection, staging and monitoring of response to treatment (Padhani 2009). It is generally recommended to use b-values ≤ 1000 s/mm^2 and perform a monoexponential curve fit in order to calculate the ADC. However, low b-values (b ≤ 100 s/mm^2) are sensitive to perfusion and therefore induce a bias in the diffusion measurements. Therefore, images obtained with b = 0 were excluded from ADC calculations. The remaining b-values (100, 300, 600 and 1000 s/mm^2) are thought to represent extra- and intracellular diffusion within the

tumors. The DW-MRI images were obtained after the DCE-MRI images, and it has been shown that ADC values obtained after contrast agent administration are slightly lower than pre-contrast ADC values (Yamada 2002). The order of imaging sequences was partly chosen to avoid blood clotting in the tail vein cannula. In addition, the same order has been used in clinical breast examinations for improved lesion detection. As the DW-MRI images were obtained approximately 45 minutes after contrast injection in all animals, the effects of residual contrast agent was assumed to be similar in all animals. Therefore the order of the imaging sequences was not considered to influence the experimental findings.

5.3 Assessment of glucose and choline metabolism

Paper I and II concerns the metabolic profile of the basal-like and luminal-like xenografts. In particular, the choline metabolism and the glycolysis were studied in detail. These two metabolic pathways were selected for several reasons. Firstly, they have been shown to be abnormally regulated in cancer. Secondly, they contain metabolites that can be observed using MRS. Finally, drugs interfering with these metabolic pathways have been shown to reduce the growth rate of solid tumors in preclinical studies.

Choline phospholipid metabolism is altered across a wide range of cancers. The most consistent abnormality is elevated PCho concentration and increased tCho signal *in vivo* (Glunde 2011). These changes have been associated with overexpression of choline kinase and phospholipase C (Glunde 2004). It is frequently stated that breast cancer cells switch from a high GPC/low PCho ratio to a low GPC/high PCho ratio during malignant transformation (Glunde 2011; Podo 1999). This is an interpretation of *in vitro* studies reported by Aboagye *et al*, where the concentrations of individual choline metabolites in an array of cell lines ranging from immortalised human epithelial breast cells to aggressive, metastatic breast cancer cell lines were assessed (Aboagye 1999). These findings have been extended to clinical *in vivo* MRS breast cancer, where a high tCho signal is associated with malignant disease, and a reduction in tCho is a marker for response to neoadjuvant therapy (Baek 2009; Gillies 2005). This consensus has been questioned on several grounds. Firstly, the metabolic profiles

obtained in cultured cell lines are not fully consistent with *ex vivo* profiles obtained from clinical cancer samples using HR MAS MRS. In clinical cancer samples, GPC:PCho ratio > 1 has been reported (Sitter 2006). In prostate cancer, GPC concentration is positively correlated to tumor grade (Keshari 2011). Secondly, it has been shown that the experimental conditions may have a profound effect on the metabolic profile of cultured cells (Morse 2009). Finally, it has been shown that microenvironmental factors contribute to the regulation of choline phospholipid metabolism (Eliyahu 2007a). These data suggest that *in vitro* metabolic profiles may not be representative for human disease. The use of tCho in therapy monitoring has also been questioned, since several studies have demonstrated that anticancer agents actually cause increased concentrations of PCho and/or GPC (Moestue 2011a; Sterin 2001).

As the role of choline phospholipid metabolism in breast cancer is not understood in detail, HR MAS MRS was performed on tissue samples from basal-like and luminal-like xenografts, in order to evaluate metabolic profile. The two models had significant differences in the concentration of PCho, GPC and glycine, and we therefore compared the expression of genes involved in this metabolic pathway. Synthesis of these datasets showed that the gene expression explained some of the differences in metabolic profile. The luminal-like xenografts had higher PCho concentration, which was attributed to higher choline kinase expression. The higher GPC concentration in basal-like xenografts could be explained by a higher expression of PLA2, in particular the Group IVa isoenzyme. Expression of genes involved in conversion of choline via betaine to glycine was also higher in the basal-like xenografts, possibly explaining the higher glycine concentration in this model. Another plausible explanation is overexpression of the PHGDH enzyme, which diverts the metabolic flux from glycolysis into serine and glycine production (Seton-Rogers 2011). Overexpression of this gene is associated with triple negative/basal-like breast cancer, which is in accordance with the high glycine levels observed in breast cancer patients with poor prognosis (Giskeodegard 2010; Sitter 2010b). This study therefore identified possible genes that are of importance for regulation of choline phospholipid metabolism. The metabolic profiles from the xenograft models were compared with corresponding human breast cancer samples, demonstrating that the xenograft models to a large

degree were representative of the metabolic profiles found in human disease. Out of necessity, the samples from basal-like and luminal-like xenografts were compared to clinical triple negative and ER+/PgR+ breast cancer, respectively. This was considered appropriate as more than 90% of triple negative breast cancers also can be assigned to the basal-like subtype. The ER+/PgR+ breast cancers were also classified as luminal-A using gene expression profiling, demonstrating that the molecular profiles were similar to that of the luminal-like xenograft model.

This study suggested that molecular subtypes of breast cancer may be associated with different metabolic profiles. It also suggested a number of enzymes that may be responsible for the differences in metabolic profile. The regulation of choline phospholipid metabolism can, however, not be deduced from the study. Differences in metabolic profile could either be associated with differences in oncogenic signal transduction, or with differences in the tumor microenvironment. As shown in paper III, the luminal-like xenografts are more hypoxic than the basal-like xenografts. Hypoxia induces HIF-1 activity, which in turn has been shown to upregulate the activity of choline kinase and increase PCho concentration (Glunde 2008). Therefore, it is possible that the difference in metabolic profile is due to microenvironmental differences rather than being an intrinsic property of luminal-like xenograft. On the other hand, similar profiles are found in both xenografts and human samples, suggesting that intrinsic factors also are of importance.

The data obtained in Paper I suggests that a high GPC concentration may be associated with aggressive breast cancer, adding complexity to the current hypothesis that PCho rather than GPC is associated with malignant transformation. The paper also suggests that *in vivo* ^{1}H MRS is unable to distinguish these subtypes based on the tCho signal. tCho levels are similar in both models despite the profound difference in metabolic profile, and ^{31}P MRS may be a better approach for studies of choline metabolism in breast cancer diagnosis and therapy monitoring.

One of the most prominent metabolic abnormalities in cancer is a high rate of aerobic glycolysis, where glucose is converted to lactate even under normoxic conditions (Warburg 1924). The low ATP yield is compensated by a high metabolic flux (Vander

Heiden 2009). This way, cancer cells can produce energy while conserving carbon for production of proteins and nucleotides, as required to maintain a high rate of proliferation. As shown in Figure 9, the oncogenic signalling pathways that regulate choline metabolism have also been shown to regulate glucose metabolism (Elstrom 2004; Lock 2011; Tennant 2009; Yeung 2008).

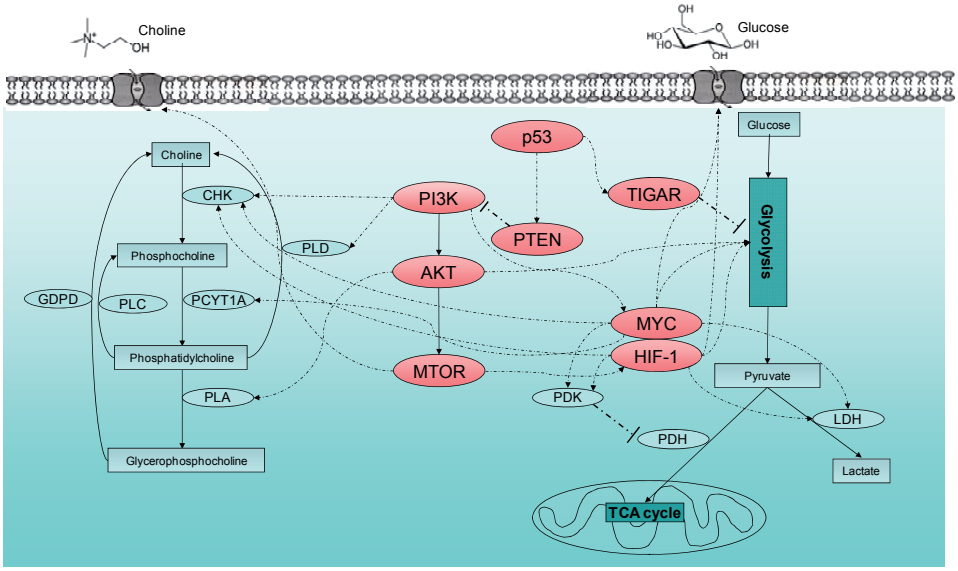

Figure 9 Oncogenic regulation of choline and glucose metabolism

The PI3K/AKT/MTOR signalling pathway regulates both choline and glucose metabolism by controlling the activity of key enzymes on different levels in both these metabolic pathways. Elliptic shapes represent proteins whereas rectangular shapes represent metabolites or metabolic pathways. Solid lines represent metabolic conversion, dotted lines represent the regulatory effects from oncogenic signalling transducers (red) on metabolic enzymes (blue). Transcription factors such as Myc or HIF-1 are also regulated by microenvironmental factors. Reproduced with permission from Moestue *et al*, Mol Oncol 2011; 5 (3); 224-241.

Glucose metabolism in cancer can be studied using various MRS techniques both *in vitro* and *in vivo*. High resolution MRS can be applied to cell cultures, tissue samples and extracts. Proton spectroscopy is routinely used in cancer diagnosis and management, and assessment of lactate production can be performed during a clinical MR examination. Advances in MRS methodology combined with increased interest in glycolysis as a therapeutic target can lead to increased use of *in vivo* lactate MRS assessment. Other metabolites in the glycolysis are present in low concentrations and

are seldom considered as biomarkers in proton spectroscopy. Most studies of the glycolytic pathway use ^{13}C MRS for tracing the metabolic fate of [1-^{13}C] glucose or other isotopically enriched substrates. ^{13}C MRS has also been used to study glucose metabolism *in vivo* in cancer (Kurhanewicz 2008; Wijnen 2010). Following administration of ^{13}C-enriched substrates to tumor-bearing animals, the fate of the substrates can be studied taking tumor microenvironmental factor into account. However, ^{13}C MRS is not yet routinely used in clinical diagnosis or management of cancer. This may change as new spectroscopic techniques, such as hyperpolarized ^{13}C MRSI, are further developed.

The objective of Paper II was to establish a protocol for ^{13}C HR MAS MRS, which allows analysis not only of [1-^{13}C] glucose metabolism but also any other ^{13}C-enriched substrates. In contrast to ^{1}H MRS, this allows evaluation of metabolic flux since the levels of both the parent compound and its downstream metabolites can be assayed. This could allow evaluation of a wide range of substrates for *in vivo* application, including hyperpolarized MRS. Abnormal glycolytic activity has repeatedly been observed in cancer, and it has also been demonstrated that the glycolytic rate can be modulated by cytotoxic drugs, direct glycolytic inhibitors or, in the case of breast cancer, endocrine treatment (Ben-Horin 1995; Neeman 1989; Poptani 2003). However, the association between glycolytic rate and malignancy is not completely understood. Lactate concentration has been suggested as a biomarker for malignant transformation both in brain and prostate cancer (Tessem 2008; Walenta 2004). There is also considerable interest in glycolytic inhibitors as anticancer agents (Tennant 2010). By tracking the fate of [1-^{13}C] glucose in basal-like and luminal-like xenografts, evaluation of the relationship between tumor growth rate and glycolytic flux could be assessed. The ^{13}C spectra demonstrated that virtually all the administered glucose was converted to alanine and lactate. However, small amounts of [4-^{13}C] glutamate were also detected in the luminal-like xenografts. This suggests that the TCA cycle is intact but downregulated. Evaluation of [1-^{13}C] glucose, [3-^{13}C] alanine and [3-^{13}C] lactate levels in the xenografts suggested that both models produced significant amounts of both alanine and lactate within 10 minutes of glucose administration. The amount of both these metabolites was increased at 15 minutes, demonstrating that the samples were collected during a

period of active tracer metabolism in the cancer cells. Interestingly, only negligible glucose levels were observed in luminal-like xenografts. This suggests that the glycolytic rate in these tumors is higher than the glucose uptake rate, which was not the case for the basal-like xenografts. The total lactate amounts were similar in the two models. As most glycolytic genes, including glucose transporters, hexokinase and lactate dehydrogenase were higher expressed in luminal-like xenografts, the combined data strongly suggest higher glycolytic rate in the luminal-like xenografts. This means that glucose consumption rate not necessarily is associated with tumor growth rate. Instead, it suggests that modulation of glucose metabolism by microenvironmental factors may be a determinant factor. The luminal-like xenografts have poorer vascularization and higher hypoxia levels than the basal-like xenografts. This may activate HIF-1 which is known to stimulate glycolysis. The mapping of glucose metabolism in these models provides a fundament for studies of inhibition of glycolysis as a therapeutic strategy. If the luminal-like xenografts are addicted to aerobic lactate production, glycolytic inhibitors may potentially be more effective in this model.

5.4 Assessment of bevacizumab treatment

In Paper III, the basal-like and luminal-like xenografts were examined by MRI and histopathology to describe the vascular and microenvironmental characteristics of the tumors. The effect of tumor growth and estradiol withdrawal was monitored by imaging the same animals with a 7-day interval. Both DCE-MRI and DW-MRI showed differences between the xenografts, and the histopathological evaluation contributed greatly to the interpretation of these differences. Furthermore, the paper provided a fundament for assessment of changes in vascular function after treatment with the VEGF inhibitor bevacizumab. Basal-like xenografts had higher K^{trans} and v_p than luminal-like xenografts, which is in accordance with the higher MVD and proliferative MVD (pMVD) observed in basal-like xenografts. Both a high K^{trans} and high MVD/pMVD are associated with poor prognosis in cancer. These results show that DCE-MRI can be used to noninvasively evaluate the vascularity of solid tumors, which may be of value in breast cancer risk stratification (Gravdal 2009; Pickles 2009; Stefansson 2006; Turnbull 2009). The study also demonstrated that contrast

agent pharmacokinetics did not change significantly over a 7-day interval. However, by comparing large tumors (> 1500 mm^3) with medium-sized tumors (200-600 mm^3), a reduction in vascularization with concomitant hypoxia and reduced K^{trans} values was observed. The differences in tumor volume represent ~3 weeks (basal-like xenografts) and 6-13 weeks (luminal-like xenografts) of growth, demonstrating that the tumor volume is an important experimental factor that should be taken into account in design and interpretation of preclinical MRI studies. The changes in DCE-MRI parameters after estradiol withdrawal suggested that the imaging protocol was adequate for assessment of changes in vascular function following treatment with anticancer drugs.

In Paper IV, the effect of the anti-VEGF antibody bevacizumab was evaluated using DCE-MRI and DW-MRI. Bevacizumab has been approved for clinical use in several cancers, including breast cancer. However, its impact on patient survival has so far been less than anticipated when the concept of antiangiogenic treatment first was conceived. Therefore, it is a need for noninvasive methods that can discriminate between responders and non-responders. Identification of the patient subpopulations which will benefit from a drug can increase its clinical utility. Previous studies using macromolecular contrast agents have shown that bevacizumab treatment reduce the K^{trans} values. As the transcapillary transport of macromolecular contrast agents mainly depend on vascular permeability, these findings show that bevacizumab reduces tumor vessel leakiness. However, such contrast agents are not approved for clinical use. It has also been shown that bevacizumab treatment reduces interstitial fluid pressure (IFP), possibly due to less leakage of serum proteins into the interstitium (Dickson 2007). This suggests that bevacizumab-induced changes should be imageable using low-molecular contrast agent DCE-MRI. An inverse correlation between IFP and transcapillary transport of gadodiamide has previously been reported (Gulliksrud 2009).

In basal-like xenografts, bevacizumab treatment has been shown to significantly inhibit tumor growth (Lindholm EM, submitted to Br J Cancer 2011). In Paper IV, it was shown that the MVD and pMVD in basal-like xenografts decreased significantly after bevacizumab treatment. A similar trend was seen in the luminal-like xenografts. In contrast, the DCE-MRI data demonstrated increased contrast agent uptake in both

xenografts. The increase was greatest in the central regions of the tumors, whereas peripheral areas showed only minor changes. In addition, the fraction of non-enhancing cells decreased significantly following bevacizumab therapy. These findings suggest that low-molecular contrast agent DCE-MRI after bevacizumab therapy reflects changes in vascular function rather than changes in MVD. Furthermore, as studies using macromolecular contrast agents have shown that bevacizumab reduces the vascular permeability, the changes observed in this study must be caused by improved perfusion, particularly in central tumor regions. Similar changes were found in both basal-like and luminal-like xenografts, suggesting that VEGF blockade may have a profound effect on vascular function also in the absence of reduced MVD or pMVD.

Although vascular normalization following bevacizumab therapy may be transient, noninvasive methods for monitoring vascular function may be useful for determining metronomic drug dosing regimens (Jain 2005). It has previously been shown that anti-VEGF therapy can enhance the delivery of anticancer drugs in solid tumors (Dickson 2007). The findings in Paper IV suggest that increased perfusion in central tumor regions may enhance the delivery of chemotherapeutic drugs. In this setting, DCE-MRI could be used to identify the optimal time point for administration of chemotherapy.

6 Conclusions and future perspectives

In this thesis, basal-like and luminal-like breast cancer xenograft models have been characterized using MRI/MRS in combination with histopathology and gene expression analysis. Several MR-derived parameters were associated with the aggressiveness of the xenografts, including high GPC and glycine concentration and high K^{trans} and v_p values.

The work has established the xenografts as relevant model systems for therapy monitoring studies in basal-like and luminal-like breast cancer. In addition, several interesting aspects of breast cancer molecular biology have been revealed using MRS. Firstly, we have shown that previous theories regarding choline metabolism may be too simplistic and not covering the entire range of breast cancer heterogeneity. While it has been suggested that high GPC/PCho ratio is associated with normal breast tissue and that malignancy predominantly correlate with PCho concentration, the findings in basal-like xenografts suggest that high GPC can be found in aggressive breast cancer subtypes. This indicates that follow-up studies should be performed, as the choline cycle may contain several targets for anticancer therapy and as drugs interfering with the choline cycle may have varying efficacy in different breast cancer subtypes. Secondly, we found that the glycolytic rate is not directly associated with tumor growth rate. The glycolytic rate is higher in the slowly growing luminal-like xenografts, due to higher expression of genes involved in glycolysis. This illustrates the importance of microenvironmental regulation of tumor metabolism. Finally, we have shown how metabolic profiles represent the expression of genes directly involved in metabolic pathways.

Using DCE-MRI, we have also shown how differences in angiogenesis and vascular function can be imaged using a clinically relevant contrast agent. The basal-like xenografts are better vascularised due to higher angiogenic activity, which is reflected in higher K^{trans} and v_e values than the luminal-like xenografts. The differences in vascular function and angiogenesis are relevant for interpretation of response to bevacizumab therapy. In contrast to classic chemotherapy (doxorubicin),

bevacizumab has a blood vessel-specific effect, leading to improved perfusion (and contrast enhancement) in central regions of the xenograft tumors. It was also found that bevacizumab therapy reduced both MVD and pMVD in basal-like xenografts. Combining these two data sets, it was concluded that bevacizumab both reduces angiogenic activity and normalises vascular function. However, DCE-MRI primarily reflects the vascular function and not the number of blood vessels. We also demonstrated that response to bevacizumab therapy was reflected by DW-MRI, which potentially also could be used for clinical therapy monitoring.

The work presented in the thesis provides a solid fundament for further studies of differential response to therapy in these experimental models of breast cancer, and the use of MRI/MRS for early evaluation of response to therapy. Of special interest is the metabolic response to drugs targeting oncogenic signaling or metabolic pathways, which hopefully can be of benefit for patients with basal-like breast cancer. Development of methods for functional analysis of metabolic pathways using ^{13}C HR MAS MRS can bridge the gap between current global metabolomic approaches and the development of ^{13}C-enhanced tracers for clinical hyperpolarized MRSI. In addition, the thorough description of vascularity in these xenograft models may be useful in development of nanoparticulate contrast agents targeting angiogenic markers.

7 Bibliography

Aboagye EO and Bhujwalla ZM: Malignant transformation alters membrane choline phospholipid metabolism of human mammary epithelial cells. Cancer Res 1999; 59(1); 80 - 84

Al-Saffar NM et al: The phosphoinositide 3-kinase inhibitor PI-103 downregulates choline kinase alpha leading to phosphocholine and total choline decrease detected by magnetic resonance spectroscopy. Cancer Res 2010; 70(13); 5507 - 5517

Aliu SO et al: MRI methods for evaluating the effects of tyrosine kinase inhibitor administration used to enhance chemotherapy efficiency in a breast tumor xenograft model. J Magn Reson Imaging 2009; 29(5); 1071 - 1079

Baar J et al: A vasculature-targeting regimen of preoperative docetaxel with or without bevacizumab for locally advanced breast cancer: impact on angiogenic biomarkers. Clin Cancer Res 2009; 15(10); 3583 - 3590

Badve S et al: Basal-like and triple-negative breast cancers: a critical review with an emphasis on the implications for pathologists and oncologists. Mod Pathol 2011a; 24(2); 157 - 167

Badve S et al: Basal-like and triple-negative breast cancers: a critical review with an emphasis on the implications for pathologists and oncologists. Mod Pathol 2011b; 24(2); 157 - 167

Baek HM et al: Predicting pathologic response to neoadjuvant chemotherapy in breast cancer by using MR imaging and quantitative 1H MR spectroscopy. Radiology 2009; 251(3); 653 - 662

Barantin L et al: A new method for absolute quantitation of MRS metabolites. Magn Reson Med 1997; 38(2); 179 - 182

Beatson G: On the treatment of inoperable cases of breast carcinoma of the mamma: suggestions for a new method of treatment, with illustrative cases. Lancet 1896; 148(3802); 104 - 107

Beloueche-Babari M et al: Modulation of melanoma cell phospholipid metabolism in response to heat shock protein 90 inhibition. Oncotarget 2010a; 1(3); 185 - 197

Beloueche-Babari M et al: Metabolic assessment of the action of targeted cancer therapeutics using magnetic resonance spectroscopy. Br J Cancer 2010b; 102(1); 1 - 7

Beloueche-Babari M et al: Identification of magnetic resonance detectable metabolic changes associated with inhibition of phosphoinositide 3-kinase signaling in human breast cancer cells. Mol Cancer Ther 2006; 5(1); 187 - 196

Ben-Horin H et al: Mechanism of action of the antineoplastic drug lonidamine: 31P and 13C nuclear magnetic resonance studies. Cancer Res 1995; 55(13); 2814 - 2821

Bergamaschi A et al: Molecular profiling and characterization of luminal-like and basal-like in vivo breast cancer xenograft models. Mol Oncol 2009; 3(5-6); 469 - 482

Bhujwalla ZM et al: Combined vascular and extracellular pH imaging of solid tumors. NMR Biomed 2002; 15(2); 114 - 119

Bhujwalla ZM et al: Vascular differences detected by MRI for metastatic versus nonmetastatic breast and prostate cancer xenografts. Neoplasia 2001; 3(2); 143 - 153

Bloch F: Nuclear Induction. 1946; 70460 - 474

Boven E et al: Phase II preclinical drug screening in human tumor xenografts: a first European multicenter collaborative study. Cancer Res 1992; 52(21); 5940 - 5947

Bray F et al: Cancer Registry of Norway. Cancer in Norway 2008 - Cancer incidence, mortality, survival and prevalence in Norway. 2009;

Brindle K: New approaches for imaging tumour responses to treatment. Nat Rev Cancer 2008; 8(2); 94 - 107

Buchholz TA et al: Neoadjuvant chemotherapy for breast carcinoma: multidisciplinary considerations of benefits and risks. Cancer 2003; 98(6); 1150 - 1160

Chen JH et al: MRI evaluation of pathologically complete response and residual tumors in breast cancer after neoadjuvant chemotherapy. Cancer 2008; 112(1); 17 - 26

Chung YL et al: Magnetic resonance spectroscopic pharmacodynamic markers of the heat shock protein 90 inhibitor 17-allylamino,17-demethoxygeldanamycin (17AAG) in human colon cancer models. J Natl Cancer Inst 2003; 95(21); 1624 - 1633

Chung YL et al: Noninvasive magnetic resonance spectroscopic pharmacodynamic markers of a novel histone deacetylase inhibitor, LAQ824, in human colon carcinoma cells and xenografts. Neoplasia 2008; 10(4); 303 - 313

de Ronde JJ et al: Concordance of clinical and molecular breast cancer subtyping in the context of preoperative chemotherapy response. Breast Cancer Res Treat 2010; 119(1); 119 - 126

Dickson PV et al: Bevacizumab-induced transient remodeling of the vasculature in neuroblastoma xenografts results in improved delivery and efficacy of

systemically administered chemotherapy. Clin Cancer Res 2007; 13(13); 3942 - 3950

Edgar R et al: Gene Expression Omnibus: NCBI gene expression and hybridization array data repository. Nucleic Acids Res 2002; 30(1); 207 - 210

Egeland TA et al: Dynamic contrast-enhanced magnetic resonance imaging of tumors: preclinical validation of parametric images. Radiat Res 2009; 172(3); 339 - 347

Ei Khouli RH et al: Diffusion-weighted imaging improves the diagnostic accuracy of conventional 3.0-T breast MR imaging. Radiology 2010; 256(1); 64 - 73

Eliyahu G et al: Choline Metabolism in Breast Cancer; The Influence of the Microenvironmental conditions [Abstract]. Proc Intl Soc Mag Reson Med 2007a; 15

Eliyahu G et al: Phosphocholine as a biomarker of breast cancer: molecular and biochemical studies. Int J Cancer 2007b; 120(8); 1721 - 1730

Ellingsen C et al: Dynamic contrast-enhanced magnetic resonance imaging of human cervical carcinoma xenografts: pharmacokinetic analysis and correlation to tumor histomorphology. Radiother Oncol 2010; 97(2); 217 - 224

Ellingsen C et al: Assessment of hypoxia in human cervical carcinoma xenografts by dynamic contrast-enhanced magnetic resonance imaging. Int J Radiat Oncol Biol Phys 2009; 73(3); 838 - 845

Elstrom RL et al: Akt stimulates aerobic glycolysis in cancer cells. Cancer Res 2004; 64(11); 3892 - 3899

Ferlay J et al: Estimates of worldwide burden of cancer in 2008: GLOBOCAN 2008. Int J Cancer 2010;

Ferrara N et al: Bevacizumab (Avastin), a humanized anti-VEGF monoclonal antibody for cancer therapy. Biochem Biophys Res Commun 2005; 333(2); 328 - 335

Folkman J: Tumor angiogenesis: therapeutic implications. N Engl J Med 1971; 285(21); 1182 - 1186

Folkman J: Anti-angiogenesis: new concept for therapy of solid tumors. Ann Surg 1972; 175(3); 409 - 416

Galbraith SM et al: Combretastatin A4 phosphate has tumor antivascular activity in rat and man as demonstrated by dynamic magnetic resonance imaging. J Clin Oncol 2003; 21(15); 2831 - 2842

Gerber HP and Ferrara N: Pharmacology and pharmacodynamics of bevacizumab as monotherapy or in combination with cytotoxic therapy in preclinical studies. Cancer Res 2005; 65(3); 671 - 680

Gillies RJ and Morse DL: In vivo magnetic resonance spectroscopy in cancer. Annu Rev Biomed Eng 2005; 7287 - 326

Giskeodegard GF et al: Multivariate modeling and prediction of breast cancer prognostic factors using MR metabolomics. J Proteome Res 2010; 9(2); 972 - 979

Glunde K et al: Magnetic resonance spectroscopy in metabolic and molecular imaging and diagnosis of cancer. Chem Rev 2010; 110(5); 3043 - 3059

Glunde K and Bhujwalla ZM: Metabolic tumor imaging using magnetic resonance spectroscopy. Semin Oncol 2011; 38(1); 26 - 41

Glunde K et al: Choline metabolism in cancer: implications for diagnosis and therapy. Expert Rev Mol Diagn 2006; 6(6); 821 - 829

Glunde K et al: Molecular causes of the aberrant choline phospholipid metabolism in breast cancer. Cancer Res 2004; 64(12); 4270 - 4276

Glunde K et al: Hypoxia regulates choline kinase expression through hypoxia-inducible factor-1 alpha signaling in a human prostate cancer model. Cancer Res 2008; 68(1); 172 - 180

Golman K et al: Metabolic imaging by hyperpolarized 13C magnetic resonance imaging for in vivo tumor diagnosis. Cancer Res 2006; 66(22); 10855 - 10860

Gottschalk S et al: Imatinib (STI571)-mediated changes in glucose metabolism in human leukemia BCR-ABL-positive cells. Clin Cancer Res 2004; 10(19); 6661 - 6668

Gown AM: Current issues in ER and HER2 testing by IHC in breast cancer. Mod Pathol 2008; 21 Suppl 2S8 - S15

Gravdal K et al: Proliferation of immature tumor vessels is a novel marker of clinical progression in prostate cancer. Cancer Res 2009; 69(11); 4708 - 4715

Gribbestad IS et al: Contrast-enhanced magnetic resonance imaging of the breast. Acta Oncol 1992; 31(8); 833 - 842

Griffiths JR and Iles RA: NMR studies of tumours. Biosci Rep 1982; 2(9); 719 - 725

Gulliksrud K et al: Dynamic contrast-enhanced magnetic resonance imaging of tumor interstitial fluid pressure. Radiother Oncol 2009; 91(1); 107 - 113

Gulliksrud K et al: Assessment of tumor hypoxia and interstitial fluid pressure by gadomelitol-based dynamic contrast-enhanced magnetic resonance imaging. Radiother Oncol 2011;

Haddadin IS et al: Metabolite quantification and high-field MRS in breast cancer. NMR Biomed 2009; 22(1); 65 - 76

Hanahan D and Weinberg RA: The hallmarks of cancer. Cell 2000; 100(1); 57 - 70

Harries M and Smith I: The development and clinical use of trastuzumab (Herceptin). Endocr Relat Cancer 2002; 9(2); 75 - 85

Hata T et al: Magnetic resonance imaging for preoperative evaluation of breast cancer: a comparative study with mammography and ultrasonography. J Am Coll Surg 2004; 198(2); 190 - 197

Hayes DF: Bevacizumab treatment for solid tumors: boon or bust? JAMA 2011; 305(5); 506 - 508

Heldahl MG et al: Prognostic value of pretreatment dynamic contrast-enhanced MR imaging in breast cancer patients receiving neoadjuvant chemotherapy: overall survival predicted from combined time course and volume analysis. Acta Radiol 2010; 51(6); 604 - 612

Heyer J et al: Non-germline genetically engineered mouse models for translational cancer research. Nat Rev Cancer 2010; 10(7); 470 - 480

Jagannathan NR: Breast MR. NMR Biomed 2009; 22(1); 1 - 2

Jain RK: Normalization of tumor vasculature: an emerging concept in antiangiogenic therapy. Science 2005; 307(5706); 58 - 62

Jain RK et al: Biomarkers of response and resistance to antiangiogenic therapy. Nat Rev Clin Oncol 2009; 6(6); 327 - 338

Jensen LR et al: Assessment of early docetaxel response in an experimental model of human breast cancer using DCE-MRI, ex vivo HR MAS, and in vivo 1H MRS. NMR Biomed 2010; 23(1); 56 - 65

Johansen R et al: Predicting survival and early clinical response to primary chemotherapy for patients with locally advanced breast cancer using DCE-MRI. J Magn Reson Imaging 2009; 29(6); 1300 - 1307

Johnston SR: New strategies in estrogen receptor-positive breast cancer. Clin Cancer Res 2010; 16(7); 1979 - 1987

Kanehisa M and Goto S: KEGG: kyoto encyclopedia of genes and genomes. Nucleic Acids Res 2000; 28(1); 27 - 30

Katz-Brull R et al: Clinical utility of proton magnetic resonance spectroscopy in characterizing breast lesions. J Natl Cancer Inst 2002a; 94(16); 1197 - 1203

Katz-Brull R et al: Metabolic markers of breast cancer: enhanced choline metabolism and reduced choline-ether-phospholipid synthesis. Cancer Res 2002b; 62(7); 1966 - 1970

Keshari KR et al: Correlation of phospholipid metabolites with prostate cancer pathologic grade, proliferative status and surgical stage - impact of tissue environment. NMR Biomed 2011; 24(6); 691 - 699

Kim H et al: Breast tumor xenografts: diffusion-weighted MR imaging to assess early therapy with novel apoptosis-inducing anti-DR5 antibody. Radiology 2008; 248(3); 844 - 851

King A and Gottlieb E: Glucose metabolism and programmed cell death: an evolutionary and mechanistic perspective. Curr Opin Cell Biol 2009; 21(6); 885 - 893

Kreike B et al: Gene expression profiling and histopathological characterization of triple-negative/basal-like breast carcinomas. Breast Cancer Res 2007; 9(5); R65 -

Kuhl CK et al: Dynamic bilateral contrast-enhanced MR imaging of the breast: trade-off between spatial and temporal resolution. Radiology 2005; 236(3); 789 - 800

Kul S et al: Contribution of diffusion-weighted imaging to dynamic contrast-enhanced MRI in the characterization of breast tumors. AJR Am J Roentgenol 2011; 196(1); 210 - 217

Kurhanewicz J et al: Current and potential applications of clinical 13C MR spectroscopy. J Nucl Med 2008; 49(3); 341 - 344

La Vecchia C. et al: Cancer mortality in Europe, 2000-2004, and an overview of trends since 1975. Ann Oncol 2010; 21(6); 1323 - 1360

Lacal JC: Choline kinase: a novel target for antitumor drugs. IDrugs 2001; 4(4); 419 - 426

Lacroix M and Leclercq G: Relevance of breast cancer cell lines as models for breast tumours: an update. Breast Cancer Res Treat 2004; 83(3); 249 - 289

Lane HA et al: mTOR inhibitor RAD001 (everolimus) has antiangiogenic/vascular properties distinct from a VEGFR tyrosine kinase inhibitor. Clin Cancer Res 2009; 15(5); 1612 - 1622

Larsson HB et al: Quantitation of blood-brain barrier defect by magnetic resonance imaging and gadolinium-DTPA in patients with multiple sclerosis and brain tumors. Magn Reson Med 1990; 16(1); 117 - 131

Leung DW et al: Vascular endothelial growth factor is a secreted angiogenic mitogen. Science 1989; 246(4935); 1306 - 1309

Levitzki A and Klein S: Signal transduction therapy of cancer. Mol Aspects Med 2010; 31(4); 287 - 329

Lock R et al: Autophagy Facilitates Glycolysis During Ras Mediated Oncogenic Transformation. Mol Biol Cell 2011; 22(2); 165 - 178

Loi S et al: Gene expression profiling identifies activated growth factor signaling in poor prognosis (Luminal-B) estrogen receptor positive breast cancer. BMC Med Genomics 2009; 237 -

Loveless ME et al: A quantitative comparison of the influence of individual versus population-derived vascular input functions on dynamic contrast enhanced-MRI in small animals. Magn Reson Med 2011;

Mann RM et al: Breast MRI: guidelines from the European Society of Breast Imaging. Eur Radiol 2008; 18(7); 1307 - 1318

Marangoni E et al: A new model of patient tumor-derived breast cancer xenografts for preclinical assays. Clin Cancer Res 2007; 13(13); 3989 - 3998

McLaughlin R and Hylton N: MRI in breast cancer therapy monitoring. NMR Biomed 2011a; 24(6); 712 - 720

McLaughlin R and Hylton N: MRI in breast cancer therapy monitoring. NMR Biomed 2011b; 24(6); 712 - 720

Moestue S et al: Metabolic effects of signal transduction inhibition in cancer assessed by magnetic resonance spectroscopy. Mol Oncol 2011a; 5(3); 224 - 241

Moestue S et al: HR MAS MR Spectroscopy in Metabolic Characterization of Cancer. Curr Top Med Chem 2011b; 11(1); 2 - 26

Moestue SA et al: Distinct choline metabolic profiles are associated with differences in gene expression for basal-like and luminal-like breast cancer xenograft models. BMC Cancer 2010; 10433 -

Morse DL et al: Characterization of breast cancers and therapy response by MRS and quantitative gene expression profiling in the choline pathway. NMR Biomed 2009; 22(1); 114 - 127

Nalwoga H et al: Vascular proliferation is increased in basal-like breast cancer. Breast Cancer Res Treat 2011;

Naume B et al: Presence of bone marrow micrometastasis is associated with different recurrence risk within molecular subtypes of breast cancer. Mol Oncol 2007; 1(2); 160 - 171

Neeman M and Degani H: Metabolic studies of estrogen- and tamoxifen-treated human breast cancer cells by nuclear magnetic resonance spectroscopy. Cancer Res 1989; 49(3); 589 - 594

Norsk bryst cancer gruppe (NBCG): Blåboka. Retningslinjer for brystkreftbehandling. www nbcg no 2011;

Osborne CK: Steroid hormone receptors in breast cancer management. Breast Cancer Res Treat 1998; 51(3); 227 - 238

Osborne CK and Schiff R: Estrogen-receptor biology: continuing progress and therapeutic implications. J Clin Oncol 2005; 23(8); 1616 - 1622

Padhani AR: MRI for assessing antivascular cancer treatments. Br J Radiol 2003; 76 Spec No 1S60 - S80

Padhani AR et al: Prediction of clinicopathologic response of breast cancer to primary chemotherapy at contrast-enhanced MR imaging: initial clinical results. Radiology 2006; 239(2); 361 - 374

Padhani AR and Koh DM: Diffusion MR imaging for monitoring of treatment response. Magn Reson Imaging Clin N Am 2011; 19(1); 181 - 209

Padhani AR et al: Diffusion-weighted magnetic resonance imaging as a cancer biomarker: consensus and recommendations. Neoplasia 2009; 11(2); 102 - 125

Park SH et al: Diffusion-weighted MR imaging: pretreatment prediction of response to neoadjuvant chemotherapy in patients with breast cancer. Radiology 2010; 257(1); 56 - 63

Partridge SC et al: Quantitative diffusion-weighted imaging as an adjunct to conventional breast MRI for improved positive predictive value. AJR Am J Roentgenol 2009; 193(6); 1716 - 1722

Perou CM and Borresen-Dale AL: Systems Biology and Genomics of Breast Cancer. Cold Spring Harb Perspect Biol 2010;

Perou CM et al: Molecular portraits of human breast tumours. Nature 2000; 406(6797); 747 - 752

Pickles MD et al: Diffusion changes precede size reduction in neoadjuvant treatment of breast cancer. Magn Reson Imaging 2006; 24(7); 843 - 847

Pickles MD et al: Role of dynamic contrast enhanced MRI in monitoring early response of locally advanced breast cancer to neoadjuvant chemotherapy. Breast Cancer Res Treat 2005; 91(1); 1 - 10

Pickles MD et al: Prognostic value of pre-treatment DCE-MRI parameters in predicting disease free and overall survival for breast cancer patients undergoing neoadjuvant chemotherapy. Eur J Radiol 2009; 71(3); 498 - 505

Podo F: Tumour phospholipid metabolism. NMR Biomed 1999; 12(7); 413 - 439

Podo F et al: Triple-negative breast cancer: present challenges and new perspectives. Mol Oncol 2010; 4(3); 209 - 229

Poptani H et al: Cyclophosphamide treatment modifies tumor oxygenation and glycolytic rates of RIF-1 tumors: 13C magnetic resonance spectroscopy,

Eppendorf electrode, and redox scanning. Cancer Res 2003; 63(24); 8813 - 8820

Portais JC et al: Glucose and glutamine metabolism in C6 glioma cells studied by carbon 13 NMR. Biochimie 1996; 78(3); 155 - 164

Preda A et al: MRI monitoring of Avastin antiangiogenesis therapy using B22956/1, a new blood pool contrast agent, in an experimental model of human cancer. J Magn Reson Imaging 2004; 20(5); 865 - 873

Purcell EM et al: Resonance absorption by nuclear magnetic moments in a solid. 1946; 6937 - 38

Rabi II et al: A new method of measuring nuclear magnetic moment. 1938; 53318 - 318

Rakha EA and Ellis IO: Triple-negative/basal-like breast cancer: review. Pathology 2009; 41(1); 40 - 47

Rofstad EK et al: Radiocurability is associated with interstitial fluid pressure in human tumor xenografts. Neoplasia 2009; 11(11); 1243 - 1251

Sankaranarayanapillai M et al: Detection of histone deacetylase inhibition by noninvasive magnetic resonance spectroscopy. Mol Cancer Ther 2006; 5(5); 1325 - 1334

Sardanelli F et al: Magnetic resonance imaging of the breast: recommendations from the EUSOMA working group. Eur J Cancer 2010; 46(8); 1296 - 1316

Sardanelli F et al: Multicenter surveillance of women at high genetic breast cancer risk using mammography, ultrasonography, and contrast-enhanced magnetic resonance imaging (the high breast cancer risk italian 1 study): final results. Invest Radiol 2011; 46(2); 94 - 105

Schnall MD et al: MRI detection of distinct incidental cancer in women with primary breast cancer studied in IBMC 6883. J Surg Oncol 2005; 92(1); 32 - 38

Schnell CR et al: Effects of the dual phosphatidylinositol 3-kinase/mammalian target of rapamycin inhibitor NVP-BEZ235 on the tumor vasculature: implications for clinical imaging. Cancer Res 2008; 68(16); 6598 - 6607

Schwartz DL et al: Radiosensitization and stromal imaging response correlates for the HIF-1 inhibitor PX-478 given with or without chemotherapy in pancreatic cancer. Mol Cancer Ther 2010; 9(7); 2057 - 2067

Segers J et al: Potentiation of cyclophosphamide chemotherapy using the anti-angiogenic drug thalidomide: importance of optimal scheduling to exploit the 'normalization' window of the tumor vasculature. Cancer Lett 2006; 244(1); 129 - 135

Seton-Rogers S: Metabolism: Flexible flux. Nat Rev Cancer 2011; 11(9); 621 -

Shao W and Brown M: Advances in estrogen receptor biology: prospects for improvements in targeted breast cancer therapy. Breast Cancer Res 2004; 6(1); 39 - 52

Singletary SE and Greene FL: Revision of breast cancer staging: the 6th edition of the TNM Classification. Semin Surg Oncol 2003; 21(1); 53 - 59

Sitter B et al: Quantification of metabolites in breast cancer patients with different clinical prognosis using HR MAS MR spectroscopy. NMR Biomed 2010a;

Sitter B et al: Quantification of metabolites in breast cancer patients with different clinical prognosis using HR MAS MR spectroscopy. NMR Biomed 2010b; 23(4); 424 - 431

Sitter B et al: Comparison of HR MAS MR spectroscopic profiles of breast cancer tissue with clinical parameters. NMR Biomed 2006; 19(1); 30 - 40

Slamon DJ et al: Studies of the HER-2/neu proto-oncogene in human breast and ovarian cancer. Science 1989; 244(4905); 707 - 712

Sorlie T et al: Gene expression patterns of breast carcinomas distinguish tumor subclasses with clinical implications. Proc Natl Acad Sci U S A 2001; 98(19); 10869 - 10874

Stefansson IM et al: Vascular proliferation is important for clinical progress of endometrial cancer. Cancer Res 2006; 66(6); 3303 - 3309

Stejskal EO and Tanner JE: Spin diffusion measurements: Spin echoes in the presence of a time-dependent field gradient. 1965; 42288 - 292

Sterin M et al: Levels of phospholipid metabolites in breast cancer cells treated with antimitotic drugs: a 31P-magnetic resonance spectroscopy study. Cancer Res 2001; 61(20); 7536 - 7543

Tennant DA et al: Metabolic transformation in cancer. Carcinogenesis 2009; 30(8); 1269 - 1280

Tennant DA et al: Targeting metabolic transformation for cancer therapy. Nat Rev Cancer 2010; 10(4); 267 - 277

Tessem MB et al: Evaluation of lactate and alanine as metabolic biomarkers of prostate cancer using 1H HR-MAS spectroscopy of biopsy tissues. Magn Reson Med 2008; 60(3); 510 - 516

Tofts PS et al: Estimating kinetic parameters from dynamic contrast-enhanced T(1)-weighted MRI of a diffusable tracer: standardized quantities and symbols. J Magn Reson Imaging 1999; 10(3); 223 - 232

Tozaki M and Fukuma E: 1H MR spectroscopy and diffusion-weighted imaging of the breast: are they useful tools for characterizing breast lesions before biopsy? AJR Am J Roentgenol 2009; 193(3); 840 - 849

Turetschek K et al: Tumor microvascular changes in antiangiogenic treatment: assessment by magnetic resonance contrast media of different molecular weights. J Magn Reson Imaging 2004; 20(1); 138 - 144

Turnbull L et al: Comparative effectiveness of MRI in breast cancer (COMICE) trial: a randomised controlled trial. Lancet 2010; 375(9714); 563 - 571

Turnbull LW: Dynamic contrast-enhanced MRI in the diagnosis and management of breast cancer. NMR Biomed 2009; 22(1); 28 - 39

Vander Heiden MG et al: Understanding the Warburg effect: the metabolic requirements of cell proliferation. Science 2009; 324(5930); 1029 - 1033

Vargo-Gogola T and Rosen JM: Modelling breast cancer: one size does not fit all. Nat Rev Cancer 2007; 7(9); 659 - 672

Walenta S et al: Lactate in solid malignant tumors: potential basis of a metabolic classification in clinical oncology. Curr Med Chem 2004; 11(16); 2195 - 2204

Warburg O: Über den stoffwechsel der carcinomzelle. 1924; 12(50); 1132 - 1137

Wedam SB et al: Antiangiogenic and antitumor effects of bevacizumab in patients with inflammatory and locally advanced breast cancer. J Clin Oncol 2006; 24(5); 769 - 777

Wider G and Dreier L: Measuring protein concentrations by NMR spectroscopy. J Am Chem Soc 2006; 128(8); 2571 - 2576

Wijnen JP et al: In vivo (13)C magnetic resonance spectroscopy of a human brain tumor after application of (13)C-1-enriched glucose. Magn Reson Imaging 2010;

Wu X et al: Tumor characterization with dynamic contrast enhanced magnetic resonance imaging and biodegradable macromolecular contrast agents in mice. Pharm Res 2009; 26(9); 2202 - 2208

Yalcin A et al: Selective inhibition of choline kinase simultaneously attenuates MAPK and PI3K/AKT signaling. Oncogene 2010; 29(1); 139 - 149

Yamada K et al: Effect of intravenous gadolinium-DTPA on diffusion-weighted images: evaluation of normal brain and infarcts. Stroke 2002; 33(7); 1799 - 1802

Yeung SJ et al: Roles of p53, MYC and HIF-1 in regulating glycolysis - the seventh hallmark of cancer. Cell Mol Life Sci 2008; 65(24); 3981 - 3999

Yu KD et al: Different Distribution of Breast Cancer Subtypes in Breast Ductal Carcinoma in situ (DCIS), DCIS with Microinvasion, and DCIS with Invasion Component. Ann Surg Oncol 2010;

Paper I

Moestue et al. BMC Cancer 2010, 10:433
http://www.biomedcentral.com/1471-2407/10/433

BMC Cancer

RESEARCH ARTICLE Open Access

Distinct choline metabolic profiles are associated with differences in gene expression for basal-like and luminal-like breast cancer xenograft models

Siver A Moestue[1*], Eldrid Borgan[1,2], Else M Huuse[1], Evita M Lindholm[3], Beathe Sitter[1], Anne-Lise Børresen-Dale[2,4], Olav Engebraaten[3,4], Gunhild M Mælandsmo[3], Ingrid S Gribbestad[1]

Abstract

Background: Increased concentrations of choline-containing compounds are frequently observed in breast carcinomas, and may serve as biomarkers for both diagnostic and treatment monitoring purposes. However, underlying mechanisms for the abnormal choline metabolism are poorly understood.

Methods: The concentrations of choline-derived metabolites were determined in xenografted primary human breast carcinomas, representing basal-like and luminal-like subtypes. Quantification of metabolites in fresh frozen tissue was performed using high-resolution magic angle spinning magnetic resonance spectroscopy (HR MAS MRS).
The expression of genes involved in phosphatidylcholine (PtdCho) metabolism was retrieved from whole genome expression microarray analyses.
The metabolite profiles from xenografts were compared with profiles from human breast cancer, sampled from patients with estrogen/progesterone receptor positive (ER+/PgR+) or triple negative (ER-/PgR-/HER2-) breast cancer.

Results: In basal-like xenografts, glycerophosphocholine (GPC) concentrations were higher than phosphocholine (PCho) concentrations, whereas this pattern was reversed in luminal-like xenografts. These differences may be explained by lower choline kinase (*CHKA*, *CHKB*) expression as well as higher PtdCho degradation mediated by higher expression of phospholipase A2 group 4A (*PLA2G4A*) and phospholipase B1 (*PLB1*) in the basal-like model. The glycine concentration was higher in the basal-like model. Although glycine could be derived from energy metabolism pathways, the gene expression data suggested a metabolic shift from PtdCho synthesis to glycine formation in basal-like xenografts. In agreement with results from the xenograft models, tissue samples from triple negative breast carcinomas had higher GPC/PCho ratio than samples from ER+/PgR+ carcinomas, suggesting that the choline metabolism in the experimental models is representative for luminal-like and basal-like human breast cancer.

Conclusions: The differences in choline metabolite concentrations corresponded well with differences in gene expression, demonstrating distinct metabolic profiles in the xenograft models representing basal-like and luminal-like breast cancer. The same characteristics of choline metabolite profiles were also observed in patient material from ER+/PgR+ and triple-negative breast cancer, suggesting that the xenografts are relevant model systems for studies of choline metabolism in luminal-like and basal-like breast cancer.

* Correspondence: siver.a.moestue@ntnu.no
[1]Department of Circulation and Medical Imaging, Norwegian University of Science and Technology (NTNU), Trondheim, Norway
Full list of author information is available at the end of the article

Background

Optimal treatment of individual breast cancer patients is still a major challenge in oncology. An approach to improve and individualize the treatment beyond the markers and stratification tools used at present, is through molecular subtyping of breast cancer [1]. Based on variation in gene expression profiles, five molecular subtypes have been identified [1-3]. The gene expression patterns of these subtypes are similar across multiple samples from the same tumor, shows no treatment-related changes and have been reproduced in a number of patient populations [2-7]. However, the current use of these molecular subgroups in clinical practice remains limited. Further understanding of the differences in biology between the various subtypes is needed in order to predict therapeutic response and provide individual treatment strategies based on gene expression profiles [8].

Elevated levels of choline metabolites is a known feature of breast cancer, and it has been shown that drugs targeting choline metabolism have selective *in vivo* and *in vitro* cytotoxic efficacy against a variety of cancer types [9-13]. Magnetic resonance spectroscopy (MRS) is a valuable tool for studies of choline metabolism both in patients and in experimental systems [14]. High resolution magic angle spinning (HR MAS) MRS of *ex vivo* tissue samples has been particularly useful, as it allows assessment of individual choline metabolites in intact tissue specimens. Increased concentrations of choline, phosphocholine (PCho) and glycerophosphocholine (GPC) has been demonstrated both in cultured breast cancer cells [15-17] and in human breast cancer biopsies [18-21]. It has also been shown that choline metabolism is altered following chemotherapy, suggesting the possibility of using MRS for therapy monitoring [22-24]. However, to utilize these findings in diagnosis and individualized therapy monitoring of breast cancer patients, a better understanding of the choline metabolism abnormalities on a molecular level is needed.

Several studies investigating expression of genes involved in metabolism of phosphatidylcholine (PtdCho) have been performed using breast cancer cell lines [16,17,25,26]. PtdCho is an important cellular membrane lipid, and this metabolic pathway directly involves choline, PCho and GPC. In addition, genes involved in transmembrane choline transport and conversion of choline to glycine have been suggested to be important for the observed choline concentrations in breast cancer cells [16,27]. The choline metabolism profiles observed in cultured breast cancer cells are more homogenous than those seen in human biopsies. In order to bridge the gap between *in vitro* research and clinical breast cancer, there is a great need for animal models representing different types of breast cancer for use in functional and mechanistic studies. Serial orthotopic transplantation of clinical tumor isolates in immunodeficient mice is considered a promising tool for investigation of human breast cancer biology [28]. Establishment of relevant experimental models of basal-like breast cancer is especially important both in order to understand the special characteristics of this subtype, to find potential new molecular targets for therapy and to establish potential biomarkers for monitoring response to therapy.

The aim of this study was to compare the choline metabolite patterns in animal models of basal-like and luminal-like subtypes of breast cancer, and to study the expression of genes related to choline metabolism in order to explain the differences between the two breast cancer subtypes. The two orthotopic xenograft models used, MAS98.12 and MAS98.06, represent basal-like and luminal-like subtypes of breast cancer, respectively [29]. Both models have been established by direct inoculation of primary human tumor material into immunodeficient animals. The content of creatine, choline, PCho, GPC, taurine and glycine in the xenografts as well as human breast cancer tissue samples was determined using HR MAS MRS. The molecular basis of the observed differences in choline metabolism was studied using gene expression microarray data. In order to evaluate if the xenograft models are representative for human disease, the metabolic profiles were compared to corresponding profiles from patients with ER+/PgR+ or triple negative breast cancer.

Methods

Animal model

The MAS98.12 and MAS98.06 tumor models were established by orthotopic implantation of biopsy tissues from primary mammary carcinomas in SCID mice as previously described [29]. Both the primary carcinomas and the xenograft models have been characterized using gene expression profiling. These analyses demonstrated that the primary carcinomas could be classified as luminal-like and basal-like subtypes of breast cancer, and that these molecular subtypes were retained in the MAS98.06 (luminal-like) and MAS98.12 (basal-like) xenografts. Relevant characteristics of the models are presented in Table 1. The tumors are serially transplanted. Tissue used for HR MAS MRS was from passage 47 (MAS98.12) and 28 (MAS98.06), and tissue used for RNA microarray analysis was from passage 45 (MAS98.12) and 25 (MAS98.06).

The animals were kept under pathogen-free conditions. Housing conditions included temperature between 19°C and 22°C, humidity between 50% and 60%, 20 air

Table 1 Summary of xenograft characteristics

	Basal-like xenograft (MAS98.12)		Luminal-like xenograft (MAS98.06)	
	Primary tumor	**Xenograft**	**Primary tumor**	**Xenograft**
Tumor grade	Grade III IDC	NA	Grade III IDC	NA
Lymph node status	No metastasis	NA	Metastasis to 12 of 25 nodes No distant metastases	NA
Differentiation	Poorly differentiated	Poorly differentiated	Well differentiated	Poorly differentiated
Hormone receptor status	ER-/PgR+**	ER-/PgR-	ER+/PgR+	ER+/PgR+
ERBB2 amplification*	Negative	Negative	Negative	Negative
Intrinsic molecular subtype	Basal-like	Basal-like	Luminal-like	Luminal-like
TP53 status	Wildtype	Mutated	Mutated	Mutated
Volume doubling time	NA	1-2 days	NA	7 days
Proliferation index (Ki67)	Missing	28%	Missing	35%

Summary of characteristics related to genotype and phenotype of the xenograft models

* Measured at the DNA level by array Comparative Genomic Hybridization (aCGH)

** The primary basal-like carcinoma had very weak cytoplasmic staining for PgR[29].

changes/hr and a 12 hr light/dark cycle. The animals were fed RM1 diet (Scanbur BK, Norway) and distilled tap water *ad libitum*. The drinking water was supplemented with 17-β-estradiol at a concentration of 4 μg/ml in order to ensure stimulation of the estrogen receptors and promote tumor growth in the MAS98.06 xenografts. With respect to tumor growth rate, this estrogen supplement correspond to the use of s.c. continuous release 17-β-estradiol pellets (1.7 mg/pellet), which were used during establishment of the animal models [29]. To provide equal experimental conditions, the MAS98.12 xenografts also received estradiol supplement. This could in theory cause non-ER-mediated effects on choline metabolite profile. However, the similarities between human tissue samples and xenograft tissue suggest that such effects are insignificant in ER-breast cancer.

Following sacrifice by cervical dislocation, tumor tissue was harvested from 10 animals from each model for the HR MAS MRS analyses and for 6 animals from each model for gene expression microarray analyses, at tumor diameters of approximately 13-15 mm. Samples were put in cryogenic vials and immersed in liquid nitrogen immediately after dissection and stored under cryogenic conditions until analysis. All procedures and experiments involving animals were approved by The National Animal Research Authority, and carried out according to the European Convention for the Protection of Vertebrates used for Scientific Purposes.

Human tissue samples

For comparison of xenograft models with human breast cancer tissue, biopsies from 22 breast cancer patients were identified in our internal database based on histopathology/immunohistochemistry data. Patients with either ER+/PgR+ (n = 14) or triple negative (n = 8) phenotype were included. Biopsy material was obtained during surgery and immediately frozen in liquid nitrogen. Histopathology and immunohistochemistry data for the selected patients was obtained from hospital records. Patient and tumor characteristics are presented in Table 2. The biopsy material was subject to HR MAS MRS analysis and subsequent histopathological evaluation using hematoxylin/eosin (HE) staining. The use of patient material was approved by the Regional Committee for Medical and Health Research Ethics, and informed written consent was obtained from all included patients.

HR MAS MRS of xenograft tissue

Storage time before HR MAS MRS analysis was less than one month for all 20 samples. Macroscopically viable tumor tissue was cut to fit a 30 μl disposable insert (Bruker Biospin Corp.), prefilled with 3 μl PBS made on D_2O containing 98.8 mM trimethylsilyltetradeuteropropionic acid (TSP) for chemical shift referencing. The average sample weight was 15 ± 3 mg (mean ± SD). HR MAS MR spectra were recorded using a Bruker AVANCE DRX600 spectrometer equipped with a $^{1}H/^{13}C$ HR MAS probe (Bruker BioSpin Corp.). Samples were spun at 5 kHz with an instrumental temperature setting of 4°C. A pulse-acquired experiment including the ERETIC sequence (ereticpr.drx; Bruker) was performed for all samples. The ERETIC signal was positioned at -1.0 ppm. The water resonance was saturated for 15 seconds (60 dB continuous wave), followed by a 60-degree pulse for excitation. Signals were collected over a sweep width of 16.7 ppm. 128 FIDs were acquired into 64K points during 3.28 seconds. Spectra were Fourier transformed into 128K after 0.3 Hz exponential line broadening and chemical shifts were calibrated to the TSP singlet at 0 ppm. Spectral

Table 2 Summary of patient characteristics

Subtype	n	Patient age (years)	Phenotype	Tumor grade1/2/3	Tumor size (cm)	Mean tumor fraction (%)	Mean connective tissue fraction (%)	Mean fatty tissue fraction (%)
ER+/PgR+	14	57 ± 16	ER+/PgR+	1/10/3	2.3 ± 1.3	23 ± 11	72 ± 11	5 ± 7
Triple negative	8	57 ± 17	ER-/PgR-/HER2-	0/3/5	2.2 ± 1.0	38 ± 32	55 ± 31	6 ± 7

Summary of patient and sample characteristics of the different subgroups of human tissue samples (mean ± SD)

assignments were performed based on a previous HR MAS MRS study of breast cancer lesions [30]. One HR MAS MRS spectrum from the MAS98.06 animals was lost due to technical error.

The regions from 0.20 to -0.20 ppm (TSP), -0.85 to -1.15 ppm (ERETIC) and 3.60 to 2.90 ppm (glycine, taurine, GPC, PCho, choline, and creatine) were selected for quantification in all spectra. Peak areas were calculated by curve fitting (PeakFit v 4, Systat Software Inc) using a combination of Gaussian and Lorentzian lineshapes (Voigt function). The correlation coefficient of the fit (r^2) was > 0.95 for all spectra. The ERETIC signal was quantified to 3.17×10^{-7} moles using a series of creatine calibration standards as previously described [31]. Concentrations of tissue metabolites ([*MET*]) were calculated relative to the ERETIC signal using equation (1):

$$[MET] = \frac{A_{MET}}{A_{ERETIC}} \times \frac{1}{k_{MET}} \times \frac{n_{ERETIC}}{m_{sample}} \quad (1)$$

A_{MET} and A_{ERETIC} are the calculated areas of the metabolite and the ERETIC signals, respectively; k_{MET} is the number of protons giving rise to the metabolite signal; n_{ERETIC} is the number of moles the ERETIC signal represents; and m_{sample} is the mass of the sample. The metabolite concentrations measured using the ERETIC signal were compared using a 2-sided Student's t-test with a significance level of $p < 0.05$ using Sigmaplot 11.0 (Systat Software Inc.).

HR MAS MRS of human tissue samples

Human tissue samples were prepared for HR MAS MRS analysis using the same procedure as the xenograft samples. Spectra were acquired using a spin-echo Carr-Purcell-Meiboom-Gill sequence (cpmgpr; Bruker) with 2 s water suppression prior to a 90° excitation pulse. The spin-echo sequence for suppression of broad peaks was performed using a delay of 1 ms repeated 136 times, resulting in an effective echo time of 285 ms. A total of 128 scans over a spectral region of 10 kHz were collected into 32k points during 1.64 s. The spectra were Fourier transformed into 128 K after 0.3 Hz exponential line broadening, and the metabolite region from 3.60 to 3.00 ppm was selected for further evaluation. The spectra were normalized by scaling the spectral data of all samples to achieve an equal total area for each spectrum. Metabolite peak areas were then obtained by curve fitting as described above.

Histopathology

Following HR MAS MRS analysis, the xenograft samples were fixed in 10% neutral buffered formalin and embedded in paraffin. One histopathological section were prepared from each sample, stained with hematoxylin/eosin/saffron (HES) according to standard protocol and evaluated microscopically. A visual evaluation with respect to the presence of viable tumor tissue and the extent of necrosis was performed. Tumor grade, hormone receptor status and HER2 expression of human tissue samples was obtained from hospital records. In addition, specimens analysed by HR MAS MRS were HES-stained and the relative areas of normal and neoplastic epithelial tissue, necrotic tissue, fat and fibrous connective tissue were scored.

Gene expression analysis

Gene expression analysis was performed on tumor tissue from 6 animals from each of the two xenograft models, using a one-color microarray-based platform (Agilent). Total RNA was isolated from snap frozen tumor tissue using TRIzol (Invitrogen) and resuspended in RNase-free water. Total RNA (700 ng) was amplified, labelled with Cy3, and 1.65 μg cRNA was hybridized to 4 × 44 k Agilent Whole Human Genome Oligo Microarrays at 60°C and 10 rpm for 17 hours, according to the manufacturer's protocol. The arrays were scanned using an Agilent G2565A DNA microarray scanner and extracted using Feature Extraction (v 10.1.1.1, Agilent). One microarray from the MAS98.06 model was removed due to poor array quality. The microarray data was normalized and analysed using R (v 2.9.0) and the LIMMA Bioconductor package [32]. The raw signals were corrected for multiplicative detrending effects and the arrays were quantile normalized and log2 transformed. Probes which were flagged as outliers by the Feature Extraction software or were present in less than 30% of the samples, were removed. The signal intensities were averaged between duplicate probes, and the probe with the highest interquartile range was selected to represent each unique transcript.

A total of 119 genes were selected for further analysis. The selection criteria were a) genes involved in KEGG *homo sapiens* glycerophospholipid pathway hsa:00564 [33], or b) genes coding for proteins reported to be directly involved in choline transport and choline and glycine metabolism [16,34-36]. Of the selected genes, 117 were represented on the microarray (full gene list supplied as additional file 1).

Testing for differential expression between the xenograft models was performed using t-tests with Empirical Bayesian correction of the test statistics [32]. To account for multiple testing, an adjusted p-value of 0.05 (using Benjamini & Hochberg's false discovery rate) was defined as the threshold for significant differential expression between the xenograft models. The microarray data from the significantly differentially expressed genes was centered across genes and clustered across genes and samples using hierarchical clustering with Euclidian distance and complete linkage. The relationship between gene expression and metabolite concentrations was explored using Ingenuity Pathways Analysis (Ingenuity Systems), and an illustration was adapted from the canonical Glycerophospholipid Metabolism and Glycine, Serine and Threonine Metabolism pathways [33]. The abovementioned gene list was also extracted from microarray data from previously described passages of the same xenograft models [29], to ensure that gene expression remain stable throughout serial transplantation of the xenografts.

Results

Histopathology

All xenograft samples were found to contain mainly viable tumor tissue and stromal connective tissue, shown previously to be recruited mouse stromal tissue [29], with negligible necrosis (< 10% area) in 18 of 19 samples. The HR MAS MRS data was therefore considered to be representative of the metabolite concentrations in the solid tumors. One sample in the MAS98.06 group contained a necrotic area, microscopically estimated to 25% area of the specimen. However, the metabolite concentrations measured in this sample differed from the group mean by less than ± 2 SD, and the sample was therefore not excluded from the data set. The mean fractions of tumor and connective tissue in the human tissue samples are presented in Table 2.

HR MAS MRS of xenograft samples

The HR MAS MRS analyses revealed several significant differences in the metabolic profiles of the two xenograft models. Mean ^{1}H HR MAS MRS spectra from the two models are shown in Figure 1 (spectral region 3.6 - 3.0 ppm). The metabolites assigned in Figure 1 were quantifiable in all spectra. The metabolite concentrations calculated using the ERETIC reference signal are presented in Table 3. There was no significant difference in choline concentration between the models. However, the concentrations of GPC and PCho were significantly higher than the choline concentration in both the basal-like and the luminal-like model. While all the samples from basal-like xenografts showed higher concentration of GPC than PCho, the samples from luminal-like xenografts invariably showed lower concentrations of GPC than PCho. The differences in GPC and PCho concentrations between the two xenograft models were statistically significant ($p < 0.001$ and $p < 0.01$, respectively). The concentration of glycine was significantly higher in the basal-like than in the luminal-like model ($p < 0.002$).

HR MAS MRS of human tissue samples

The HR MAS MRS spectra from the tissue samples were retrieved from our internal database, and mean spectra from the two groups are shown in Figure 1. The mean metabolite profiles demonstrated that triple negative breast cancer tissue had high GPC and low PCho concentrations, whereas tissue from ER+/PgR+ patients had low GPC and high PCho. There was a significant difference in the GPC/PCho peak area ratio between ER+/PgR+ and triple negative samples (0.8 ± 0.5 and 1.5 ± 0.7, respectively. $p = 0.01$), corresponding to the findings from the xenograft models. The mean spectra from human tissue samples also suggested that the glycine concentration was higher in triple negative breast cancer tissue samples. Using the glycine/total peak area ratio as marker for glycine content, this trend was not statistically significant ($p = 0.19$). The relative choline peak area was significantly higher in triple negative tissue ($p < 0.00003$) and the relative creatine peak area was significantly lower ($p = 0.024$).

Gene expression analysis of xenograft tissue

Of the 119 investigated genes, 67 were differentially expressed between the xenograft models at a 5% adjusted (false discovery rate) significance level. Microarray data from earlier passages of the same xenograft models [29] showed similar trends of differential expression (data not shown). The complete results from the gene expression analysis are available as additional file. A heatmap of the differentially expressed genes is presented in Figure 2, with hierarchical clustering of genes and samples. In the following sections, only genes directly involved in synthesis and degradation of PtdCho from choline are considered.

Among the five selected genes coding for proteins known to be involved in transmembrane choline transport, only solute carrier family 44, member 1 (*SLC44A1*) showed significantly different expression between the two models. The expression of this transporter, also known as choline transporter-like protein 1 (*CTL1*), was

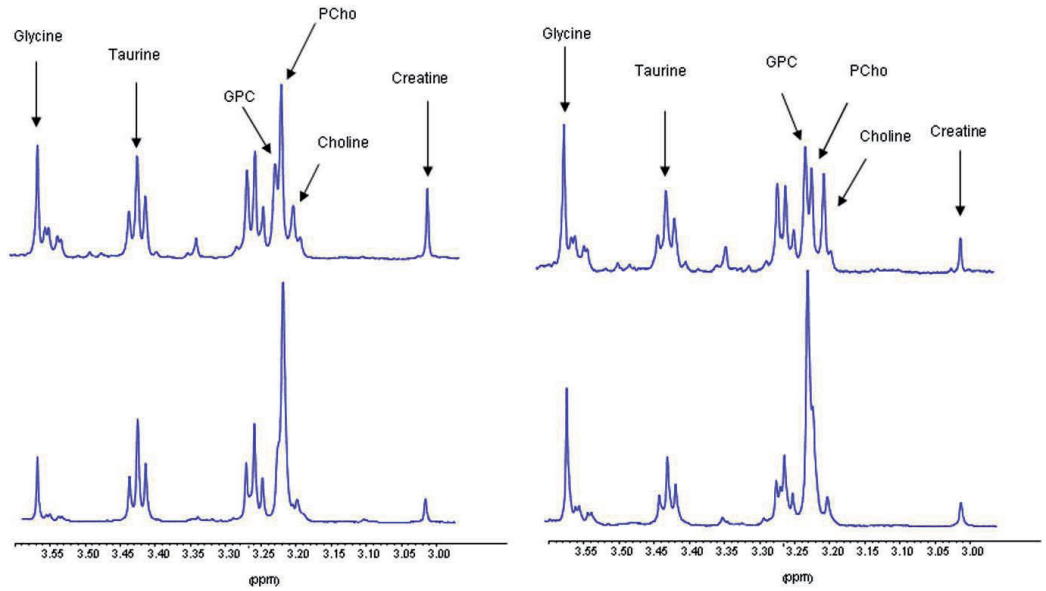

Figure 1 Mean HR MAS MRS spectra from human tissue samples and xenograft tissue. HR MAS MRS spectra (spectral region 3.6 to 3.0 ppm) of ER+/PgR+ (top left) and triple negative (top right) human tissue samples, and luminal-like (bottom left) and basal-like (bottom right) xenograft samples. Spectral assignments are provided for peaks used in quantification.

lower in basal-like than luminal-like xenografts. Solute carrier family 22, member 1 (*SLC22A1*) and solute carrier family 44, member 2 (*SLC44A2*) were similarly expressed in the two models, whereas solute carrier family 5 (choline transporter), member 7 (*SLC5A7*) and solute carrier family 22 (organic cation transporter), member 2 (*SLC22A2*), were expressed below the limit of detection. *SLC5A7* is also known as choline transporter 1 (*CHT1*), a high-affinity choline-specific transporter protein, whereas *SLC44A2* is also known as choline-transporter like protein 2 (*CTL2*).

Genes directly involved in choline metabolism which were differentially expressed between the xenograft models are listed in Table 4 and 5. A schematic overview of intracellular choline metabolite concentrations and the comparative gene expression (the anabolic Kennedy pathway, PtdCho breakdown and conversion of choline to glycine) between the xenograft models is presented in Figure 3. As shown in Figure 3, choline is converted to PCho through the action of two isoforms of the same enzyme, choline kinase alpha and beta. The expression of the genes (*CHKA*, *CHKB*) coding for both isoforms was significantly lower in the basal-like than in the luminal-like model.

Conversion of PCho to CDP-choline is mediated through the alpha and beta isoforms of phosphate cytidylyl transferase 1 (*PCYT1A* and *PCYT1B*). The expression of *PCYT1B* was significantly higher, and *PCYT1A* was significantly lower in the basal-like than the luminal-like model. The gene coding for choline phosphotransferase 1 (*CHPT1*), which converts CDP-PCho to PtdCho, had a significantly lower expression level in the basal-like than in the luminal-like model.

PtdCho is degraded by several different phospholipases. Enzymes in the phosphoplipase A2 group (*PLA2*) convert PtdCho to acyl-GPC. Of the 13 *PLA2* isoforms studied, two were significantly higher expressed in the basal-like model, three were significantly lower expressed, five showed no significant difference in expression and three were below the limit of detection.

Table 3 Metabolite concentrations

	MAS98.12 (n = 10)	MAS98.06 (n = 9)
Creatine	4.1 ± 1.4	3.4 ± 1.7
Choline	1.2 ± 0.7	0.9 ± 0.6
Phosphocholine *	4.5 ± 2.1	9.1 ± 4.4
Glycerophosphocholine **	9.8 ± 2.5	2.7 ± 1.7
Taurine	14.7 ± 4.1	19.1 ± 9.1
Glycine *	8.2 ± 3.0	4.0 ± 1.8

Metabolite concentrations in basal-like (MAS98.12) and luminal-like (MAS98.06) xenografts calculated from HR MAS MRS spectra using the ERETIC method (μmol/g, mean ± SD, * $p < 0.01$, ** $p < 0.001$)

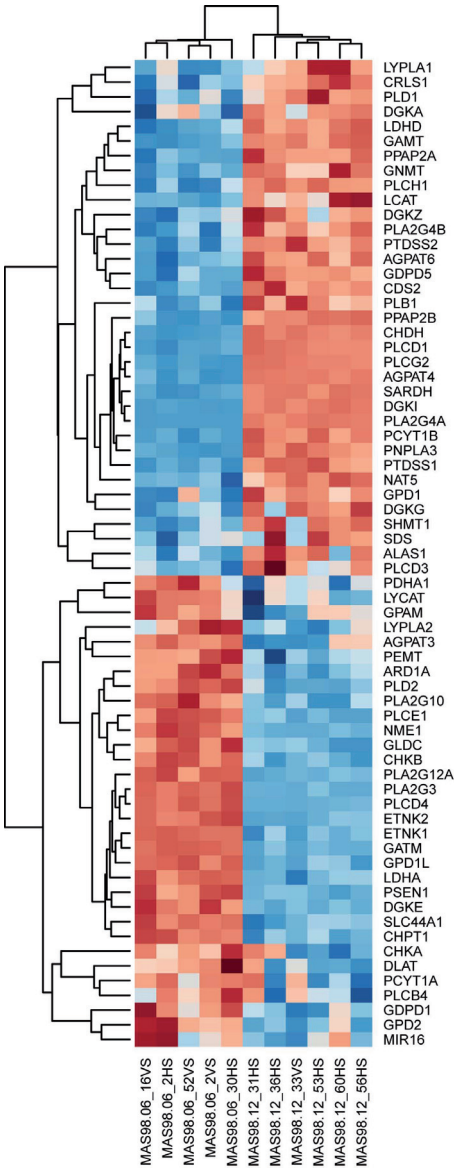

Figure 2 Heatmap of differentially expressed genes in xenograft models. Hierarchical clustering of the 67 differentially expressed genes (false discovery rate < 0.05) involved in the KEGG *homo sapiens* glycerophospholipid pathway hsa:00564, choline transport or directly involved in conversion from choline to glycine (Red: high expression compared to mean expression in xenograft samples. Blue: low expression compared to mean expression in xenograft samples). The microarray data was centred across genes and clustered across genes and samples using Euclidian distance and complete linkage.

The largest difference in gene expression between the two models was found for *PLA2G4A*, where a log2-fold difference of 6.4 in gene expression was observed. Phospholipase B1 (*PLB1*) is involved in both deacetylation steps from PtdCho to GPC, and was significantly higher expressed in the basal-like than in the luminal-like model.

Phospholipase D, with the two isoforms *PLD1* and *PLD2*, converts PtdCho to choline. The expression of *PLD1* was significantly higher and the expression of *PLD2* was significantly lower in the basal-like compared to the luminal-like model. Other genes related to the degradation of PtdCho, such as lecithin-cholesterol acetyltransferase (*LCAT*) and phosphatidylserine synthase 1 (*PTDSS1*) also had significantly higher expression levels in the basal-like than in the luminal-like model. The *GDPD5* gene, coding for glycerophosphodiester phosphodiesterase (GDPD) was significantly higher expressed in the basal-like model than in the luminal-like model, indicating that GPC degradation may occur at a higher rate in basal-like xenografts. However, an isoform of this gene, *GDPD1*, was higher expressed in the luminal-like xenografts. As shown in Figure 3, choline dehydrogenase (*CHDH*) mediates the irreversible conversion of choline to betaine, which is a key precursor in the synthesis of glycine. The expression of *CHDH* was significantly higher in the basal-like than in the luminal-like model. Sarcosine dehydrogenase (*SARDH*), involved in the conversion of betaine to glycine, also had significantly higher expression levels in the basal-like model.

Discussion

The HR MAS MRS data demonstrated significant differences in choline metabolite pattern between the basal-like and luminal-like xenograft models. In particular, the difference in GPC and PCho concentrations is an interesting finding, as the pattern seen in the basal-like model does not correspond to typical *in vitro* choline metabolite patterns [15,17]. In addition, expression data showed that several genes directly associated with choline metabolism differed significantly between the two models. Differences in expression of genes involved in choline metabolism corresponded to differences in metabolite concentrations, suggesting that transcriptional differences between the models are reflected in the HR MAS MRS spectra. The relative amounts of GPC and PCho in human tissue samples from triple negative and ER+/PgR+ subtypes of breast cancer corresponded well with the data from the xenografts.

In order to evaluate if the choline metabolism in the xenograft models is representative for basal-like and luminal-like breast cancer in humans, they were compared to data from triple negative and ER+/PgR+ breast cancer patients. It is assumed that the triple-negative

Table 4 Differentially expressed genes

Entrez ID	Probe name	Gene name	Encoded protein	Log2-fold difference	Adjusted p-value (false discovery rate)
5321	A_23_P11685	PLA2G4A	Phospholipase A2, group IV A	6.4	$4.4E^{-16}$
55349	A_23_P69293	CHDH	Choline dehydrogenase	3.3	$4.0E^{-13}$
1757	A_24_P35400	SARDH	Sarcosine dehydrogenase	2.5	$7.6E^{-12}$
9468	A_24_P941353	PCYT1B	Phosphate cytidylyltransferase 1, choline, beta	1.7	$3.7E^{-9}$
31896	A_23_P87401	GDPD5	Glycerophosphodiester phosphodiesterase domain containing 5	1.0	$4.2E^{-6}$
8681	A_23_P403424	PLA2G4B	Phospholipase A2, group IV B	0.9	$9.8E^{-5}$
9791	A_23_P168868	PTDSS1	Phosphatidylserine synthase I	0.9	$9.6E^{-7}$
10434	A_23_P19192	LYPLA1	Lysophospholipase 1	0.9	0.001
3931	A_23_P218237	LCAT	Lecithin-cholesterol acyltransferase	0.8	0.0002
151056	A_23_P56356	PLB1	Phospholipase B1	0.7	0.0001
5337	A_23_P155335	PLD1	Phospholipase D1	0.7	0.0005

Genes directly involved in choline metabolism with significantly higher expression in basal-like (MAS98.12) than luminal-like (MAS98.06) tumors

phenotype is a valid surrogate marker for basal-like breast cancer, as approximately 90% of triple-negative breast carcinomas can be classified as basal-like based on the intrinsic molecular subtyping developed by Sørlie *et al* [3,37]. On the other hand, expression of estrogen and/or progesterone receptors is a typical feature of luminal A and B subtypes, whereas the ERBB2 and basal-like subtypes of breast cancer rarely express hormone receptors [38,39]. Therefore, the ER+/PgR+ phenotype is considered to be a valid surrogate marker for luminal-like subtypes of breast cancer.

Using gene expression profiling, the molecular causes for the differences in choline metabolism was further explored in the xenograft models. The heatmap of all 64 significantly differentially expressed genes in Figure 2, clearly shows that different sets of genes related to phospholipid metabolism are higher expressed the basal-like model compared to the luminal-like models. This indicates that the regulation of choline metabolism differ between the two xenograft models. Although this study does not provide data on metabolic flux, the methods used are suitable for highlighting key steps in choline metabolism. Comparison of these two disease models does not, however, give any information with respect to the difference between choline metabolism in normal breast versus breast cancer tissue. Nevertheless, gene expression profiling of the xenograft models showed significant differences in the expression of genes directly involved in choline metabolism, suggesting that these genes may play key roles in regulation of choline metabolite concentrations in human breast cancer.

Increased choline transport has been associated with the abnormally high concentrations of PCho observed in breast cancer [16,27,40]. In our study, the influx of choline in the two models could not be fully evaluated from the gene expression data, as only one of five investigated

Table 5 Differentially expressed genes

Entrez ID	Probe name	Gene name	Encoded protein	Log2-fold difference	Adjusted p-value (false discovery rate)
50487	A_23_P17814	PLA2G3	Phospholipase A2, group III	-3.1	$1.1E^{-12}$
81579	A_23_P30020	PLA2G12A	Phospholipase A2, group XII A	-1.6	$2.5E^{-9}$
56994	A_23_P105571	CHPT1	Choline phosphotransferase 1	-1.4	$1.6E^{-7}$
23446	A_23_P216630	SLC44A1	Solute carrier family 44, member 1 (CTL1)	-1.1	$7.9E^{-7}$
5338	A_23_P4308	PLD2	Phospholipase D2	-1.1	$1.2E^{-6}$
8399	A_23_P88767	PLA2G10	Phospholipase A2, group X	-1.1	$3.1E^{-6}$
1119	A_23_P314120	CHKB	Choline kinase beta	-0.8	$2.0E^{-6}$
11313	A_24_P276490	LYPLA2	Lysophospholipase II	-0.4	0.005
5130	A_23_P252681	PCYT1A	Phosphate cytidylyltransferase 1, choline, alpha	-0.4	0.035
24657	A_23_P84666	GDPD1	Glycerophosphodiester phosphodiesterase domain containing I	-0.4	0.005
1119	A_23_P124742	CHKA	Choline kinase, alpha	-0.3	0.047

Genes directly involved in choline metabolism with significantly lower expression in basal-like (MAS98.12) than luminal-like (MAS98.06) tumors

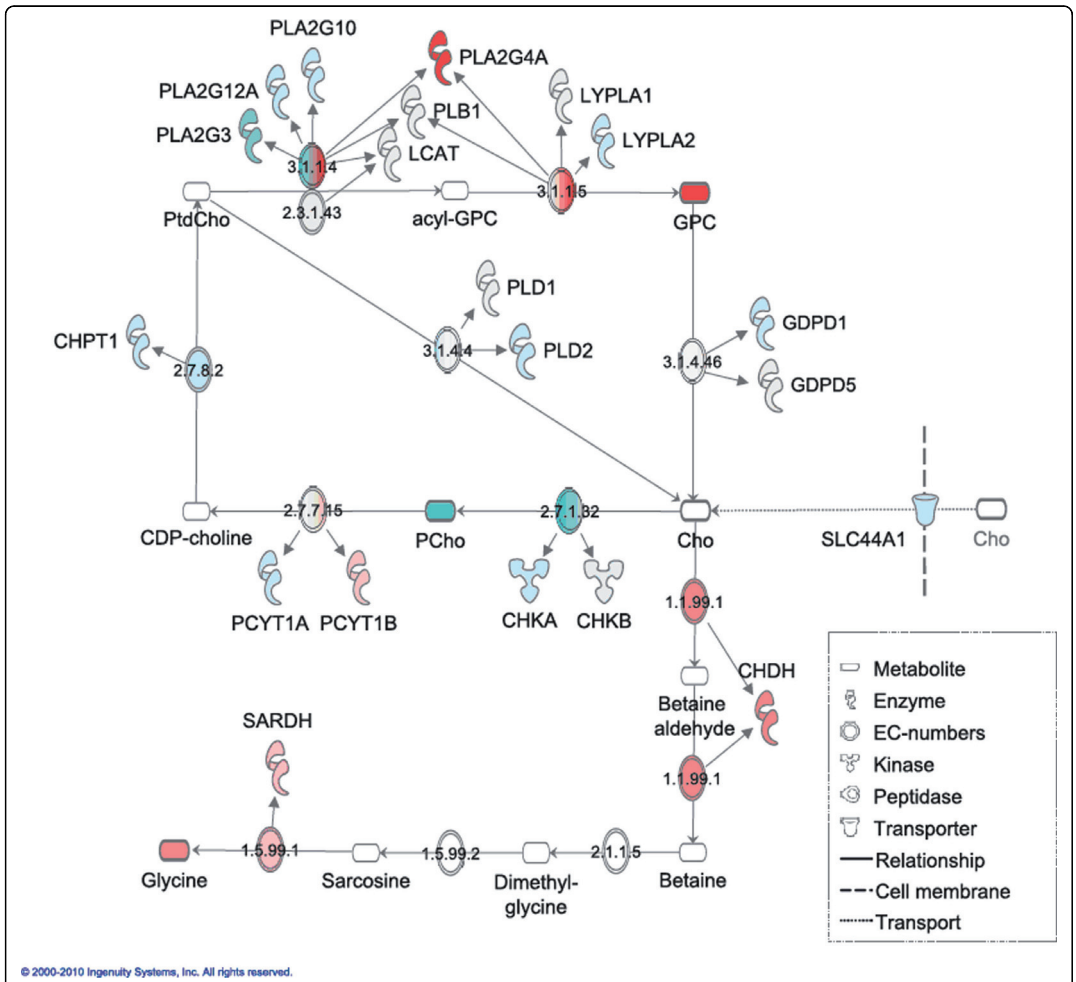

Figure 3 Differences in gene expression and metabolite concentrations. Differences in intracellular choline metabolism, choline transport and glycine formation between basal-like and luminal-like xenografts. Red: higher gene expression/metabolite concentration in basal-like xenografts. Blue: higher gene expression/metabolite concentration in luminal-like xenografts. White: Non-significant difference in expression/concentration. Log2-fold difference between models is indicated by color intensity. Only significantly differentially expressed genes are illustrated at each EC number, which represents specific enzymatic reactions. The metabolites which were measured with HR MAS MRS are outlined with a thicker line.

choline transporters was differentially expressed. Choline transport has been shown to be less important than PtdCho turnover for total choline metabolite concentrations [17]. Differences in choline uptake may still have impact on the choline metabolite concentrations, and specific studies using isotopically labelled choline could possibly allow accurate evaluation of choline transport rate in the two xenograft models.

In breast cancer cells, the intracellular metabolism of choline is divided in two major pathways as shown in Figure 3: Betaine production or PtdCho synthesis [27,34]. In the betaine synthesis pathway, choline is oxidized to betaine through the action of choline dehydrogenase (*CHDH*). Betaine is then demethylated to glycine. *In vitro* studies of MCF7-cells have shown that PtdCho synthesis is the pathway predominantly accountable for choline turnover [34]. The first step in the PtdCho synthesis pathway is the phosphorylation of choline through choline kinase, yielding PCho (Figure 3). It has been shown that increased expression of *CHKA* is

critical for proliferation both of mammary epithelial cells and breast cancer [41], but *in vitro* studies of different breast cancer cell lines have not conclusively demonstrated a correlation between *CHKA* expression and PCho concentration [16,26]. In our study, the expression of *CHKA* and *CHKB* was significantly lower in the basal-like than in the luminal-like model, although some variability in expression was observed (Figure 2). This is consistent with the lower PCho concentrations measured in the basal-like model. Betaine production is thought to contribute only slightly to the overall conversion of choline, and neither choline transport nor GPC degradation is conclusive with respect to their contribution to the choline pool. As normal breast tissue or benign breast lesions rarely exhibit increased choline metabolite levels, the xenograft models are believed to represent typical choline metabolism abnormalities of breast carcinomas [42,43]. Therefore, it should be stressed that *CHKA* and *CHKB* expression is likely to be upregulated in both xenograft models compared to normal breast tissue. The lower PCho concentrations in the basal-like xenografts may also in part be a result of higher *CHDH* expression. This suggests that conversion of choline to betaine is upregulated, shifting the metabolic flux in favour of glycine formation. *SARDH*, related to conversion of betaine to glycine, was also significantly higher expressed in the basal-like model. The concentration of glycine in the basal-like model was indeed higher than in the luminal-like model, suggesting that there is a difference in choline routing and glycine production between the two breast cancer subtypes. An association between tumor aggressiveness and glycine concentration has been noted also in clinical breast cancer tissue biopsies [21]. Abnormalities in cancer energy metabolism are widely recognized, and differences in glycine concentration between the two xenograft models in this study could well be an indirect result of this phenomenon.

Degradation of PtdCho is the primary source of GPC. The expression of *PLA2G4A*, *PLA2G4B*, *LCAT*, *LYPLA1* and *PLB1*, which all are associated with this pathway, was higher in the basal-like model. Other genes (*PLA2G3*, *PLA2G12A*, *PLA2G10*, *LYPLA2*) were lower expressed in the basal-like model, and a clear association between PtdCho degradation and GPC concentration could not be concluded. However, *in vitro* studies have suggested that GPC concentrations are associated with *PLA2G4A* levels, which is consistent with our findings [17]. A lower rate of GPC degradation could account for the higher GPC concentration observed in the basal-like xenograft model. The expression of *GDPD5* was, however, higher in basal-like xenografts. The observed differences between the two models in the relative expression of different genes assigned to the abovementioned enzymatic steps could be reflecting the relative importance of different gene products coding for proteins with the same enzymatic activity in the two models.

By associating choline metabolite concentrations with tumor cell phenotype, it has been proposed that PCho concentration increase with the malignancy of the tumor cell line when grown in culture [15]. However, other *in vitro* studies have failed to show a correlation between malignancy and choline metabolite concentrations [16]. It has been suggested that differences in experimental design, particularly the stage of cell growth, are accountable for these discrepancies [26]. In all the abovementioned *in vitro* studies of breast cancer cells, PCho concentrations were significantly higher than GPC concentrations. However, both in xenograft models of breast cancer and in clinical tissue samples, GPC concentrations higher than PCho concentrations have been observed [21,44]. GPC concentration has been shown to be negatively correlated with estrogen receptor content in breast carcinomas, which agrees with the relatively high GPC content in the basal-like xenograft [45]. Our data show that GPC concentration is significantly lower and PCho concentration is significantly higher in the luminal-like animal model, which represents a less aggressive disease than the basal-like model. This suggests that the relationship between choline metabolite concentrations and malignancy of solid tumors is more complex than indicated by studies of breast cancer cell lines. Discrepancies between *in vitro* data and clinical data may be attributed to the microenvironment of solid tumors. It has recently been shown that the metabolic profiles change when the same breast cancer cell lines are studied both *in vitro* and *in vivo* [46]. In addition, *in vitro* simulation of microenvironmental factors in solid tumors has demonstrated that PCho and GPC concentrations respond to changes in acidity, oxygenation level and glucose accessibility [44].

The relevance of the basal-like and luminal-like xenografts used in this study was further supported by comparing the choline metabolite pattern with that of human tissue samples from ER+/PgR+ and triple negative breast cancer. Evaluation of metabolite levels through relative peak areas demonstrated that the mean GPC/PCho ratio was significantly higher in triple negative breast cancer than in ER+/PgR+ breast cancer. The relative PCho area was significantly higher in ER+/PgR+ samples than in samples from triple negative breast cancer. A trend towards higher glycine concentration was also found in triple negative tissue samples. Interestingly, the choline concentration in triple negative breast cancer was higher than in ER+/PgR+ breast cancer. Overall, the striking similarity between xenografts and human tissue samples with respect to GPC and PCho levels suggest that the xenografts have maintained genetic and/or microenvironmental features from the primary carcinomas which are relevant for the choline

metabolite pattern. The spectra from human tissue samples also suggest that PCho concentrations alone are not a reliable prognostic biomarker. The triple negative samples represent disease with poor prognosis, yet the PCho level in these samples appear to be significantly lower than in ER+/PgR+ samples. This finding encourages large-scale studies of the metabolite pattern and gene expression in the different molecular subtypes of breast cancer, as this may reveal new drug targets or suggest strategies for individualised therapy using drugs targeting the choline metabolism pathways.

When interpreting the gene expression data from the two xenograft models, it should be kept in mind that gene expression not always represents the actual enzymatic activity. Isoforms of the same enzyme may exhibit differences in transcriptional regulation, and mRNA concentrations do not account for post-translational modification of enzymes. In addition, the concentrations of all investigated choline-containing compounds are determined by more than one metabolic reaction. Thus, a simplistic model for correlating gene expression with metabolite concentration is not applicable. The net rate of all relevant metabolic reactions governs the metabolite concentrations, and the relative importance of each metabolic reaction is unknown. This must be kept in mind when interpreting the data. However, the gene expression data provide significant information in terms of highlighting the reactions that are most likely to be relevant for the observed differences in metabolic pattern. Hypotheses generated on the basis of microarray data should be evaluated by tracking the flux of metabolites through the different pathways.

Comparing our data with pre-existing studies of choline metabolism in cultured cells and *in vivo* models with data from human biopsies, we suggest that primary tumor xenografts are more relevant model systems than cell cultures with respect to investigation of metabolic profiles in different breast cancer subtypes, and may be a better approach to studies of therapeutic efficacy in the different breast cancer subtypes. As the choline metabolite profile of the xenograft models used in the study appear representative of basal-like and luminal-like human breast cancer, the models are considered valuable tools for testing of targeted drugs and for monitoring response to treatment in these subtypes of breast cancer.

Conclusions

HR MAS MRS analyses of a basal-like and a luminal-like xenograft model demonstrated significant differences in choline metabolite concentrations. In the more aggressive basal-like tumor, GPC concentrations were higher than PCho concentrations, whereas this pattern was reversed in the luminal-like model. Glycine concentration was also significantly higher in the basal-like model. These differences could at least in part be explained by lower choline kinase expression and increased PtdCho degradation in the basal-like model. The gene expression data also suggested a possible shift in metabolic flux from PtdCho synthesis to glycine formation in the basal-like model. The choline metabolism pattern in the xenografts corresponded well with spectra from tissue samples from triple negative and ER+/PgR+ human breast carcinomas, suggesting that the basal-like and luminal-like xenografts may be a relevant model system for studies of choline metabolism in these two subtypes of human breast cancer.

Additional material

Additional file 1: Differential gene expression. Excel spreadsheet containing results from the differential gene expression analysis of the 119 investigated genes.

Acknowledgements
The authors wish to thank Unn Granli and Borgny Ytterhus for staining of histology sections and Alexandr Kristian for assistance in animal surgery. The work presented is sponsored by the Research Council of Norway, grants no. 175459/V50, 186479/V50, 183379/S10 and 183621/S10.

Author details
[1]Department of Circulation and Medical Imaging, Norwegian University of Science and Technology (NTNU), Trondheim, Norway. [2]Department of Genetics, Institute for Cancer Research, Oslo University Hospital Radiumhospitalet, Oslo, Norway. [3]Department of Tumor Biology, Institute for Cancer Research, Oslo University Hospital Radiumhospitalet, Oslo, Norway. [4]Institute for Clinical Medicine, Faculty of Medicine, University of Oslo, Oslo, Norway.

Authors' contributions
SAM conceived and designed the study, performed the HR MAS MRS analysis, performed the histopathological analysis, interpreted the data and wrote the manuscript. EB performed the gene expression analysis and interpreted the microarray data. EMH performed the HR MAS MRS analysis. EL carried out the *in vivo* experiments. BS established the HR MAS MRS protocol and supervised the analyses. ALBD contributed with expertise in molecular biology techniques. OE designed and coordinated the *in vivo* experiments. GMM participated in design and coordination of the study. ISG designed and coordinated the study and gave final approval of the manuscript. All co-authors critically revised the manuscript and approved the final version.

Competing interests
The authors declare that they have no competing interests.

Received: 15 April 2010 Accepted: 17 August 2010
Published: 17 August 2010

References

1. Perou CM, Sorlie T, Eisen MB, van de RM, Jeffrey SS, Rees CA, *et al*: **Molecular portraits of human breast tumours.** *Nature* 2000, **406**:747-752.
2. Sorlie T, Perou CM, Tibshirani R, Aas T, Geisler S, Johnsen H, *et al*: **Gene expression patterns of breast carcinomas distinguish tumor subclasses with clinical implications.** *Proc Natl Acad Sci USA* 2001, **98**:10869-10874.
3. Sorlie T, Tibshirani R, Parker J, Hastie T, Marron JS, Nobel A, *et al*: **Repeated observation of breast tumor subtypes in independent gene expression data sets.** *Proc Natl Acad Sci USA* 2003, **100**:8418-8423.
4. Calza S, Hall P, Auer G, Bjohle J, Klaar S, Kronenwett U, *et al*: **Intrinsic molecular signature of breast cancer in a population-based cohort of 412 patients.** *Breast Cancer Res* 2006, **8**:R34.

5. Kurebayashi J, Moriya T, Ishida T, Hirakawa H, Kurosumi M, Akiyama F, *et al*: **The prevalence of intrinsic subtypes and prognosis in breast cancer patients of different races.** *Breast* 2007, **16(Suppl 2)**:S72-S77.
6. Mullins M, Perreard L, Quackenbush JF, Gauthier N, Bayer S, Ellis M, *et al*: **Agreement in breast cancer classification between microarray and quantitative reverse transcription PCR from fresh-frozen and formalin-fixed, paraffin-embedded tissues.** *Clin Chem* 2007, **53**:1273-1279.
7. Sorlie T, Wang Y, Xiao C, Johnsen H, Naume B, Samaha RR, *et al*: **Distinct molecular mechanisms underlying clinically relevant subtypes of breast cancer: gene expression analyses across three different platforms.** *BMC Genomics* 2006, **7**:127.
8. Stadler ZK, Come SE: **Review of gene-expression profiling and its clinical use in breast cancer.** *Crit Rev Oncol Hematol* 2009, **69**:1-11.
9. Banez-Coronel M, de Molina AR, Rodriguez-Gonzalez A, Sarmentero J, Ramos MA, Garcia-Cabezas MA, *et al*: **Choline kinase alpha depletion selectively kills tumoral cells.** *Curr Cancer Drug Targets* 2008, **8**:709-719.
10. Hernandez-Alcoceba R, Fernandez F, Lacal JC: **In vivo antitumor activity of choline kinase inhibitors: a novel target for anticancer drug discovery.** *Cancer Res* 1999, **59**:3112-3118.
11. Lacal JC: **Choline kinase: a novel target for antitumor drugs.** *IDrugs* 2001, **4**:419-426.
12. Rodriguez-Gonzalez A, Ramirez de MA, Fernandez F, Ramos MA, del Carmen NM, Campos J, *et al*: **Inhibition of choline kinase as a specific cytotoxic strategy in oncogene-transformed cells.** *Oncogene* 2003, **22**:8803-8812.
13. Rodriguez-Gonzalez A, Ramirez de MA, Banez-Coronel M, Megias D, Lacal JC: **Inhibition of choline kinase renders a highly selective cytotoxic effect in tumour cells through a mitochondrial independent mechanism.** *Int J Oncol* 2005, **26**:999-1008.
14. Tozaki M: **Proton MR spectroscopy of the breast.** *Breast Cancer* 2008, **15**:218-223.
15. Aboagye EO, Bhujwalla ZM: **Malignant transformation alters membrane choline phospholipid metabolism of human mammary epithelial cells.** *Cancer Res* 1999, **59**:80-84.
16. Eliyahu G, Kreizman T, Degani H: **Phosphocholine as a biomarker of breast cancer: molecular and biochemical studies.** *Int J Cancer* 2007, **120**:1721-1730.
17. Glunde K, Jie C, Bhujwalla ZM: **Molecular causes of the aberrant choline phospholipid metabolism in breast cancer.** *Cancer Res* 2004, **64**:4270-4276.
18. Gillies RJ, Morse DL: **In vivo magnetic resonance spectroscopy in cancer.** *Annu Rev Biomed Eng* 2005, **7**:287-326.
19. Mackinnon WB, Barry PA, Malycha PL, Gillett DJ, Russell P, Lean CL, *et al*: **Fine-needle biopsy specimens of benign breast lesions distinguished from invasive cancer ex vivo with proton MR spectroscopy.** *Radiology* 1997, **204**:661-666.
20. Negendank W: **Studies of human tumors by MRS: a review.** *NMR Biomed* 1992, **5**:303-324.
21. Sitter B, Lundgren S, Bathen TF, Halgunset J, Fjosne HE, Gribbestad IS: **Comparison of HR MAS MR spectroscopic profiles of breast cancer tissue with clinical parameters.** *NMR Biomed* 2006, **19**:30-40.
22. Meisamy S, Bolan PJ, Baker EH, Bliss RL, Gulbahce E, Everson LI, *et al*: **Neoadjuvant chemotherapy of locally advanced breast cancer: predicting response with in vivo (1)H MR spectroscopy–a pilot study at 4 T.** *Radiology* 2004, **233**:424-431.
23. Morse DL, Raghunand N, Sadarangani P, Murthi S, Job C, Day S, *et al*: **Response of choline metabolites to docetaxel therapy is quantified in vivo by localized (31)P MRS of human breast cancer xenografts and in vitro by high-resolution (31)P NMR spectroscopy of cell extracts.** *Magn Reson Med* 2007, **58**:270-280.
24. Neeman M, Eldar H, Rushkin E, Degani H: **Chemotherapy-induced changes in the energetics of human breast cancer cells; 31P- and 13C-NMR studies.** *Biochim Biophys Acta* 1990, **1052**:255-263.
25. Glunde K, Jie C, Bhujwalla ZM: **Mechanisms of indomethacin-induced alterations in the choline phospholipid metabolism of breast cancer cells.** *Neoplasia* 2006, **8**:758-771.
26. Morse DL, Carroll D, Day S, Gray H, Sadarangani P, Murthi S, *et al*: **Characterization of breast cancers and therapy response by MRS and quantitative gene expression profiling in the choline pathway.** *NMR Biomed* 2009, **22**:114-127.
27. Katz-Brull R, Seger D, Rivenson-Segal D, Rushkin E, Degani H: **Metabolic markers of breast cancer: enhanced choline metabolism and reduced choline-ether-phospholipid synthesis.** *Cancer Res* 2002, **62**:1966-1970.
28. Vargo-Gogola T, Rosen JM: **Modelling breast cancer: one size does not fit all.** *Nat Rev Cancer* 2007, **7**:659-672.
29. Bergamaschi A, Hjortland GO, Triulzi T, Sorlie T, Johnsen H, Ree AH, *et al*: **Molecular profiling and characterization of luminal-like and basal-like in vivo breast cancer xenograft models.** *Mol Oncol* 2009, **3**:469-482.
30. Sitter B, Sonnewald U, Spraul M, Fjosne HE, Gribbestad IS: **High-resolution magic angle spinning MRS of breast cancer tissue.** *NMR Biomed* 2002, **15**:327-337.
31. Sitter B, Bathen TF, Singstad TE, Fjosne HE, Lundgren S, Halgunset J, *et al*: **Quantification of metabolites in breast cancer patients with different clinical prognosis using HR MAS MR spectroscopy.** *NMR Biomed* 2010, **23**:424-431.
32. Smyth GK: **Linear models and empirical bayes methods for assessing differential expression in microarray experiments.** *Stat Appl Genet Mol Biol* 2004, **3, Article3.**
33. Kanehisa M, Goto S: **KEGG: kyoto encyclopedia of genes and genomes.** *Nucleic Acids Res* 2000, **28**:27-30.
34. Katz-Brull R, Margalit R, Degani H: **Differential routing of choline in implanted breast cancer and normal organs.** *Magn Reson Med* 2001, **46**:31-38.
35. Michel V, Yuan Z, Ramsubir S, Bakovic M: **Choline transport for phospholipid synthesis.** *Exp Biol Med (Maywood)* 2006, **231**:490-504.
36. Gallazzini M, Ferraris JD, Burg MB: **GDPD5 is a glycerophosphocholine phosphodiesterase that osmotically regulates the osmoprotective organic osmolyte GPC.** *Proc Natl Acad Sci USA* 2008, **105**:11026-11031.
37. Kreike B, van KM, Horlings H, Weigelt B, Peterse H, Bartelink H, *et al*: **Gene expression profiling and histopathological characterization of triple-negative/basal-like breast carcinomas.** *Breast Cancer Res* 2007, **9**:R65.
38. Sorlie T: **Molecular portraits of breast cancer: tumour subtypes as distinct disease entities.** *Eur J Cancer* 2004, **40**:2667-2675.
39. Bhargava R, Striebel J, Beriwal S, Flickinger JC, Onisko A, Ahrendt G, *et al*: **Prevalence, morphologic features and proliferation indices of breast carcinoma molecular classes using immunohistochemical surrogate markers.** *Int J Clin Exp Pathol* 2009, **2**:444-455.
40. Katz-Brull R, Degani H: **Kinetics of choline transport and phosphorylation in human breast cancer cells; NMR application of the zero trans method.** *Anticancer Res* 1996, **16**:1375-1380.
41. Ramirez de MA, Banez-Coronel M, Gutierrez R, Rodriguez-Gonzalez A, Olmeda D, Megias D, *et al*: **Choline kinase activation is a critical requirement for the proliferation of primary human mammary epithelial cells and breast tumor progression.** *Cancer Res* 2004, **64**:6732-6739.
42. Gribbestad IS, Petersen SB, Fjosne HE, Kvinnsland S, Krane J: **1H NMR spectroscopic characterization of perchloric acid extracts from breast carcinomas and non-involved breast tissue.** *NMR Biomed* 1994, **7**:181-194.
43. Kvistad KA, Bakken IJ, Gribbestad IS, Ehrnholm B, Lundgren S, Fjosne HE, *et al*: **Characterization of neoplastic and normal human breast tissues with in vivo (1)H MR spectroscopy.** *J Magn Reson Imaging* 1999, **10**:159-164.
44. Eliyahu G, Maril N, Margalit R, Degani H: **Choline Metabolism in Breast Cancer; The Influence of the Microenvironmental conditions [Abstract].** *Proc Intl Soc Mag Reson Med* 2007, **15.**
45. Giskeodegard GF, Grinde MT, Sitter B, Axelson DE, Lundgren S, Fjosne HE, *et al*: **Multivariate modeling and prediction of breast cancer prognostic factors using MR metabolomics.** *J Proteome Res* 2010, **9**:972-979.
46. Mori N, Glunde K, Takagi T, Xiong L, Wides F, Bhujwalla Z: **Tumor microenvironmental alterations of lipid metabolism detected by comparing cancer cells with tumors [Abstract].** *Proc Intl Soc Mag Reson Med* 2009, **17**:2310.

Pre-publication history

The pre-publication history for this paper can be accessed here:
http://www.biomedcentral.com/1471-2407/10/433/prepub

doi:10.1186/1471-2407-10-433
Cite this article as: Moestue *et al.*: Distinct choline metabolic profiles are associated with differences in gene expression for basal-like and luminal-like breast cancer xenograft models. *BMC Cancer* 2010 **10**:433.

Paper II

Is not included due to copyright

Paper III

Is not included due to copyright

Paper IV

Is not included due to copyright

Dissertations at the Faculty of Medicine, NTNU

1977

1. Knut Joachim Berg: EFFECT OF ACETYLSALICYLIC ACID ON RENAL FUNCTION
2. Karl Erik Viken and Arne Ødegaard: STUDIES ON HUMAN MONOCYTES CULTURED *IN VITRO*

1978

3. Karel Bjørn Cyvin: CONGENITAL DISLOCATION OF THE HIP JOINT.
4. Alf O. Brubakk: METHODS FOR STUDYING FLOW DYNAMICS IN THE LEFT VENTRICLE AND THE AORTA IN MAN.

1979

5. Geirmund Unsgaard: CYTOSTATIC AND IMMUNOREGULATORY ABILITIES OF HUMAN BLOOD MONOCYTES CULTURED IN VITRO

1980

6. Størker Jørstad: URAEMIC TOXINS
7. Arne Olav Jenssen: SOME RHEOLOGICAL, CHEMICAL AND STRUCTURAL PROPERTIES OF MUCOID SPUTUM FROM PATIENTS WITH CHRONIC OBSTRUCTIVE BRONCHITIS

1981

8. Jens Hammerstrøm: CYTOSTATIC AND CYTOLYTIC ACTIVITY OF HUMAN MONOCYTES AND EFFUSION MACROPHAGES AGAINST TUMOR CELLS *IN VITRO*

1983

9. Tore Syversen: EFFECTS OF METHYLMERCURY ON RAT BRAIN PROTEIN.
10. Torbjørn Iversen: SQUAMOUS CELL CARCINOMA OF THE VULVA.

1984

11. Tor-Erik Widerøe: ASPECTS OF CONTINUOUS AMBULATORY PERITONEAL DIALYSIS.
12. Anton Hole: ALTERATIONS OF MONOCYTE AND LYMPHOCYTE FUNCTIONS IN REALTION TO SURGERY UNDER EPIDURAL OR GENERAL ANAESTHESIA.
13. Terje Terjesen: FRACTURE HEALING AND STRESS-PROTECTION AFTER METAL PLATE FIXATION AND EXTERNAL FIXATION.
14. Carsten Saunte: CLUSTER HEADACHE SYNDROME.
15. Inggard Lereim: TRAFFIC ACCIDENTS AND THEIR CONSEQUENCES.
16. Bjørn Magne Eggen: STUDIES IN CYTOTOXICITY IN HUMAN ADHERENT MONONUCLEAR BLOOD CELLS.
17. Trond Haug: FACTORS REGULATING BEHAVIORAL EFFECTS OG DRUGS.

1985

18. Sven Erik Gisvold: RESUSCITATION AFTER COMPLETE GLOBAL BRAIN ISCHEMIA.
19. Terje Espevik: THE CYTOSKELETON OF HUMAN MONOCYTES.
20. Lars Bevanger: STUDIES OF THE Ibc (c) PROTEIN ANTIGENS OF GROUP B STREPTOCOCCI.
21. Ole-Jan Iversen: RETROVIRUS-LIKE PARTICLES IN THE PATHOGENESIS OF PSORIASIS.
22. Lasse Eriksen: EVALUATION AND TREATMENT OF ALCOHOL DEPENDENT BEHAVIOUR.
23. Per I. Lundmo: ANDROGEN METABOLISM IN THE PROSTATE.

1986

24. Dagfinn Berntzen: ANALYSIS AND MANAGEMENT OF EXPERIMENTAL AND CLINICAL PAIN.
25. Odd Arnold Kildahl-Andersen: PRODUCTION AND CHARACTERIZATION OF MONOCYTE-DERIVED CYTOTOXIN AND ITS ROLE IN MONOCYTE-MEDIATED CYTOTOXICITY.
26. Ola Dale: VOLATILE ANAESTHETICS.

1987

27. Per Martin Kleveland: STUDIES ON GASTRIN.
28. Audun N. Øksendal: THE CALCIUM PARADOX AND THE HEART.
29. Vilhjalmur R. Finsen: HIP FRACTURES

1988

30. Rigmor Austgulen: TUMOR NECROSIS FACTOR: A MONOCYTE-DERIVED REGULATOR OF CELLULAR GROWTH.
31. Tom-Harald Edna: HEAD INJURIES ADMITTED TO HOSPITAL.
32. Joseph D. Borsi: NEW ASPECTS OF THE CLINICAL PHARMACOKINETICS OF METHOTREXATE.
33. Olav F. M. Sellevold: GLUCOCORTICOIDS IN MYOCARDIAL PROTECTION.
34. Terje Skjærpe: NONINVASIVE QUANTITATION OF GLOBAL PARAMETERS ON LEFT VENTRICULAR FUNCTION: THE SYSTOLIC PULMONARY ARTERY PRESSURE AND CARDIAC OUTPUT.
35. Eyvind Rødahl: STUDIES OF IMMUNE COMPLEXES AND RETROVIRUS-LIKE ANTIGENS IN PATIENTS WITH ANKYLOSING SPONDYLITIS.
36. Ketil Thorstensen: STUDIES ON THE MECHANISMS OF CELLULAR UPTAKE OF IRON FROM TRANSFERRIN.
37. Anna Midelfart: STUDIES OF THE MECHANISMS OF ION AND FLUID TRANSPORT IN THE BOVINE CORNEA.
38. Eirik Helseth: GROWTH AND PLASMINOGEN ACTIVATOR ACTIVITY OF HUMAN GLIOMAS AND BRAIN METASTASES - WITH SPECIAL REFERENCE TO TRANSFORMING GROWTH FACTOR BETA AND THE EPIDERMAL GROWTH FACTOR RECEPTOR.
39. Petter C. Borchgrevink: MAGNESIUM AND THE ISCHEMIC HEART.
40. Kjell-Arne Rein: THE EFFECT OF EXTRACORPOREAL CIRCULATION ON SUBCUTANEOUS TRANSCAPILLARY FLUID BALANCE.
41. Arne Kristian Sandvik: RAT GASTRIC HISTAMINE.
42. Carl Bredo Dahl: ANIMAL MODELS IN PSYCHIATRY.

1989

43. Torbjørn A. Fredriksen: CERVICOGENIC HEADACHE.
44. Rolf A. Walstad: CEFTAZIDIME.
45. Rolf Salvesen: THE PUPIL IN CLUSTER HEADACHE.
46. Nils Petter Jørgensen: DRUG EXPOSURE IN EARLY PREGNANCY.
47. Johan C. Ræder: PREMEDICATION AND GENERAL ANAESTHESIA IN OUTPATIENT GYNECOLOGICAL SURGERY.
48. M. R. Shalaby: IMMUNOREGULATORY PROPERTIES OF TNF-α AND THE RELATED CYTOKINES.
49. Anders Waage: THE COMPLEX PATTERN OF CYTOKINES IN SEPTIC SHOCK.
50. Bjarne Christian Eriksen: ELECTROSTIMULATION OF THE PELVIC FLOOR IN FEMALE URINARY INCONTINENCE.
51. Tore B. Halvorsen: PROGNOSTIC FACTORS IN COLORECTAL CANCER.

1990

52. Asbjørn Nordby: CELLULAR TOXICITY OF ROENTGEN CONTRAST MEDIA.
53. Kåre E. Tvedt: X-RAY MICROANALYSIS OF BIOLOGICAL MATERIAL.
54. Tore C. Stiles: COGNITIVE VULNERABILITY FACTORS IN THE DEVELOPMENT AND MAINTENANCE OF DEPRESSION.
55. Eva Hofsli: TUMOR NECROSIS FACTOR AND MULTIDRUG RESISTANCE.
56. Helge S. Haarstad: TROPHIC EFFECTS OF CHOLECYSTOKININ AND SECRETIN ON THE RAT PANCREAS.
57. Lars Engebretsen: TREATMENT OF ACUTE ANTERIOR CRUCIATE LIGAMENT INJURIES.
58. Tarjei Rygnestad: DELIBERATE SELF-POISONING IN TRONDHEIM.
59. Arne Z. Henriksen: STUDIES ON CONSERVED ANTIGENIC DOMAINS ON MAJOR OUTER MEMBRANE PROTEINS FROM ENTEROBACTERIA.
60. Steinar Westin: UNEMPLOYMENT AND HEALTH: Medical and social consequences of a factory closure in a ten-year controlled follow-up study.
61. Ylva Sahlin: INJURY REGISTRATION, a tool for accident preventive work.
62. Helge Bjørnstad Pettersen: BIOSYNTHESIS OF COMPLEMENT BY HUMAN ALVEOLAR MACROPHAGES WITH SPECIAL REFERENCE TO SARCOIDOSIS.
63. Berit Schei: TRAPPED IN PAINFUL LOVE.
64. Lars J. Vatten: PROSPECTIVE STUDIES OF THE RISK OF BREAST CANCER IN A COHORT OF NORWEGIAN WOMAN.

1991

65. Kåre Bergh: APPLICATIONS OF ANTI-C5a SPECIFIC MONOCLONAL ANTIBODIES FOR THE ASSESSMENT OF COMPLEMENT ACTIVATION.
66. Svein Svenningsen: THE CLINICAL SIGNIFICANCE OF INCREASED FEMORAL ANTEVERSION.
67. Olbjørn Klepp: NONSEMINOMATOUS GERM CELL TESTIS CANCER: THERAPEUTIC OUTCOME AND PROGNOSTIC FACTORS.
68. Trond Sand: THE EFFECTS OF CLICK POLARITY ON BRAINSTEM AUDITORY EVOKED POTENTIALS AMPLITUDE, DISPERSION, AND LATENCY VARIABLES.
69. Kjetil B. Åsbakk: STUDIES OF A PROTEIN FROM PSORIATIC SCALE, PSO P27, WITH RESPECT TO ITS POTENTIAL ROLE IN IMMUNE REACTIONS IN PSORIASIS.
70. Arnulf Hestnes: STUDIES ON DOWN´S SYNDROME.
71. Randi Nygaard: LONG-TERM SURVIVAL IN CHILDHOOD LEUKEMIA.
72. Bjørn Hagen: THIO-TEPA.
73. Svein Anda: EVALUATION OF THE HIP JOINT BY COMPUTED TOMOGRAMPHY AND ULTRASONOGRAPHY.

1992

74. Martin Svartberg: AN INVESTIGATION OF PROCESS AND OUTCOME OF SHORT-TERM PSYCHODYNAMIC PSYCHOTHERAPY.
75. Stig Arild Slørdahl: AORTIC REGURGITATION.
76. Harold C Sexton: STUDIES RELATING TO THE TREATMENT OF SYMPTOMATIC NON-PSYCHOTIC PATIENTS.
77. Maurice B. Vincent: VASOACTIVE PEPTIDES IN THE OCULAR/FOREHEAD AREA.
78. Terje Johannessen: CONTROLLED TRIALS IN SINGLE SUBJECTS.
79. Turid Nilsen: PYROPHOSPHATE IN HEPATOCYTE IRON METABOLISM.
80. Olav Haraldseth: NMR SPECTROSCOPY OF CEREBRAL ISCHEMIA AND REPERFUSION IN RAT.
81. Eiliv Brenna: REGULATION OF FUNCTION AND GROWTH OF THE OXYNTIC MUCOSA.

1993

82. Gunnar Bovim: CERVICOGENIC HEADACHE.
83. Jarl Arne Kahn: ASSISTED PROCREATION.
84. Bjørn Naume: IMMUNOREGULATORY EFFECTS OF CYTOKINES ON NK CELLS.
85. Rune Wiseth: AORTIC VALVE REPLACEMENT.
86. Jie Ming Shen: BLOOD FLOW VELOCITY AND RESPIRATORY STUDIES.
87. Piotr Kruszewski: SUNCT SYNDROME WITH SPECIAL REFERENCE TO THE AUTONOMIC NERVOUS SYSTEM.
88. Mette Haase Moen: ENDOMETRIOSIS.
89. Anne Vik: VASCULAR GAS EMBOLISM DURING AIR INFUSION AND AFTER DECOMPRESSION IN PIGS.
90. Lars Jacob Stovner: THE CHIARI TYPE I MALFORMATION.
91. Kjell Å. Salvesen: ROUTINE ULTRASONOGRAPHY IN UTERO AND DEVELOPMENT IN CHILDHOOD.

1994

92. Nina-Beate Liabakk: DEVELOPMENT OF IMMUNOASSAYS FOR TNF AND ITS SOLUBLE RECEPTORS.
93. Sverre Helge Torp: *erb*B ONCOGENES IN HUMAN GLIOMAS AND MENINGIOMAS.
94. Olav M. Linaker: MENTAL RETARDATION AND PSYCHIATRY. Past and present.
95. Per Oscar Feet: INCREASED ANTIDEPRESSANT AND ANTIPANIC EFFECT IN COMBINED TREATMENT WITH DIXYRAZINE AND TRICYCLIC ANTIDEPRESSANTS.
96. Stein Olav Samstad: CROSS SECTIONAL FLOW VELOCITY PROFILES FROM TWO-DIMENSIONAL DOPPLER ULTRASOUND: Studies on early mitral blood flow.
97. Bjørn Backe: STUDIES IN ANTENATAL CARE.
98. Gerd Inger Ringdal: QUALITY OF LIFE IN CANCER PATIENTS.
99. Torvid Kiserud: THE DUCTUS VENOSUS IN THE HUMAN FETUS.
100. Hans E. Fjøsne: HORMONAL REGULATION OF PROSTATIC METABOLISM.
101. Eylert Brodtkorb: CLINICAL ASPECTS OF EPILEPSY IN THE MENTALLY RETARDED.
102. Roar Juul: PEPTIDERGIC MECHANISMS IN HUMAN SUBARACHNOID HEMORRHAGE.
103. Unni Syversen: CHROMOGRANIN A. Phsysiological and Clinical Role.

1995

104. Odd Gunnar Brakstad: THERMOSTABLE NUCLEASE AND THE *nuc* GENE IN THE DIAGNOSIS OF *Staphylococcus aureus* INFECTIONS.
105. Terje Engan: NUCLEAR MAGNETIC RESONANCE (NMR) SPECTROSCOPY OF PLASMA IN MALIGNANT DISEASE.
106. Kirsten Rasmussen: VIOLENCE IN THE MENTALLY DISORDERED.
107. Finn Egil Skjeldestad: INDUCED ABORTION: Timetrends and Determinants.
108. Roar Stenseth: THORACIC EPIDURAL ANALGESIA IN AORTOCORONARY BYPASS SURGERY.
109. Arild Faxvaag: STUDIES OF IMMUNE CELL FUNCTION *in mice infected with* MURINE RETROVIRUS.

1996

110. Svend Aakhus: NONINVASIVE COMPUTERIZED ASSESSMENT OF LEFT VENTRICULAR FUNCTION AND SYSTEMIC ARTERIAL PROPERTIES. Methodology and some clinical applications.
111. Klaus-Dieter Bolz: INTRAVASCULAR ULTRASONOGRAPHY.
112. Petter Aadahl: CARDIOVASCULAR EFFECTS OF THORACIC AORTIC CROSS-CLAMPING.
113. Sigurd Steinshamn: CYTOKINE MEDIATORS DURING GRANULOCYTOPENIC INFECTIONS.
114. Hans Stifoss-Hanssen: SEEKING MEANING OR HAPPINESS?
115. Anne Kvikstad: LIFE CHANGE EVENTS AND MARITAL STATUS IN RELATION TO RISK AND PROGNOSIS OF CANCER.
116. Torbjørn Grøntvedt: TREATMENT OF ACUTE AND CHRONIC ANTERIOR CRUCIATE LIGAMENT INJURIES. A clinical and biomechanical study.
117. Sigrid Hørven Wigers: CLINICAL STUDIES OF FIBROMYALGIA WITH FOCUS ON ETIOLOGY, TREATMENT AND OUTCOME.
118. Jan Schjøtt: MYOCARDIAL PROTECTION: Functional and Metabolic Characteristics of Two Endogenous Protective Principles.
119. Marit Martinussen: STUDIES OF INTESTINAL BLOOD FLOW AND ITS RELATION TO TRANSITIONAL CIRCULATORY ADAPATION IN NEWBORN INFANTS.
120. Tomm B. Müller: MAGNETIC RESONANCE IMAGING IN FOCAL CEREBRAL ISCHEMIA.
121. Rune Haaverstad: OEDEMA FORMATION OF THE LOWER EXTREMITIES.
122. Magne Børset: THE ROLE OF CYTOKINES IN MULTIPLE MYELOMA, WITH SPECIAL REFERENCE TO HEPATOCYTE GROWTH FACTOR.
123. Geir Smedslund: A THEORETICAL AND EMPIRICAL INVESTIGATION OF SMOKING, STRESS AND DISEASE: RESULTS FROM A POPULATION SURVEY.

1997

124. Torstein Vik: GROWTH, MORBIDITY, AND PSYCHOMOTOR DEVELOPMENT IN INFANTS WHO WERE GROWTH RETARDED *IN UTERO*.
125. Siri Forsmo: ASPECTS AND CONSEQUENCES OF OPPORTUNISTIC SCREENING FOR CERVICAL CANCER. Results based on data from three Norwegian counties.
126. Jon S. Skranes: CEREBRAL MRI AND NEURODEVELOPMENTAL OUTCOME IN VERY LOW BIRTH WEIGHT (VLBW) CHILDREN. A follow-up study of a geographically based year cohort of VLBW children at ages one and six years.
127. Knut Bjørnstad: COMPUTERIZED ECHOCARDIOGRAPHY FOR EVALUTION OF CORONARY ARTERY DISEASE.
128. Grethe Elisabeth Borchgrevink: DIAGNOSIS AND TREATMENT OF WHIPLASH/NECK SPRAIN INJURIES CAUSED BY CAR ACCIDENTS.
129. Tor Elsås: NEUROPEPTIDES AND NITRIC OXIDE SYNTHASE IN OCULAR AUTONOMIC AND SENSORY NERVES.
130. Rolf W. Gråwe: EPIDEMIOLOGICAL AND NEUROPSYCHOLOGICAL PERSPECTIVES ON SCHIZOPHRENIA.
131. Tonje Strømholm: CEREBRAL HAEMODYNAMICS DURING THORACIC AORTIC CROSSCLAMPING. An experimental study in pigs

1998

132. Martinus Bråten: STUDIES ON SOME PROBLEMS REALTED TO INTRAMEDULLARY NAILING OF FEMORAL FRACTURES.

133. Ståle Nordgård: PROLIFERATIVE ACTIVITY AND DNA CONTENT AS PROGNOSTIC INDICATORS IN ADENOID CYSTIC CARCINOMA OF THE HEAD AND NECK.
134. Egil Lien: SOLUBLE RECEPTORS FOR **TNF** AND **LPS**: RELEASE PATTERN AND POSSIBLE SIGNIFICANCE IN DISEASE.
135. Marit Bjørgaas: HYPOGLYCAEMIA IN CHILDREN WITH DIABETES MELLITUS
136. Frank Skorpen: GENETIC AND FUNCTIONAL ANALYSES OF DNA REPAIR IN HUMAN CELLS.
137. Juan A. Pareja: SUNCT SYNDROME. ON THE CLINICAL PICTURE. ITS DISTINCTION FROM OTHER, SIMILAR HEADACHES.
138. Anders Angelsen: NEUROENDOCRINE CELLS IN HUMAN PROSTATIC CARCINOMAS AND THE PROSTATIC COMPLEX OF RAT, GUINEA PIG, CAT AND DOG.
139. Fabio Antonaci: CHRONIC PAROXYSMAL HEMICRANIA AND HEMICRANIA CONTINUA: TWO DIFFERENT ENTITIES?
140. Sven M. Carlsen: ENDOCRINE AND METABOLIC EFFECTS OF METFORMIN WITH SPECIAL EMPHASIS ON CARDIOVASCULAR RISK FACTORES.

1999

141. Terje A. Murberg: DEPRESSIVE SYMPTOMS AND COPING AMONG PATIENTS WITH CONGESTIVE HEART FAILURE.
142. Harm-Gerd Karl Blaas: THE EMBRYONIC EXAMINATION. Ultrasound studies on the development of the human embryo.
143. Noèmi Becser Andersen:THE CEPHALIC SENSORY NERVES IN UNILATERAL HEADACHES. Anatomical background and neurophysiological evaluation.
144. Eli-Janne Fiskerstrand: LASER TREATMENT OF PORT WINE STAINS. A study of the efficacy and limitations of the pulsed dye laser. Clinical and morfological analyses aimed at improving the therapeutic outcome.
145. Bård Kulseng: A STUDY OF ALGINATE CAPSULE PROPERTIES AND CYTOKINES IN RELATION TO INSULIN DEPENDENT DIABETES MELLITUS.
146. Terje Haug: STRUCTURE AND REGULATION OF THE HUMAN UNG GENE ENCODING URACIL-DNA GLYCOSYLASE.
147. Heidi Brurok: MANGANESE AND THE HEART. A Magic Metal with Diagnostic and Therapeutic Possibilites.
148. Agnes Kathrine Lie: DIAGNOSIS AND PREVALENCE OF HUMAN PAPILLOMAVIRUS INFECTION IN CERVICAL INTRAEPITELIAL NEOPLASIA. Relationship to Cell Cycle Regulatory Proteins and HLA DQBI Genes.
149. Ronald Mårvik: PHARMACOLOGICAL, PHYSIOLOGICAL AND PATHOPHYSIOLOGICAL STUDIES ON ISOLATED STOMACS.
150. Ketil Jarl Holen: THE ROLE OF ULTRASONOGRAPHY IN THE DIAGNOSIS AND TREATMENT OF HIP DYSPLASIA IN NEWBORNS.
151. Irene Hetlevik: THE ROLE OF CLINICAL GUIDELINES IN CARDIOVASCULAR RISK INTERVENTION IN GENERAL PRACTICE.
152. Katarina Tunòn: ULTRASOUND AND PREDICTION OF GESTATIONAL AGE.
153. Johannes Soma: INTERACTION BETWEEN THE LEFT VENTRICLE AND THE SYSTEMIC ARTERIES.
154. Arild Aamodt: DEVELOPMENT AND PRE-CLINICAL EVALUATION OF A CUSTOM-MADE FEMORAL STEM.
155. Agnar Tegnander: DIAGNOSIS AND FOLLOW-UP OF CHILDREN WITH SUSPECTED OR KNOWN HIP DYSPLASIA.
156. Bent Indredavik: STROKE UNIT TREATMENT: SHORT AND LONG-TERM EFFECTS
157. Jolanta Vanagaite Vingen: PHOTOPHOBIA AND PHONOPHOBIA IN PRIMARY HEADACHES

2000

158. Ola Dalsegg Sæther: PATHOPHYSIOLOGY DURING PROXIMAL AORTIC CROSS-CLAMPING CLINICAL AND EXPERIMENTAL STUDIES
159. xxxxxxxxx (blind number)
160. Christina Vogt Isaksen: PRENATAL ULTRASOUND AND POSTMORTEM FINDINGS – A TEN YEAR CORRELATIVE STUDY OF FETUSES AND INFANTS WITH DEVELOPMENTAL ANOMALIES.
161. Holger Seidel: HIGH-DOSE METHOTREXATE THERAPY IN CHILDREN WITH ACUTE LYMPHOCYTIC LEUKEMIA: DOSE, CONCENTRATION, AND EFFECT CONSIDERATIONS.

162. Stein Hallan: IMPLEMENTATION OF MODERN MEDICAL DECISION ANALYSIS INTO CLINICAL DIAGNOSIS AND TREATMENT.
163. Malcolm Sue-Chu: INVASIVE AND NON-INVASIVE STUDIES IN CROSS-COUNTRY SKIERS WITH ASTHMA-LIKE SYMPTOMS.
164. Ole-Lars Brekke: EFFECTS OF ANTIOXIDANTS AND FATTY ACIDS ON TUMOR NECROSIS FACTOR-INDUCED CYTOTOXICITY.
165. Jan Lundbom: AORTOCORONARY BYPASS SURGERY: CLINICAL ASPECTS, COST CONSIDERATIONS AND WORKING ABILITY.
166. John-Anker Zwart: LUMBAR NERVE ROOT COMPRESSION, BIOCHEMICAL AND NEUROPHYSIOLOGICAL ASPECTS.
167. Geir Falck: HYPEROSMOLALITY AND THE HEART.
168. Eirik Skogvoll: CARDIAC ARREST Incidence, Intervention and Outcome.
169. Dalius Bansevicius: SHOULDER-NECK REGION IN CERTAIN HEADACHES AND CHRONIC PAIN SYNDROMES.
170. Bettina Kinge: REFRACTIVE ERRORS AND BIOMETRIC CHANGES AMONG UNIVERSITY STUDENTS IN NORWAY.
171. Gunnar Qvigstad: CONSEQUENCES OF HYPERGASTRINEMIA IN MAN
172. Hanne Ellekjær: EPIDEMIOLOGICAL STUDIES OF STROKE IN A NORWEGIAN POPULATION. INCIDENCE, RISK FACTORS AND PROGNOSIS
173. Hilde Grimstad: VIOLENCE AGAINST WOMEN AND PREGNANCY OUTCOME.
174. Astrid Hjelde: SURFACE TENSION AND COMPLEMENT ACTIVATION: Factors influencing bubble formation and bubble effects after decompression.
175. Kjell A. Kvistad: MR IN BREAST CANCER – A CLINICAL STUDY.
176. Ivar Rossvoll: ELECTIVE ORTHOPAEDIC SURGERY IN A DEFINED POPULATION. Studies on demand, waiting time for treatment and incapacity for work.
177. Carina Seidel: PROGNOSTIC VALUE AND BIOLOGICAL EFFECTS OF HEPATOCYTE GROWTH FACTOR AND SYNDECAN-1 IN MULTIPLE MYELOMA.

2001

178. Alexander Wahba: THE INFLUENCE OF CARDIOPULMONARY BYPASS ON PLATELET FUNCTION AND BLOOD COAGULATION – DETERMINANTS AND CLINICAL CONSEQUENSES
179. Marcus Schmitt-Egenolf: THE RELEVANCE OF THE MAJOR hISTOCOMPATIBILITY COMPLEX FOR THE GENETICS OF PSORIASIS
180. Odrun Arna Gederaas: BIOLOGICAL MECHANISMS INVOLVED IN 5-AMINOLEVULINIC ACID BASED PHOTODYNAMIC THERAPY
181. Pål Richard Romundstad: CANCER INCIDENCE AMONG NORWEGIAN ALUMINIUM WORKERS
182. Henrik Hjorth-Hansen: NOVEL CYTOKINES IN GROWTH CONTROL AND BONE DISEASE OF MULTIPLE MYELOMA
183. Gunnar Morken: SEASONAL VARIATION OF HUMAN MOOD AND BEHAVIOUR
184. Bjørn Olav Haugen: MEASUREMENT OF CARDIAC OUTPUT AND STUDIES OF VELOCITY PROFILES IN AORTIC AND MITRAL FLOW USING TWO- AND THREE-DIMENSIONAL COLOUR FLOW IMAGING
185. Geir Bråthen: THE CLASSIFICATION AND CLINICAL DIAGNOSIS OF ALCOHOL-RELATED SEIZURES
186. Knut Ivar Aasarød: RENAL INVOLVEMENT IN INFLAMMATORY RHEUMATIC DISEASE. A Study of Renal Disease in Wegener's Granulomatosis and in Primary Sjögren's Syndrome
187. Trude Helen Flo: RESEPTORS INVOLVED IN CELL ACTIVATION BY DEFINED URONIC ACID POLYMERS AND BACTERIAL COMPONENTS
188. Bodil Kavli: HUMAN URACIL-DNA GLYCOSYLASES FROM THE UNG GENE: STRUCTRUAL BASIS FOR SUBSTRATE SPECIFICITY AND REPAIR
189. Liv Thommesen: MOLECULAR MECHANISMS INVOLVED IN TNF- AND GASTRIN-MEDIATED GENE REGULATION
190. Turid Lingaas Holmen: SMOKING AND HEALTH IN ADOLESCENCE; THE NORD-TRØNDELAG HEALTH STUDY, 1995-97
191. Øyvind Hjertner: MULTIPLE MYELOMA: INTERACTIONS BETWEEN MALIGNANT PLASMA CELLS AND THE BONE MICROENVIRONMENT

192. Asbjørn Støylen: STRAIN RATE IMAGING OF THE LEFT VENTRICLE BY ULTRASOUND. FEASIBILITY, CLINICAL VALIDATION AND PHYSIOLOGICAL ASPECTS
193. Kristian Midthjell: DIABETES IN ADULTS IN NORD-TRØNDELAG. PUBLIC HEALTH ASPECTS OF DIABETES MELLITUS IN A LARGE, NON-SELECTED NORWEGIAN POPULATION.
194. Guanglin Cui: FUNCTIONAL ASPECTS OF THE ECL CELL IN RODENTS
195. Ulrik Wisløff: CARDIAC EFFECTS OF AEROBIC ENDURANCE TRAINING: HYPERTROPHY, CONTRACTILITY AND CALCUIM HANDLING IN NORMAL AND FAILING HEART
196. Øyvind Halaas: MECHANISMS OF IMMUNOMODULATION AND CELL-MEDIATED CYTOTOXICITY INDUCED BY BACTERIAL PRODUCTS
197. Tore Amundsen: PERFUSION MR IMAGING IN THE DIAGNOSIS OF PULMONARY EMBOLISM
198. Nanna Kurtze: THE SIGNIFICANCE OF ANXIETY AND DEPRESSION IN FATIQUE AND PATTERNS OF PAIN AMONG INDIVIDUALS DIAGNOSED WITH FIBROMYALGIA: RELATIONS WITH QUALITY OF LIFE, FUNCTIONAL DISABILITY, LIFESTYLE, EMPLOYMENT STATUS, CO-MORBIDITY AND GENDER
199. Tom Ivar Lund Nilsen: PROSPECTIVE STUDIES OF CANCER RISK IN NORD-TRØNDELAG: THE HUNT STUDY. Associations with anthropometric, socioeconomic, and lifestyle risk factors
200. Asta Kristine Håberg: A NEW APPROACH TO THE STUDY OF MIDDLE CEREBRAL ARTERY OCCLUSION IN THE RAT USING MAGNETIC RESONANCE TECHNIQUES

2002

201. Knut Jørgen Arntzen: PREGNANCY AND CYTOKINES
202. Henrik Døllner: INFLAMMATORY MEDIATORS IN PERINATAL INFECTIONS
203. Asta Bye: LOW FAT, LOW LACTOSE DIET USED AS PROPHYLACTIC TREATMENT OF ACUTE INTESTINAL REACTIONS DURING PELVIC RADIOTHERAPY. A PROSPECTIVE RANDOMISED STUDY.
204. Sylvester Moyo: STUDIES ON STREPTOCOCCUS AGALACTIAE (GROUP B STREPTOCOCCUS) SURFACE-ANCHORED MARKERS WITH EMPHASIS ON STRAINS AND HUMAN SERA FROM ZIMBABWE.
205. Knut Hagen: HEAD-HUNT: THE EPIDEMIOLOGY OF HEADACHE IN NORD-TRØNDELAG
206. Li Lixin: ON THE REGULATION AND ROLE OF UNCOUPLING PROTEIN-2 IN INSULIN PRODUCING ß-CELLS
207. Anne Hildur Henriksen: SYMPTOMS OF ALLERGY AND ASTHMA VERSUS MARKERS OF LOWER AIRWAY INFLAMMATION AMONG ADOLESCENTS
208. Egil Andreas Fors: NON-MALIGNANT PAIN IN RELATION TO PSYCHOLOGICAL AND ENVIRONTENTAL FACTORS. EXPERIENTAL AND CLINICAL STUDES OF PAIN WITH FOCUS ON FIBROMYALGIA
209. Pål Klepstad: MORPHINE FOR CANCER PAIN
210. Ingunn Bakke: MECHANISMS AND CONSEQUENCES OF PEROXISOME PROLIFERATOR-INDUCED HYPERFUNCTION OF THE RAT GASTRIN PRODUCING CELL
211. Ingrid Susann Gribbestad: MAGNETIC RESONANCE IMAGING AND SPECTROSCOPY OF BREAST CANCER
212. Rønnaug Astri Ødegård: PREECLAMPSIA – MATERNAL RISK FACTORS AND FETAL GROWTH
213. Johan Haux: STUDIES ON CYTOTOXICITY INDUCED BY HUMAN NATURAL KILLER CELLS AND DIGITOXIN
214. Turid Suzanne Berg-Nielsen: PARENTING PRACTICES AND MENTALLY DISORDERED ADOLESCENTS
215. Astrid Rydning: BLOOD FLOW AS A PROTECTIVE FACTOR FOR THE STOMACH MUCOSA. AN EXPERIMENTAL STUDY ON THE ROLE OF MAST CELLS AND SENSORY AFFERENT NEURONS

2003

216. Jan Pål Loennechen: HEART FAILURE AFTER MYOCARDIAL INFARCTION. Regional Differences, Myocyte Function, Gene Expression, and Response to Cariporide, Losartan, and Exercise Training.

217. Elisabeth Qvigstad: EFFECTS OF FATTY ACIDS AND OVER-STIMULATION ON INSULIN SECRETION IN MAN
218. Arne Åsberg: EPIDEMIOLOGICAL STUDIES IN HEREDITARY HEMOCHROMATOSIS: PREVALENCE, MORBIDITY AND BENEFIT OF SCREENING.
219. Johan Fredrik Skomsvoll: REPRODUCTIVE OUTCOME IN WOMEN WITH RHEUMATIC DISEASE. A population registry based study of the effects of inflammatory rheumatic disease and connective tissue disease on reproductive outcome in Norwegian women in 1967-1995.
220. Siv Mørkved: URINARY INCONTINENCE DURING PREGNANCY AND AFTER DELIVERY: EFFECT OF PELVIC FLOOR MUSCLE TRAINING IN PREVENTION AND TREATMENT
221. Marit S. Jordhøy: THE IMPACT OF COMPREHENSIVE PALLIATIVE CARE
222. Tom Christian Martinsen: HYPERGASTRINEMIA AND HYPOACIDITY IN RODENTS – CAUSES AND CONSEQUENCES
223. Solveig Tingulstad: CENTRALIZATION OF PRIMARY SURGERY FOR OVARAIN CANCER. FEASIBILITY AND IMPACT ON SURVIVAL
224. Haytham Eloqayli: METABOLIC CHANGES IN THE BRAIN CAUSED BY EPILEPTIC SEIZURES
225. Torunn Bruland: STUDIES OF EARLY RETROVIRUS-HOST INTERACTIONS – VIRAL DETERMINANTS FOR PATHOGENESIS AND THE INFLUENCE OF SEX ON THE SUSCEPTIBILITY TO FRIEND MURINE LEUKAEMIA VIRUS INFECTION
226. Torstein Hole: DOPPLER ECHOCARDIOGRAPHIC EVALUATION OF LEFT VENTRICULAR FUNCTION IN PATIENTS WITH ACUTE MYOCARDIAL INFARCTION
227. Vibeke Nossum: THE EFFECT OF VASCULAR BUBBLES ON ENDOTHELIAL FUNCTION
228. Sigurd Fasting: ROUTINE BASED RECORDING OF ADVERSE EVENTS DURING ANAESTHESIA – APPLICATION IN QUALITY IMPROVEMENT AND SAFETY
229. Solfrid Romundstad: EPIDEMIOLOGICAL STUDIES OF MICROALBUMINURIA. THE NORD-TRØNDELAG HEALTH STUDY 1995-97 (HUNT 2)
230. Geir Torheim: PROCESSING OF DYNAMIC DATA SETS IN MAGNETIC RESONANCE IMAGING
231. Catrine Ahlén: SKIN INFECTIONS IN OCCUPATIONAL SATURATION DIVERS IN THE NORTH SEA AND THE IMPACT OF THE ENVIRONMENT
232. Arnulf Langhammer: RESPIRATORY SYMPTOMS, LUNG FUNCTION AND BONE MINERAL DENSITY IN A COMPREHENSIVE POPULATION SURVEY. THE NORD-TRØNDELAG HEALTH STUDY 1995-97. THE BRONCHIAL OBSTRUCTION IN NORD-TRØNDELAG STUDY
233. Einar Kjelsås: EATING DISORDERS AND PHYSICAL ACTIVITY IN NON-CLINICAL SAMPLES
234. Arne Wibe: RECTAL CANCER TREATMENT IN NORWAY – STANDARDISATION OF SURGERY AND QUALITY ASSURANCE

2004

235. Eivind Witsø: BONE GRAFT AS AN ANTIBIOTIC CARRIER
236. Anne Mari Sund: DEVELOPMENT OF DEPRESSIVE SYMPTOMS IN EARLY ADOLESCENCE
237. Hallvard Lærum: EVALUATION OF ELECTRONIC MEDICAL RECORDS – A CLINICAL TASK PERSPECTIVE
238. Gustav Mikkelsen: ACCESSIBILITY OF INFORMATION IN ELECTRONIC PATIENT RECORDS; AN EVALUATION OF THE ROLE OF DATA QUALITY
239. Steinar Krokstad: SOCIOECONOMIC INEQUALITIES IN HEALTH AND DISABILITY. SOCIAL EPIDEMIOLOGY IN THE NORD-TRØNDELAG HEALTH STUDY (HUNT), NORWAY
240. Arne Kristian Myhre: NORMAL VARIATION IN ANOGENITAL ANATOMY AND MICROBIOLOGY IN NON-ABUSED PRESCHOOL CHILDREN
241. Ingunn Dybedal: NEGATIVE REGULATORS OF HEMATOPOIETEC STEM AND PROGENITOR CELLS
242. Beate Sitter: TISSUE CHARACTERIZATION BY HIGH RESOLUTION MAGIC ANGLE SPINNING MR SPECTROSCOPY
243. Per Arne Aas: MACROMOLECULAR MAINTENANCE IN HUMAN CELLS – REPAIR OF URACIL IN DNA AND METHYLATIONS IN DNA AND RNA

244. Anna Bofin: FINE NEEDLE ASPIRATION CYTOLOGY IN THE PRIMARY INVESTIGATION OF BREAST TUMOURS AND IN THE DETERMINATION OF TREATMENT STRATEGIES
245. Jim Aage Nøttestad: DEINSTITUTIONALIZATION AND MENTAL HEALTH CHANGES AMONG PEOPLE WITH MENTAL RETARDATION
246. Reidar Fossmark: GASTRIC CANCER IN JAPANESE COTTON RATS
247. Wibeke Nordhøy: MANGANESE AND THE HEART, INTRACELLULAR MR RELAXATION AND WATER EXCHANGE ACROSS THE CARDIAC CELL MEMBRANE

2005

248. Sturla Molden: QUANTITATIVE ANALYSES OF SINGLE UNITS RECORDED FROM THE HIPPOCAMPUS AND ENTORHINAL CORTEX OF BEHAVING RATS
249. Wenche Brenne Drøyvold: EPIDEMIOLOGICAL STUDIES ON WEIGHT CHANGE AND HEALTH IN A LARGE POPULATION. THE NORD-TRØNDELAG HEALTH STUDY (HUNT)
250. Ragnhild Støen: ENDOTHELIUM-DEPENDENT VASODILATION IN THE FEMORAL ARTERY OF DEVELOPING PIGLETS
251. Aslak Steinsbekk: HOMEOPATHY IN THE PREVENTION OF UPPER RESPIRATORY TRACT INFECTIONS IN CHILDREN
252. Hill-Aina Steffenach: MEMORY IN HIPPOCAMPAL AND CORTICO-HIPPOCAMPAL CIRCUITS
253. Eystein Stordal: ASPECTS OF THE EPIDEMIOLOGY OF DEPRESSIONS BASED ON SELF-RATING IN A LARGE GENERAL HEALTH STUDY (THE HUNT-2 STUDY)
254. Viggo Pettersen: FROM MUSCLES TO SINGING: THE ACTIVITY OF ACCESSORY BREATHING MUSCLES AND THORAX MOVEMENT IN CLASSICAL SINGING
255. Marianne Fyhn: SPATIAL MAPS IN THE HIPPOCAMPUS AND ENTORHINAL CORTEX
256. Robert Valderhaug: OBSESSIVE-COMPULSIVE DISORDER AMONG CHILDREN AND ADOLESCENTS: CHARACTERISTICS AND PSYCHOLOGICAL MANAGEMENT OF PATIENTS IN OUTPATIENT PSYCHIATRIC CLINICS
257. Erik Skaaheim Haug: INFRARENAL ABDOMINAL AORTIC ANEURYSMS – COMORBIDITY AND RESULTS FOLLOWING OPEN SURGERY
258. Daniel Kondziella: GLIAL-NEURONAL INTERACTIONS IN EXPERIMENTAL BRAIN DISORDERS
259. Vegard Heimly Brun: ROUTES TO SPATIAL MEMORY IN HIPPOCAMPAL PLACE CELLS
260. Kenneth McMillan: PHYSIOLOGICAL ASSESSMENT AND TRAINING OF ENDURANCE AND STRENGTH IN PROFESSIONAL YOUTH SOCCER PLAYERS
261. Marit Sæbø Indredavik: MENTAL HEALTH AND CEREBRAL MAGNETIC RESONANCE IMAGING IN ADOLESCENTS WITH LOW BIRTH WEIGHT
262. Ole Johan Kemi: ON THE CELLULAR BASIS OF AEROBIC FITNESS, INTENSITY-DEPENDENCE AND TIME-COURSE OF CARDIOMYOCYTE AND ENDOTHELIAL ADAPTATIONS TO EXERCISE TRAINING
263. Eszter Vanky: POLYCYSTIC OVARY SYNDROME – METFORMIN TREATMENT IN PREGNANCY
264. Hild Fjærtoft: EXTENDED STROKE UNIT SERVICE AND EARLY SUPPORTED DISCHARGE. SHORT AND LONG-TERM EFFECTS
265. Grete Dyb: POSTTRAUMATIC STRESS REACTIONS IN CHILDREN AND ADOLESCENTS
266. Vidar Fykse: SOMATOSTATIN AND THE STOMACH
267. Kirsti Berg: OXIDATIVE STRESS AND THE ISCHEMIC HEART: A STUDY IN PATIENTS UNDERGOING CORONARY REVASCULARIZATION
268. Björn Inge Gustafsson: THE SEROTONIN PRODUCING ENTEROCHROMAFFIN CELL, AND EFFECTS OF HYPERSEROTONINEMIA ON HEART AND BONE

2006

269. Torstein Baade Rø: EFFECTS OF BONE MORPHOGENETIC PROTEINS, HEPATOCYTE GROWTH FACTOR AND INTERLEUKIN-21 IN MULTIPLE MYELOMA
270. May-Britt Tessem: METABOLIC EFFECTS OF ULTRAVIOLET RADIATION ON THE ANTERIOR PART OF THE EYE
271. Anne-Sofie Helvik: COPING AND EVERYDAY LIFE IN A POPULATION OF ADULTS WITH HEARING IMPAIRMENT

272. Therese Standal: MULTIPLE MYELOMA: THE INTERPLAY BETWEEN MALIGNANT PLASMA CELLS AND THE BONE MARROW MICROENVIRONMENT
273. Ingvild Saltvedt: TREATMENT OF ACUTELY SICK, FRAIL ELDERLY PATIENTS IN A GERIATRIC EVALUATION AND MANAGEMENT UNIT – RESULTS FROM A PROSPECTIVE RANDOMISED TRIAL
274. Birger Henning Endreseth: STRATEGIES IN RECTAL CANCER TREATMENT – FOCUS ON EARLY RECTAL CANCER AND THE INFLUENCE OF AGE ON PROGNOSIS
275. Anne Mari Aukan Rokstad: ALGINATE CAPSULES AS BIOREACTORS FOR CELL THERAPY
276. Mansour Akbari: HUMAN BASE EXCISION REPAIR FOR PRESERVATION OF GENOMIC STABILITY
277. Stein Sundstrøm: IMPROVING TREATMENT IN PATIENTS WITH LUNG CANCER – RESULTS FROM TWO MULITCENTRE RANDOMISED STUDIES
278. Hilde Pleym: BLEEDING AFTER CORONARY ARTERY BYPASS SURGERY - STUDIES ON HEMOSTATIC MECHANISMS, PROPHYLACTIC DRUG TREATMENT AND EFFECTS OF AUTOTRANSFUSION
279. Line Merethe Oldervoll: PHYSICAL ACTIVITY AND EXERCISE INTERVENTIONS IN CANCER PATIENTS
280. Boye Welde: THE SIGNIFICANCE OF ENDURANCE TRAINING, RESISTANCE TRAINING AND MOTIVATIONAL STYLES IN ATHLETIC PERFORMANCE AMONG ELITE JUNIOR CROSS-COUNTRY SKIERS
281. Per Olav Vandvik: IRRITABLE BOWEL SYNDROME IN NORWAY, STUDIES OF PREVALENCE, DIAGNOSIS AND CHARACTERISTICS IN GENERAL PRACTICE AND IN THE POPULATION
282. Idar Kirkeby-Garstad: CLINICAL PHYSIOLOGY OF EARLY MOBILIZATION AFTER CARDIAC SURGERY
283. Linn Getz: SUSTAINABLE AND RESPONSIBLE PREVENTIVE MEDICINE. CONCEPTUALISING ETHICAL DILEMMAS ARISING FROM CLINICAL IMPLEMENTATION OF ADVANCING MEDICAL TECHNOLOGY
284. Eva Tegnander: DETECTION OF CONGENITAL HEART DEFECTS IN A NON-SELECTED POPULATION OF 42,381 FETUSES
285. Kristin Gabestad Nørsett: GENE EXPRESSION STUDIES IN GASTROINTESTINAL PATHOPHYSIOLOGY AND NEOPLASIA
286. Per Magnus Haram: GENETIC VS. AQUIRED FITNESS: METABOLIC, VASCULAR AND CARDIOMYOCYTE ADAPTATIONS
287. Agneta Johansson: GENERAL RISK FACTORS FOR GAMBLING PROBLEMS AND THE PREVALENCE OF PATHOLOGICAL GAMBLING IN NORWAY
288. Svein Artur Jensen: THE PREVALENCE OF SYMPTOMATIC ARTERIAL DISEASE OF THE LOWER LIMB
289. Charlotte Björk Ingul: QUANITIFICATION OF REGIONAL MYOCARDIAL FUNCTION BY STRAIN RATE AND STRAIN FOR EVALUATION OF CORONARY ARTERY DISEASE. AUTOMATED VERSUS MANUAL ANALYSIS DURING ACUTE MYOCARDIAL INFARCTION AND DOBUTAMINE STRESS ECHOCARDIOGRAPHY
290. Jakob Nakling: RESULTS AND CONSEQUENCES OF ROUTINE ULTRASOUND SCREENING IN PREGNANCY – A GEOGRAPHIC BASED POPULATION STUDY
291. Anne Engum: DEPRESSION AND ANXIETY – THEIR RELATIONS TO THYROID DYSFUNCTION AND DIABETES IN A LARGE EPIDEMIOLOGICAL STUDY
292. Ottar Bjerkeset: ANXIETY AND DEPRESSION IN THE GENERAL POPULATION: RISK FACTORS, INTERVENTION AND OUTCOME – THE NORD-TRØNDELAG HEALTH STUDY (HUNT)
293. Jon Olav Drogset: RESULTS AFTER SURGICAL TREATMENT OF ANTERIOR CRUCIATE LIGAMENT INJURIES – A CLINICAL STUDY
294. Lars Fosse: MECHANICAL BEHAVIOUR OF COMPACTED MORSELLISED BONE – AN EXPERIMENTAL IN VITRO STUDY
295. Gunilla Klensmeden Fosse: MENTAL HEALTH OF PSYCHIATRIC OUTPATIENTS BULLIED IN CHILDHOOD
296. Paul Jarle Mork: MUSCLE ACTIVITY IN WORK AND LEISURE AND ITS ASSOCIATION TO MUSCULOSKELETAL PAIN

297. Björn Stenström: LESSONS FROM RODENTS: I: MECHANISMS OF OBESITY SURGERY – ROLE OF STOMACH. II: CARCINOGENIC EFFECTS OF *HELICOBACTER PYLORI* AND SNUS IN THE STOMACH

2007

298. Haakon R. Skogseth: INVASIVE PROPERTIES OF CANCER – A TREATMENT TARGET ? IN VITRO STUDIES IN HUMAN PROSTATE CANCER CELL LINES
299. Janniche Hammer: GLUTAMATE METABOLISM AND CYCLING IN MESIAL TEMPORAL LOBE EPILEPSY
300. May Britt Drugli: YOUNG CHILDREN TREATED BECAUSE OF ODD/CD: CONDUCT PROBLEMS AND SOCIAL COMPETENCIES IN DAY-CARE AND SCHOOL SETTINGS
301. Arne Skjold: MAGNETIC RESONANCE KINETICS OF MANGANESE DIPYRIDOXYL DIPHOSPHATE (MnDPDP) IN HUMAN MYOCARDIUM. STUDIES IN HEALTHY VOLUNTEERS AND IN PATIENTS WITH RECENT MYOCARDIAL INFARCTION
302. Siri Malm: LEFT VENTRICULAR SYSTOLIC FUNCTION AND MYOCARDIAL PERFUSION ASSESSED BY CONTRAST ECHOCARDIOGRAPHY
303. Valentina Maria do Rosario Cabral Iversen: MENTAL HEALTH AND PSYCHOLOGICAL ADAPTATION OF CLINICAL AND NON-CLINICAL MIGRANT GROUPS
304. Lasse Løvstakken: SIGNAL PROCESSING IN DIAGNOSTIC ULTRASOUND: ALGORITHMS FOR REAL-TIME ESTIMATION AND VISUALIZATION OF BLOOD FLOW VELOCITY
305. Elisabeth Olstad: GLUTAMATE AND GABA: MAJOR PLAYERS IN NEURONAL METABOLISM
306. Lilian Leistad: THE ROLE OF CYTOKINES AND PHOSPHOLIPASE A_2s IN ARTICULAR CARTILAGE CHONDROCYTES IN RHEUMATOID ARTHRITIS AND OSTEOARTHRITIS
307. Arne Vaaler: EFFECTS OF PSYCHIATRIC INTENSIVE CARE UNIT IN AN ACUTE PSYCIATHRIC WARD
308. Mathias Toft: GENETIC STUDIES OF LRRK2 AND PINK1 IN PARKINSON'S DISEASE
309. Ingrid Løvold Mostad: IMPACT OF DIETARY FAT QUANTITY AND QUALITY IN TYPE 2 DIABETES WITH EMPHASIS ON MARINE N-3 FATTY ACIDS
310. Torill Eidhammer Sjøbakk: MR DETERMINED BRAIN METABOLIC PATTERN IN PATIENTS WITH BRAIN METASTASES AND ADOLESCENTS WITH LOW BIRTH WEIGHT
311. Vidar Beisvåg: PHYSIOLOGICAL GENOMICS OF HEART FAILURE: FROM TECHNOLOGY TO PHYSIOLOGY
312. Olav Magnus Søndenå Fredheim: HEALTH RELATED QUALITY OF LIFE ASSESSMENT AND ASPECTS OF THE CLINICAL PHARMACOLOGY OF METHADONE IN PATIENTS WITH CHRONIC NON-MALIGNANT PAIN
313. Anne Brantberg: FETAL AND PERINATAL IMPLICATIONS OF ANOMALIES IN THE GASTROINTESTINAL TRACT AND THE ABDOMINAL WALL
314. Erik Solligård: GUT LUMINAL MICRODIALYSIS
315. Elin Tollefsen: RESPIRATORY SYMPTOMS IN A COMPREHENSIVE POPULATION BASED STUDY AMONG ADOLESCENTS 13-19 YEARS. YOUNG-HUNT 1995-97 AND 2000-01; THE NORD-TRØNDELAG HEALTH STUDIES (HUNT)
316. Anne-Tove Brenne: GROWTH REGULATION OF MYELOMA CELLS
317. Heidi Knobel: FATIGUE IN CANCER TREATMENT – ASSESSMENT, COURSE AND ETIOLOGY
318. Torbjørn Dahl: CAROTID ARTERY STENOSIS. DIAGNOSTIC AND THERAPEUTIC ASPECTS
319. Inge-Andre Rasmussen jr.: FUNCTIONAL AND DIFFUSION TENSOR MAGNETIC RESONANCE IMAGING IN NEUROSURGICAL PATIENTS
320. Grete Helen Bratberg: PUBERTAL TIMING – ANTECEDENT TO RISK OR RESILIENCE ? EPIDEMIOLOGICAL STUDIES ON GROWTH, MATURATION AND HEALTH RISK BEHAVIOURS; THE YOUNG HUNT STUDY, NORD-TRØNDELAG, NORWAY
321. Sveinung Sørhaug: THE PULMONARY NEUROENDOCRINE SYSTEM. PHYSIOLOGICAL, PATHOLOGICAL AND TUMOURIGENIC ASPECTS
322. Olav Sande Eftedal: ULTRASONIC DETECTION OF DECOMPRESSION INDUCED VASCULAR MICROBUBBLES
323. Rune Bang Leistad: PAIN, AUTONOMIC ACTIVATION AND MUSCULAR ACTIVITY RELATED TO EXPERIMENTALLY-INDUCED COGNITIVE STRESS IN HEADACHE PATIENTS

324. Svein Brekke: TECHNIQUES FOR ENHANCEMENT OF TEMPORAL RESOLUTION IN THREE-DIMENSIONAL ECHOCARDIOGRAPHY
325. Kristian Bernhard Nilsen: AUTONOMIC ACTIVATION AND MUSCLE ACTIVITY IN RELATION TO MUSCULOSKELETAL PAIN
326. Anne Irene Hagen: HEREDITARY BREAST CANCER IN NORWAY. DETECTION AND PROGNOSIS OF BREAST CANCER IN FAMILIES WITH *BRCA1*GENE MUTATION
327. Ingebjørg S. Juel : INTESTINAL INJURY AND RECOVERY AFTER ISCHEMIA. AN EXPERIMENTAL STUDY ON RESTITUTION OF THE SURFACE EPITHELIUM, INTESTINAL PERMEABILITY, AND RELEASE OF BIOMARKERS FROM THE MUCOSA
328. Runa Heimstad: POST-TERM PREGNANCY
329. Jan Egil Afset: ROLE OF ENTEROPATHOGENIC *ESCHERICHIA COLI* IN CHILDHOOD DIARRHOEA IN NORWAY
330. Bent Håvard Hellum: *IN VITRO* INTERACTIONS BETWEEN MEDICINAL DRUGS AND HERBS ON CYTOCHROME P-450 METABOLISM AND P-GLYCOPROTEIN TRANSPORT
331. Morten André Høydal: CARDIAC DYSFUNCTION AND MAXIMAL OXYGEN UPTAKE MYOCARDIAL ADAPTATION TO ENDURANCE TRAINING

2008

332. Andreas Møllerløkken: REDUCTION OF VASCULAR BUBBLES: METHODS TO PREVENT THE ADVERSE EFFECTS OF DECOMPRESSION
333. Anne Hege Aamodt: COMORBIDITY OF HEADACHE AND MIGRAINE IN THE NORD-TRØNDELAG HEALTH STUDY 1995-97
334. Brage Høyem Amundsen: MYOCARDIAL FUNCTION QUANTIFIED BY SPECKLE TRACKING AND TISSUE DOPPLER ECHOCARDIOGRAPHY – VALIDATION AND APPLICATION IN EXERCISE TESTING AND TRAINING
335. Inger Anne Næss: INCIDENCE, MORTALITY AND RISK FACTORS OF FIRST VENOUS THROMBOSIS IN A GENERAL POPULATION. RESULTS FROM THE SECOND NORD-TRØNDELAG HEALTH STUDY (HUNT2)
336. Vegard Bugten: EFFECTS OF POSTOPERATIVE MEASURES AFTER FUNCTIONAL ENDOSCOPIC SINUS SURGERY
337. Morten Bruvold: MANGANESE AND WATER IN CARDIAC MAGNETIC RESONANCE IMAGING
338. Miroslav Fris: THE EFFECT OF SINGLE AND REPEATED ULTRAVIOLET RADIATION ON THE ANTERIOR SEGMENT OF THE RABBIT EYE
339. Svein Arne Aase: METHODS FOR IMPROVING QUALITY AND EFFICIENCY IN QUANTITATIVE ECHOCARDIOGRAPHY – ASPECTS OF USING HIGH FRAME RATE
340. Roger Almvik: ASSESSING THE RISK OF VIOLENCE: DEVELOPMENT AND VALIDATION OF THE BRØSET VIOLENCE CHECKLIST
341. Ottar Sundheim: STRUCTURE-FUNCTION ANALYSIS OF HUMAN ENZYMES INITIATING NUCLEOBASE REPAIR IN DNA AND RNA
342. Anne Mari Undheim: SHORT AND LONG-TERM OUTCOME OF EMOTIONAL AND BEHAVIOURAL PROBLEMS IN YOUNG ADOLESCENTS WITH AND WITHOUT READING DIFFICULTIES
343. Helge Garåsen: THE TRONDHEIM MODEL. IMPROVING THE PROFESSIONAL COMMUNICATION BETWEEN THE VARIOUS LEVELS OF HEALTH CARE SERVICES AND IMPLEMENTATION OF INTERMEDIATE CARE AT A COMMUNITY HOSPITAL COULD PROVIDE BETTER CARE FOR OLDER PATIENTS. SHORT AND LONG TERM EFFECTS
344. Olav A. Foss: "THE ROTATION RATIOS METHOD". A METHOD TO DESCRIBE ALTERED SPATIAL ORIENTATION IN SEQUENTIAL RADIOGRAPHS FROM ONE PELVIS
345. Bjørn Olav Åsvold: THYROID FUNCTION AND CARDIOVASCULAR HEALTH
346. Torun Margareta Melø: NEURONAL GLIAL INTERACTIONS IN EPILEPSY
347. Irina Poliakova Eide: FETAL GROWTH RESTRICTION AND PRE-ECLAMPSIA: SOME CHARACTERISTICS OF FETO-MATERNAL INTERACTIONS IN DECIDUA BASALIS
348. Torunn Askim: RECOVERY AFTER STROKE. ASSESSMENT AND TREATMENT; WITH FOCUS ON MOTOR FUNCTION
349. Ann Elisabeth Åsberg: NEUTROPHIL ACTIVATION IN A ROLLER PUMP MODEL OF CARDIOPULMONARY BYPASS. INFLUENCE ON BIOMATERIAL, PLATELETS AND COMPLEMENT

350. Lars Hagen: REGULATION OF DNA BASE EXCISION REPAIR BY PROTEIN INTERACTIONS AND POST TRANSLATIONAL MODIFICATIONS
351. Sigrun Beate Kjøtrød: POLYCYSTIC OVARY SYNDROME – METFORMIN TREATMENT IN ASSISTED REPRODUCTION
352. Steven Keita Nishiyama: PERSPECTIVES ON LIMB-VASCULAR HETEROGENEITY: IMPLICATIONS FOR HUMAN AGING, SEX, AND EXERCISE
353. Sven Peter Näsholm: ULTRASOUND BEAMS FOR ENHANCED IMAGE QUALITY
354. Jon Ståle Ritland: PRIMARY OPEN-ANGLE GLAUCOMA & EXFOLIATIVE GLAUCOMA. SURVIVAL, COMORBIDITY AND GENETICS
355. Sigrid Botne Sando: ALZHEIMER'S DISEASE IN CENTRAL NORWAY. GENETIC AND EDUCATIONAL ASPECTS
356. Parvinder Kaur: CELLULAR AND MOLECULAR MECHANISMS BEHIND METHYLMERCURY-INDUCED NEUROTOXICITY
357. Ismail Cüneyt Güzey: DOPAMINE AND SEROTONIN RECEPTOR AND TRANSPORTER GENE POLYMORPHISMS AND EXTRAPYRAMIDAL SYMPTOMS. STUDIES IN PARKINSON'S DISEASE AND IN PATIENTS TREATED WITH ANTIPSYCHOTIC OR ANTIDEPRESSANT DRUGS
358. Brit Dybdahl: EXTRA-CELLULAR INDUCIBLE HEAT-SHOCK PROTEIN 70 (Hsp70) – A ROLE IN THE INFLAMMATORY RESPONSE ?
359. Kristoffer Haugarvoll: IDENTIFYING GENETIC CAUSES OF PARKINSON'S DISEASE IN NORWAY
360. Nadra Nilsen: TOLL-LIKE RECEPTOR 2 –EXPRESSION, REGULATION AND SIGNALING
361. Johan Håkon Bjørngaard: PATIENT SATISFACTION WITH OUTPATIENT MENTAL HEALTH SERVICES – THE INFLUENCE OF ORGANIZATIONAL FACTORS.
362. Kjetil Høydal : EFFECTS OF HIGH INTENSITY AEROBIC TRAINING IN HEALTHY SUBJECTS AND CORONARY ARTERY DISEASE PATIENTS; THE IMPORTANCE OF INTENSITY,, DURATION AND FREQUENCY OF TRAINING.
363. Trine Karlsen: TRAINING IS MEDICINE: ENDURANCE AND STRENGTH TRAINING IN CORONARY ARTERY DISEASE AND HEALTH.
364. Marte Thuen: MANGANASE-ENHANCED AND DIFFUSION TENSOR MR IMAGING OF THE NORMAL, INJURED AND REGENERATING RAT VISUAL PATHWAY
365. Cathrine Broberg Vågbø: DIRECT REPAIR OF ALKYLATION DAMAGE IN DNA AND RNA BY 2-OXOGLUTARATE- AND IRON-DEPENDENT DIOXYGENASES
366. Arnt Erik Tjønna: AEROBIC EXERCISE AND CARDIOVASCULAR RISK FACTORS IN OVERWEIGHT AND OBESE ADOLESCENTS AND ADULTS
367. Marianne W. Furnes: FEEDING BEHAVIOR AND BODY WEIGHT DEVELOPMENT: LESSONS FROM RATS
368. Lene N. Johannessen: FUNGAL PRODUCTS AND INFLAMMATORY RESPONSES IN HUMAN MONOCYTES AND EPITHELIAL CELLS
369. Anja Bye: GENE EXPRESSION PROFILING OF *INHERITED* AND *ACQUIRED* MAXIMAL OXYGEN UPTAKE – RELATIONS TO THE METABOLIC SYNDROME.
370. Oluf Dimitri Røe: MALIGNANT MESOTHELIOMA: VIRUS, BIOMARKERS AND GENES. A TRANSLATIONAL APPROACH
371. Ane Cecilie Dale: DIABETES MELLITUS AND FATAL ISCHEMIC HEART DISEASE. ANALYSES FROM THE HUNT1 AND 2 STUDIES
372. Jacob Christian Hølen: PAIN ASSESSMENT IN PALLIATIVE CARE: VALIDATION OF METHODS FOR SELF-REPORT AND BEHAVIOURAL ASSESSMENT
373. Erming Tian: THE GENETIC IMPACTS IN THE ONCOGENESIS OF MULTIPLE MYELOMA
374. Ole Bosnes: KLINISK UTPRØVING AV NORSKE VERSJONER AV NOEN SENTRALE TESTER PÅ KOGNITIV FUNKSJON
375. Ola M. Rygh: 3D ULTRASOUND BASED NEURONAVIGATION IN NEUROSURGERY. A CLINICAL EVALUATION
376. Astrid Kamilla Stunes: ADIPOKINES, PEROXISOME PROFILERATOR ACTIVATED RECEPTOR (PPAR) AGONISTS AND SEROTONIN. COMMON REGULATORS OF BONE AND FAT METABOLISM
377. Silje Engdal: HERBAL REMEDIES USED BY NORWEGIAN CANCER PATIENTS AND THEIR ROLE IN HERB-DRUG INTERACTIONS
378. Kristin Offerdal: IMPROVED ULTRASOUND IMAGING OF THE FETUS AND ITS CONSEQUENCES FOR SEVERE AND LESS SEVERE ANOMALIES

379. Øivind Rognmo: HIGH-INTENSITY AEROBIC EXERCISE AND CARDIOVASCULAR HEALTH
380. Jo-Åsmund Lund: RADIOTHERAPY IN ANAL CARCINOMA AND PROSTATE CANCER

2009

381. Tore Grüner Bjåstad: HIGH FRAME RATE ULTRASOUND IMAGING USING PARALLEL BEAMFORMING
382. Erik Søndenaa: INTELLECTUAL DISABILITIES IN THE CRIMINAL JUSTICE SYSTEM
383. Berit Rostad: SOCIAL INEQUALITIES IN WOMEN'S HEALTH, HUNT 1984-86 AND 1995-97, THE NORD-TRØNDELAG HEALTH STUDY (HUNT)
384. Jonas Crosby: ULTRASOUND-BASED QUANTIFICATION OF MYOCARDIAL DEFORMATION AND ROTATION
385. Erling Tronvik: MIGRAINE, BLOOD PRESSURE AND THE RENIN-ANGIOTENSIN SYSTEM
386. Tom Christensen: BRINGING THE GP TO THE FOREFRONT OF EPR DEVELOPMENT
387. Håkon Bergseng: ASPECTS OF GROUP B STREPTOCOCCUS (GBS) DISEASE IN THE NEWBORN. EPIDEMIOLOGY, CHARACTERISATION OF INVASIVE STRAINS AND EVALUATION OF INTRAPARTUM SCREENING
388. Ronny Myhre: GENETIC STUDIES OF CANDIDATE TENE3S IN PARKINSON'S DISEASE
389. Torbjørn Moe Eggebø: ULTRASOUND AND LABOUR
390. Eivind Wang: TRAINING IS MEDICINE FOR PATIENTS WITH PERIPHERAL ARTERIAL DISEASE
391. Thea Kristin Våtsveen: GENETIC ABERRATIONS IN MYELOMA CELLS
392. Thomas Jozefiak: QUALITY OF LIFE AND MENTAL HEALTH IN CHILDREN AND ADOLESCENTS: CHILD AND PARENT PERSPECTIVES
393. Jens Erik Slagsvold: N-3 POLYUNSATURATED FATTY ACIDS IN HEALTH AND DISEASE – CLINICAL AND MOLECULAR ASPECTS
394. Kristine Misund: A STUDY OF THE TRANSCRIPTIONAL REPRESSOR ICER. REGULATORY NETWORKS IN GASTRIN-INDUCED GENE EXPRESSION
395. Franco M. Impellizzeri: HIGH-INTENSITY TRAINING IN FOOTBALL PLAYERS. EFFECTS ON PHYSICAL AND TECHNICAL PERFORMANCE
396. Kari Hanne Gjeilo: HEALTH-RELATED QUALITY OF LIFE AND CHRONIC PAIN IN PATIENTS UNDERGOING CARDIAC SURGERY
397. Øyvind Hauso: NEUROENDOCRINE ASPECTS OF PHYSIOLOGY AND DISEASE
398. Ingvild Bjellmo Johnsen: INTRACELLULAR SIGNALING MECHANISMS IN THE INNATE IMMUNE RESPONSE TO VIRAL INFECTIONS
399. Linda Tømmerdal Roten: GENETIC PREDISPOSITION FOR DEVELOPMENT OF PREEMCLAMPSIA – CANDIDATE GENE STUDIES IN THE HUNT (NORD-TRØNDELAG HEALTH STUDY) POPULATION
400. Trude Teoline Nausthaug Rakvåg: PHARMACOGENETICS OF MORPHINE IN CANCER PAIN
401. Hanne Lehn: MEMORY FUNCTIONS OF THE HUMAN MEDIAL TEMPORAL LOBE STUDIED WITH fMRI
402. Randi Utne Holt: ADHESION AND MIGRATION OF MYELOMA CELLS – IN VITRO STUDIES –
403. Trygve Solstad: NEURAL REPRESENTATIONS OF EUCLIDEAN SPACE
404. Unn-Merete Fagerli: MULTIPLE MYELOMA CELLS AND CYTOKINES FROM THE BONE MARROW ENVIRONMENT; ASPECTS OF GROWTH REGULATION AND MIGRATION
405. Sigrid Bjørnelv: EATING– AND WEIGHT PROBLEMS IN ADOLESCENTS, THE YOUNG HUNT-STUDY
406. Mari Hoff: CORTICAL HAND BONE LOSS IN RHEUMATOID ARTHRITIS. EVALUATING DIGITAL X-RAY RADIOGRAMMETRY AS OUTCOME MEASURE OF DISEASE ACTIVITY, RESPONSE VARIABLE TO TREATMENT AND PREDICTOR OF BONE DAMAGE
407. Siri Bjørgen: AEROBIC HIGH INTENSITY INTERVAL TRAINING IS AN EFFECTIVE TREATMENT FOR PATIENTS WITH CHRONIC OBSTRUCTIVE PULMONARY DISEASE
408. Susanne Lindqvist: VISION AND BRAIN IN ADOLESCENTS WITH LOW BIRTH WEIGHT
409. Torbjørn Hergum: 3D ULTRASOUND FOR QUANTITATIVE ECHOCARDIOGRAPHY

410. Jørgen Urnes: PATIENT EDUCATION IN GASTRO-OESOPHAGEAL REFLUX DISEASE. VALIDATION OF A DIGESTIVE SYMPTOMS AND IMPACT QUESTIONNAIRE AND A RANDOMISED CONTROLLED TRIAL OF PATIENT EDUCATION
411. Elvar Eyjolfsson: 13C NMRS OF ANIMAL MODELS OF SCHIZOPHRENIA
412. Marius Steiro Fimland: CHRONIC AND ACUTE NEURAL ADAPTATIONS TO STRENGTH TRAINING
413. Øyvind Støren: RUNNING AND CYCLING ECONOMY IN ATHLETES; DETERMINING FACTORS, TRAINING INTERVENTIONS AND TESTING
414. Håkon Hov: HEPATOCYTE GROWTH FACTOR AND ITS RECEPTOR C-MET. AUTOCRINE GROWTH AND SIGNALING IN MULTIPLE MYELOMA CELLS
415. Maria Radtke: ROLE OF AUTOIMMUNITY AND OVERSTIMULATION FOR BETA-CELL DEFICIENCY. EPIDEMIOLOGICAL AND THERAPEUTIC PERSPECTIVES
416. Liv Bente Romundstad: ASSISTED FERTILIZATION IN NORWAY: SAFETY OF THE REPRODUCTIVE TECHNOLOGY
417. Erik Magnus Berntsen: PREOPERATIV PLANNING AND FUNCTIONAL NEURONAVIGATION – WITH FUNCTIONAL MRI AND DIFFUSION TENSOR TRACTOGRAPHY IN PATIENTS WITH BRAIN LESIONS
418. Tonje Strømmen Steigedal: MOLECULAR MECHANISMS OF THE PROLIFERATIVE RESPONSE TO THE HORMONE GASTRIN
419. Vidar Rao: EXTRACORPOREAL PHOTOCHEMOTHERAPY IN PATIENTS WITH CUTANEOUS T CELL LYMPHOMA OR GRAFT-vs-HOST DISEASE
420. Torkild Visnes: DNA EXCISION REPAIR OF URACIL AND 5-FLUOROURACIL IN HUMAN CANCER CELL LINES

2010

421. John Munkhaugen: BLOOD PRESSURE, BODY WEIGHT, AND KIDNEY FUNCTION IN THE NEAR-NORMAL RANGE: NORMALITY, RISK FACTOR OR MORBIDITY ?
422. Ingrid Castberg: PHARMACOKINETICS, DRUG INTERACTIONS AND ADHERENCE TO TREATMENT WITH ANTIPSYCHOTICS: STUDIES IN A NATURALISTIC SETTING
423. Jian Xu: BLOOD-OXYGEN-LEVEL-DEPENDENT-FUNCTIONAL MAGNETIC RESONANCE IMAGING AND DIFFUSION TENSOR IMAGING IN TRAUMATIC BRAIN INJURY RESEARCH
424. Sigmund Simonsen: ACCEPTABLE RISK AND THE REQUIREMENT OF PROPORTIONALITY IN EUROPEAN BIOMEDICAL RESEARCH LAW. WHAT DOES THE REQUIREMENT THAT BIOMEDICAL RESEARCH SHALL NOT INVOLVE RISKS AND BURDENS DISPROPORTIONATE TO ITS POTENTIAL BENEFITS MEAN?
425. Astrid Woodhouse: MOTOR CONTROL IN WHIPLASH AND CHRONIC NON-TRAUMATIC NECK PAIN
426. Line Rørstad Jensen: EVALUATION OF TREATMENT EFFECTS IN CANCER BY MR IMAGING AND SPECTROSCOPY
427. Trine Moholdt: AEROBIC EXERCISE IN CORONARY HEART DISEASE
428. Øystein Olsen: ANALYSIS OF MANGANESE ENHANCED MRI OF THE NORMAL AND INJURED RAT CENTRAL NERVOUS SYSTEM
429. Bjørn H. Grønberg: PEMETREXED IN THE TREATMENT OF ADVANCED LUNG CANCER
430. Vigdis Schnell Husby: REHABILITATION OF PATIENTS UNDERGOING TOTAL HIP ARTHROPLASTY WITH FOCUS ON MUSCLE STRENGTH, WALKING AND AEROBIC ENDURANCE PERFORMANCE
431. Torbjørn Øien: CHALLENGES IN PRIMARY PREVENTION OF ALLERGY. THE PREVENTION OF ALLERGY AMONG CHILDREN IN TRONDHEIM (PACT) STUDY.
432. Kari Anne Indredavik Evensen: BORN TOO SOON OR TOO SMALL: MOTOR PROBLEMS IN ADOLESCENCE
433. Lars Adde: PREDICTION OF CEREBRAL PALSY IN YOUNG INFANTS. COMPUTER BASED ASSESSMENT OF GENERAL MOVEMENTS
434. Magnus Fasting: PRE- AND POSTNATAL RISK FACTORS FOR CHILDHOOD ADIPOSITY
435. Vivi Talstad Monsen: MECHANISMS OF ALKYLATION DAMAGE REPAIR BY HUMAN AlkB HOMOLOGUES
436. Toril Skandsen: MODERATE AND SEVERE TRAUMATIC BRAIN INJURY. MAGNETIC RESONANCE IMAGING FINDINGS, COGNITION AND RISK FACTORS FOR DISABILITY

437. Ingeborg Smidesang: ALLERGY RELATED DISORDERS AMONG 2-YEAR OLDS AND ADOLESCENTS IN MID-NORWAY – PREVALENCE, SEVERITY AND IMPACT. THE PACT STUDY 2005, THE YOUNG HUNT STUDY 1995-97
438. Vidar Halsteinli: MEASURING EFFICIENCY IN MENTAL HEALTH SERVICE DELIVERY: A STUDY OF OUTPATIENT UNITS IN NORWAY
439. Karen Lehrmann Ægidius: THE PREVALENCE OF HEADACHE AND MIGRAINE IN RELATION TO SEX HORMONE STATUS IN WOMEN. THE HUNT 2 STUDY
440. Madelene Ericsson: EXERCISE TRAINING IN GENETIC MODELS OF HEART FAILURE
441. Marianne Klokk: THE ASSOCIATION BETWEEN SELF-REPORTED ECZEMA AND COMMON MENTAL DISORDERS IN THE GENERAL POPULATION. THE HORDALAND HEALTH STUDY (HUSK)
442. Tomas Ottemo Stølen: IMPAIRED CALCIUM HANDLING IN ANIMAL AND HUMAN CARDIOMYOCYTES REDUCE CONTRACTILITY AND INCREASE ARRHYTHMIA POTENTIAL – EFFECTS OF AEROBIC EXERCISE TRAINING
443. Bjarne Hansen: ENHANCING TREATMENT OUTCOME IN COGNITIVE BEHAVIOURAL THERAPY FOR OBSESSIVE COMPULSIVE DISORDER: THE IMPORTANCE OF COGNITIVE FACTORS
444. Mona Løvlien: WHEN EVERY MINUTE COUNTS. FROM SYMPTOMS TO ADMISSION FOR ACUTE MYOCARDIAL INFARCTION WITH SPECIAL EMPHASIS ON GENDER DIFFERECES
445. Karin Margaretha Gilljam: DNA REPAIR PROTEIN COMPLEXES, FUNCTIONALITY AND SIGNIFICANCE FOR REPAIR EFFICIENCY AND CELL SURVIVAL
446. Anne Byriel Walls: NEURONAL GLIAL INTERACTIONS IN CEREBRAL ENERGY – AND AMINO ACID HOMEOSTASIS – IMPLICATIONS OF GLUTAMATE AND GABA
447. Cathrine Fallang Knetter: MECHANISMS OF TOLL-LIKE RECEPTOR 9 ACTIVATION
448. Marit Følsvik Svindseth: A STUDY OF HUMILIATION, NARCISSISM AND TREATMENT OUTCOME IN PATIENTS ADMITTED TO PSYCHIATRIC EMERGENCY UNITS
449. Karin Elvenes Bakkelund: GASTRIC NEUROENDOCRINE CELLS – ROLE IN GASTRIC NEOPLASIA IN MAN AND RODENTS
450. Kirsten Brun Kjelstrup: DORSOVENTRAL DIFFERENCES IN THE SPATIAL REPRESENTATION AREAS OF THE RAT BRAIN
451. Roar Johansen: MR EVALUATION OF BREAST CANCER PATIENTS WITH POOR PROGNOSIS
452. Rigmor Myran: POST TRAUMATIC NECK PAIN. EPIDEMIOLOGICAL, NEURORADIOLOGICAL AND CLINICAL ASPECTS
453. Krisztina Kunszt Johansen: GENEALOGICAL, CLINICAL AND BIOCHEMICAL STUDIES IN *LRRK2* – ASSOCIATED PARKINSON'S DISEASE
454. Pål Gjerden: THE USE OF ANTICHOLINERGIC ANTIPARKINSON AGENTS IN NORWAY. EPIDEMIOLOGY, TOXICOLOGY AND CLINICAL IMPLICATIONS
455. Else Marie Huuse: ASSESSMENT OF TUMOR MICROENVIRONMENT AND TREATMENT EFFECTS IN HUMAN BREAST CANCER XENOGRAFTS USING MR IMAGING AND SPECTROSCOPY
456. Khalid S. Ibrahim: INTRAOPERATIVE ULTRASOUND ASSESSMENT IN CORONARY ARTERY BYPASS SURGERY – WITH SPECIAL REFERENCE TO CORONARY ANASTOMOSES AND THE ASCENDING AORTA
457. Bjørn Øglænd: ANTHROPOMETRY, BLOOD PRESSURE AND REPRODUCTIVE DEVELOPMENT IN ADOLESCENCE OF OFFSPRING OF MOTHERS WHO HAD PREECLAMPSIA IN PREGNANCY
458. John Olav Roaldset: RISK ASSESSMENT OF VIOLENT, SUICIDAL AND SELF-INJURIOUS BEHAVIOUR IN ACUTE PSYCHIATRY – A BIO-PSYCHO-SOCIAL APPROACH
459. Håvard Dalen: ECHOCARDIOGRAPHIC INDICES OF CARDIAC FUNCTION – NORMAL VALUES AND ASSOCIATIONS WITH CARDIAC RISK FACTORS IN A POPULATION FREE FROM CARDIOVASCULAR DISEASE, HYPERTENSION AND DIABETES: THE HUNT 3 STUDY
460. Beate André: CHANGE CAN BE CHALLENGING. INTRODUCTION TO CHANGES AND IMPLEMENTATION OF COMPUTERIZED TECHNOLOGY IN HEALTH CARE
461. Latha Nrugham: ASSOCIATES AND PREDICTORS OF ATTEMPTED SUICIDE AMONG DEPRESSED ADOLESCENTS – A 6-YEAR PROSPECTIVE STUDY

462. Håvard Bersås Nordgaard: TRANSIT-TIME FLOWMETRY AND WALL SHEAR STRESS ANALYSIS OF CORONARY ARTERY BYPASS GRAFTS – A CLINICAL AND EXPERIMENTAL STUDY

Cotutelle with University of Ghent: Abigail Emily Swillens: A MULTIPHYSICS MODEL FOR IMPROVING THE ULTRASONIC ASSESSMENT OF LARGE ARTERIES

2011

463. Marte Helene Bjørk: DO BRAIN RHYTHMS CHANGE BEFORE THE MIGRAINE ATTACK? A LONGITUDINAL CONTROLLED EEG STUDY
464. Carl-Jørgen Arum: A STUDY OF UROTHELIAL CARCINOMA: GENE EXPRESSION PROFILING, TUMORIGENESIS AND THERAPIES IN ORTHOTOPIC ANIMAL MODELS
465. Ingunn Harstad: TUBERCULOSIS INFECTION AND DISEASE AMONG ASYLUM SEEKERS IN NORWAY. SCREENING AND FOLLOW-UP IN PUBLIC HEALTH CARE
466. Leif Åge Strand: EPIDEMIOLOGICAL STUDIES AMONG ROYAL NORWEGIAN NAVY SERVICEMEN. COHORT ESTABLISHMENT, CANCER INCIDENCE AND CAUSE-SPECIFIC MORTALITY
467. Katrine Høyer Holgersen: SURVIVORS IN THEIR THIRD DECADE AFTER THE NORTH SEA OIL RIG DISASTER OF 1980. LONG-TERM PERSPECTIVES ON MENTAL HEALTH
468. MarianneWallenius: PREGNANCY RELATED ASPECTS OF CHRONIC INFLAMMATORY ARTHRITIDES: DISEASE ONSET POSTPARTUM, PREGNANCY OUTCOMES AND FERTILITY. DATA FROM A NORWEGIAN PATIENT REGISTRY LINKED TO THE MEDICAL BIRTH REGISTRY OF NORWAY
469. Ole Vegard Solberg: 3D ULTRASOUND AND NAVIGATION – APPLICATIONS IN LAPAROSCOPIC SURGERY
470. Inga Ekeberg Schjerve: EXERCISE-INDUCED IMPROVEMENT OF MAXIMAL OXYGEN UPTAKE AND ENDOTHELIAL FUNCTION IN OBESE AND OVERWEIGHT INDIVIDUALS ARE DEPENDENT ON EXERCISE-INTENSITY
471. Eva Veslemøy Tyldum: CARDIOVASCULAR FUNCTION IN PREECLAMPSIA – WITH REFERENCE TO ENDOTHELIAL FUNCTION, LEFT VENTRICULAR FUNCTION AND PRE-PREGNANCY PHYSICAL ACTIVITY
472. Benjamin Garzón Jiménez de Cisneros: CLINICAL APPLICATIONS OF MULTIMODAL MAGNETIC RESONANCE IMAGING
473. Halvard Knut Nilsen: ASSESSING CODEINE TREATMENT TO PATIENTS WITH CHRONIC NON-MALIGNANT PAIN: NEUROPSYCHOLOGICAL FUNCTIONING, DRIVING ABILITY AND WEANING
474. Eiliv Brenner: GLUTAMATE RELATED METABOLISM IN ANIMAL MODELS OF SCHIZOPHRENIA
475. Egil Jonsbu: CHEST PAIN AND PALPITATIONS IN A CARDIAC SETTING; PSYCHOLOGICAL FACTORS, OUTCOME AND TREATMENT
476. Mona Høysæter Fenstad: GENETIC SUSCEPTIBILITY TO PREECLAMPSIA : STUDIES ON THE NORD-TRØNDELAG HEALTH STUDY (HUNT) COHORT, AN AUSTRALIAN/NEW ZEALAND FAMILY COHORT AND DECIDUA BASALIS TISSUE
477. Svein Erik Gaustad: CARDIOVASCULAR CHANGES IN DIVING: FROM HUMAN RESPONSE TO CELL FUNCTION
478. Karin Torvik: PAIN AND QUALITY OF LIFE IN PATIENTS LIVING IN NURSING HOMES
479. Arne Solberg: OUTCOME ASSESSMENTS IN NON-METASTATIC PROSTATE CANCER
480. Henrik Sahlin Pettersen: CYTOTOXICITY AND REPAIR OF URACIL AND 5-FLUOROURACIL IN DNA
481. Pui-Lam Wong: PHYSICAL AND PHYSIOLOGICAL CAPACITY OF SOCCER PLAYERS: EFFECTS OF STRENGTH AND CONDITIONING
482. Ole Solheim: ULTRASOUND GUIDED SURGERY IN PATIENTS WITH INTRACRANIAL TUMOURS
483. Sten Roar Snare: QUANTITATIVE CARDIAC ANALYSIS ALGORITHMS FOR POCKET-SIZED ULTRASOUND DEVICES
484. Marit Skyrud Bratlie: LARGE-SCALE ANALYSIS OF ORTHOLOGS AND PARALOGS IN VIRUSES AND PROKARYOTES
485. Anne Elisabeth F. Isern: BREAST RECONSTRUCTION AFTER MASTECTOMY – RISK OF RECURRENCE AFTER DELAYED LARGE FLAP RECONSTRUCTION – AESTHETIC OUTCOME, PATIENT SATISFACTION, QUALITY OF LIFE AND SURGICAL RESULTS;

HISTOPATHOLOGICAL FINDINGS AND FOLLOW-UP AFTER PROPHYLACTIC MASTECTOMY IN HEREDITARY BREAST CANCER

486. Guro L. Andersen: CEREBRAL PALSY IN NORWAY – SUBTYPES, SEVERITY AND RISK FACTORS
487. Frode Kolstad: CERVICAL DISC DISEASE – BIOMECHANICAL ASPECTS
488. Bente Nordtug: CARING BURDEN OF COHABITANTS LIVING WITH PARTNERS SUFFERING FROM CHRONIC OBSTRUCTIVE PULMONARY DISEASE OR DEMENTIA
489. Mariann Gjervik Heldahl: EVALUATION OF NEOADJUVANT CHEMOTHERAPY IN LOCALLY ADVANCED BREAST CANCER BASED ON MR METHODOLOGY
490. Lise Tevik Løvseth: THE SUBJECTIVE BURDEN OF CONFIDENTIALITY
491. Marie Hjelmseth Aune: INFLAMMATORY RESPONSES AGAINST GRAM NEGATIVE BACTERIA INDUCED BY TLR4 AND NLRP12
492. Tina Strømdal Wik: EXPERIMENTAL EVALUATION OF NEW CONCEPTS IN HIP ARTHROPLASTY
493. Solveig Sigurdardottir: CLINICAL ASPECTS OF CEREBRAL PALSY IN ICELAND. A POPULATION-BASED STUDY OF PRESCHOOL CHILDREN
494. Arne Reimers: CLINICAL PHARMACOKINETICS OF LAMOTRIGINE
495. Monica Wegling: KULTURMENNESKETS BYRDE OG SYKDOMMENS VELSIGNELSE. KAN MEDISINSK UTREDNING OG INTERVENSJON HA EN SELVSTENDIG FUNKSJON UAVHENGIG AV DET KURATIVE?
496. Silje Alvestad: ASTROCYTE-NEURON INTERACTIONS IN EXPERIMENTAL MESIAL TEMPORAL LOBE EPILEPSY – A STUDY OF UNDERLYING MECHANISMS AND POSSIBLE BIOMARKERS OF EPILEPTOGENESIS
497. Javaid Nauman: RESTING HEART RATE: A MATTER OF LIFE OR DEATH – PROSPECTIVE STUDIES OF RESTING HEART RATE AND CARDIOVASCULAR RISK (THE HUNT STUDY, NORWAY)
498. Thuy Nguyen: THE ROLE OF C-SRC TYROSINE KINASE IN ANTIVIRAL IMMUNE RESPONSES
499. Trine Naalsund Andreassen: PHARMACOKINETIC, PHARMACODYNAMIC AND PHARMACOGENETIC ASPECTS OF OXYCODONE TREATMENT IN CANCER PAIN
500. Eivor Alette Laugsand: SYMPTOMS IN PATIENTS RECEIVING OPIOIDS FOR CANCER PAIN – CLINICAL AND PHARMACOGENETIC ASPECTS
501. Dorthe Stensvold: PHYSICAL ACTIVITY, CARDIOVASCULAR HEALTH AND LONGEVITY IN PATIENTS WITH METABOLIC SYNDROME
502. Stian Thoresen Aspenes: PEAK OXYGEN UPTAKE AMONG HEALTHY ADULTS – CROSS-SECTIONAL DESCRIPTIONS AND PROSPECTIVE ANALYSES OF PEAK OXYGEN UPTAKE, PHYSICAL ACTIVITY AND CARDIOVASCULAR RISK FACTORS IN HEALTHY ADULTS (20-90 YEARS)
503. Reidar Alexander Vigen: PATHOBIOLOGY OF GASTRIC CARCINOIDS AND ADENOCARCINOMAS IN RODENT MODELS AND PATIENTS. STUDIES OF GASTROCYSTOPLASTY, GENDER-RELATED FACTORS, AND AUTOPHAGY
504. Halvard Høilund-Kaupang: MODELS AND METHODS FOR INVESTIGATION OF REVERBERATIONS IN NONLINEAR ULTRASOUND IMAGING
505. Audhild Løhre: WELLBEING AMONG SCHOOL CHILDREN IN GRADES 1-10: PROMOTING AND ADVERSE FACTORS
506. Torgrim Tandstad: VOX POPULI. POPULATION-BASED OUTCOME STUDIES IN TESTICULAR CANCER
507. Anna Brenne Grønskag: THE EPIDEMIOLOGY OF HIP FRACTURES AMONG ELDERLY WOMEN IN NORD-TRØNDELAG. HUNT 1995-97, THE NORD-TRØNDELAG HEALTH STUDY
508. Kari Ravndal Risnes: BIRTH SIZE AND ADULT MORTALITY: A SYSTEMATIC REVIEW AND A LONG-TERM FOLLOW-UP OF NEARLY 40 000 INDIVIDUALS BORN AT ST. OLAV UNIVERSITY HOSPITAL IN TRONDHEIM 1920-1960
509. Hans Jakob Bøe: LONG-TERM POSTTRAUMATIC STRESS AFTER DISASTER – A CONTROLLED STUDY OF SURVIVORS' HEALTH 27 YEARS AFTER THE CAPSIZED NORTH SEA OIL RIG
510. Cathrin Barbara Canto, Cotutelle with University of Amsterdam: LAYER SPECIFIC INTEGRATIVE PROPERTIES OF ENTORHINAL PRINCIPAL NEURONS
511. Ioanna Sandvig: THE ROLE OF OLFACTORY ENSHEATHING CELLS, MRI, AND BIOMATERIALS IN TRANSPLANT-MEDIATED CNS REPAIR

512. Karin Fahl Wader: HEPATOCYTE GROWTH FACTOR, C-MET AND SYNDECAN-1 IN MULTIPLE MYELOMA
513. Gerd Tranø: FAMILIAL COLORECTAL CANCER
514. Bjarte Bergstrøm: INNATE ANTIVIRAL IMMUNITY – MECHANISMS OF THE RIG-I-MEDIATED RESPONSE
515. Marie Søfteland Sandvei: INCIDENCE, MORTALITY, AND RISK FACTORS FOR ANEURYSMAL SUBARACHNOID HEMORRHAGE. PROSPECTIVE ANALYZES OF THE HUNT AND TROMSØ STUDIES
516. Mary-Elizabeth Bradley Eilertsen: CHILDREN AND ADOLESCENTS SURVIVING CANCER: PSYCHOSOCIAL HEALTH, QUALITY OF LIFE AND SOCIAL SUPPORT
517. Takaya Saito: COMPUTATIONAL ANALYSIS OF REGULATORY MECHANISM AND INTERACTIONS OF MICRORNAS

Godkjent for disputas, publisert post mortem: Eivind Jullumstrø: COLORECTAL CANCER AT LEVANGER HOSPITAL 1980-2004

518. Christian Gutvik: A PHYSIOLOGICAL APPROACH TO A NEW DECOMPRESSION ALGORITHM USING NONLINEAR MODEL PREDICTIVE CONTROL
519. Ola Storrø: MODIFICATION OF ADJUVANT RISK FACTOR BEHAVIOURS FOR ALLERGIC DISEASE AND ASSOCIATION BETWEEN EARLY GUT MICROBIOTA AND ATOPIC SENSITIZATION AND ECZEMA. EARLY LIFE EVENTS DEFINING THE FUTURE HEALTH OF OUR CHILDREN
520. Guro Fanneløb Giskeødegård: IDENTIFICATION AND CHARACTERIZATION OF PROGNOSTIC FACTORS IN BREAST CANCER USING MR METABOLOMICS
521. Gro Christine Christensen Løhaugen: BORN PRETERM WITH VERY LOW BIRTH WEIGHT – NEVER ENDING COGNITIVE CONSEQUENCES?
522. Sigrid Nakrem: MEASURING QUALITY OF CARE IN NURSING HOMES – WHAT MATTERS?
523. Brita Pukstad: CHARACTERIZATION OF INNATE INFLAMMATORY RESPONSES IN ACUTE AND CHRONIC WOUNDS

2012

524. Hans Wasmuth: ILEAL POUCHES
525. Inger Økland: BIASES IN SECOND-TRIMESTER ULTRASOUND DATING RELATED TO PREDICTION MODELS AND FETAL MEASUREMENTS
526. Bjørn Mørkedal: BLOOD PRESSURE, OBESITY, SERUM IRON AND LIPIDS AS RISK FACTORS OF ISCHAEMIC HEART DISEASE
527. Siver Andreas Moestue: MOLECULAR AND FUNCTIONAL CHARACTERIZATION OF BREAST CANCER THROUGH A COMBINATION OF MR IMAGING, TRANSCRIPTOMICS AND METABOLOMICS